Independent Component Analysis: Applications in ECG signal processing

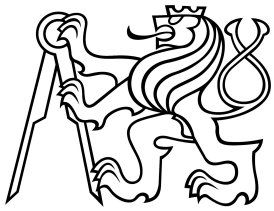

Jakub Kuzilek

Department of Cybernetics

Faculty of Electrical Engineering

Czech Technical University in Prague

Supervisor: Lenka Lhotska

Study Programme No. P2612-Electrotechnics and Informatics

Domain No. 3902V035-Artificial Intelligence and Biocybernetics

A thesis submitted for the degree of Doctor of Philosophy (PhD)

2013

I would like to dedicate this thesis to my loving beautiful wife, my parents and my brother for their support during my whole academic career.

Acknowledgements

And I would like to thank to my supervisor Lenka Lhotska for her help with thesis and all problems I ever dealt with. I would like to thank my colleagues and Department of Cybernetics for stimulating workspace.

Abstract

Our work aims at processing of ECG signals using Independent Component Analysis (ICA). ICA serves in many biomedical applications as a preprocessing or feature extraction technique. These applications are listed in state-of-the-art chapter, which describes ICA algorithms in general and also presents basic algorithms and their applications in processing of various biomedical signals. ICA represents a solution of the Blind Source Separation (BSS) problem, which can be stated as extraction of signals based merely on their mixtures. In our work we used JADE algorithm for solving two problems: de-noising of electrocardiographic (ECG) signals and beat detection. The de-noising algorithm, which we have developed, is an automatic method capable to deal with strong uncommon noises, present in nearly every holter ECG recording. The method is based on detection of noisy components and their removal from ECG data. The results show that our method is able to reduce both normal and uncommon noises. The algorithm for beat detection is based on extraction of ECG activity from noisy recording using JADE algorithm. The method is an extension of the well-known Christov's beat detection algorithm, which detects beats using combined adaptive threshold on transformed ECG signal (complex lead). Our extension adds estimation of independent components of measured signal into the transformation of ECG creating a signal called complex component, which enhances ECG activity and enables beat detection in presence of strong noises. This makes the beat detection algorithm much more robust in cases of unpredictable noise appearances typical for holter ECGs and telemedical applications of ECG. Methods were tested and compared with other state-of-the-art methods using standard databases.

Contents

List of Figures

Nomenclature

Notation

α	step size variable
x	random variable, random signal
x_i or $x[i]$	ith sample of random signal x
$\overline{x}$	sample mean of x
$\mathbf{x}$	vector, vector of signals
$\mathbf{x}(t)$	vector of signals in time t
$\mathbf{X}$	matrix, signal matrix
$\mathbf{X}^T$	matrix transpose
$\mathbf{X}^{-1}$	matrix inversion
$\widehat{\mathbf{X}}$	matrix estimate
$\rho_{x,y}$	Pearson correlation coeficient
E{}	expectation operator
$kurt(\mathbf{x})$	kurtosis of x
$var(x)$	variance of x
$sign(\mathbf{x})$	signum function of x
$\|\|\mathbf{x}\|\|$	Euclidian norm of vector $\mathbf{x}$

Nomenclature

Symbols and abbreviations

AMUSE Algortihm for Multiple Unknown Source Extraction based on EVD

BSS Blind Source Separation

ECG Electrocardiograph/y

EEG Electroencephalograph/y

EMG Electromyograph/y

efica Efficient Fast ICA

FastICA Fast ICA

fMRI functional Magnetic Resonance Imaging

FOBI Fourth Order Blind Identification

ICA Independent Component Analysis

JADE Joint Approximate Diagonalization of Eigen matrices

MRS Magnetic Resonance Spectroscopy

SOBI Second Order Blind Identification

Chapter 1

Introduction

Independent Component Analysis (ICA) represents one solution of the Blind Source Separation (BSS) problem, which is the extraction of the set of signals based merely on their mixtures. The BSS/ICA methods were successfully applied in wide variety of problems ranging from economy to medicine. One of the main research areas, in which ICA methods were used is biomedical signal processing.

For the last decade ICA methods have been employed in variety of biomedical applications. Most works use only limited number of ICA algorithms such as SOBI [1], FastICA [2] or JADE [3]. In addition, separation performance of electro-physiological sources is still unknown. Due to this uncertainty a single best method for biomedical area cannot be selected [4].

At present many problems in biomedical engineering have been solved by application of ICA. The main research area is electroencephalography (EEG) followed by functional magnetic resonance imaging (fMRI) analysis and electrocardiography (ECG). These three mainstream application fields are followed by several minor research areas such as magnetic resonance spectroscopy (MRS) or electromyography (EMG).

In ECG signal processing there are several problems, which are yet unsolved optimally and one of them is noise reduction/removal. Due to the nature of noises presented in the ECG recording one can employ traditional techniques, which perform well in controlled environment, however these methods do not work properly with holter and telemedical applications. ICA provides the solution for dealing with unpredictable and uncommon noises – it can separate the ECG activity and the noises presented in recording thus enabling further processing. It has been observed [5, 6, 4] that ECG activity has super-Gaussian distribution and due to this nature it is easily separable from other signals (noise and arte-

facts) presented in normal ECG recording. Thus we can employ it in tasks that require cleaning of ECG signals (noise reduction, beat detection, etc.).

Our work aims at using ICA algorithm in ECG signal processing. First we developed a de-noising algorithm for ECG recordings. We created method for detection and estimation of noise in records. This method is then compared to the state-of-the-art methods and its efficiency is proven.

Second we developed the enhanced Christov's beat detection algorithm, which detects beats on transformed ECG signal (complex lead) using combined adaptive threshold. Our offline extension adds estimation of independent components of measured signal into the ECG transformation creating a signal called complex component, which enhances ECG activity and enables beat detection in presence of strong noises. We compared our algorithm with the performance of our implementation of the Christov's and Tompkins's beat detection algorithms.

Following chapters are organized as follows. Chapter 2 covers the Aims of the Thesis. Chapter 3 deals with state-of-the-art in biomedical signal processing using ICA. Chapter 4 sumarizes medical minimum required for understanding ECG signals. Following two chapters describes our proposed algorithms. Chapter 7 describes evaluation methodology and referential methods used for testing of developed methods. Chapter 8 summarizes results of our evaluation process. Finally Chapter 9 contains conclusions of the thesis.

Chapter 2

Aims of the Thesis

The main aim of the thesis is to propose and implement a new methods based on ICA that enable ECG processing with higher accuracy. The aim can be divided into several control points covering the whole problem:

Create state-of-the-art of ICA applications in Biomedical Engineering research area with main focus on application in ECG signal processing.

As the Independent Component Analysis is the general tool for signal processing and analysis, extensive research has been done in the field of biomedical engineering using the ICA algorithms. This implicates the necessity for creation of state-of-the-art of the most common algorithms and their applications. We provide such a state-of-the-art and we summarize briefly the merits and flaws of ICA algorithms family. We will also discuss the reproducibility of research results. Based on state-of-the-art we will be able to propose modifications and new algorithms that will avoid the flaws of ICA.

Propose and develop an algorithm for denoising of ECG signals using ICA.

Since noise presence in measured ECG signal is one of the most common problems, especially in case of holter and telemedical ECG recordings, we decided to create an algorithm for ECG de-noising based on ICA. The algorithm should be efficient in case of common noises (50/60 Hz grid noise, breathing and muscle artefacts, etc.), in addition it should

provide filtering capability in case of uncommon noises, which can be added to ECG measurement in case of holter ECG. The algorithm should preserve the morphology in temporo-spatial domain and also the waveform of the ECG in order to keep ECG informative for medical personnel. It should be also fully automatic to enable deploying in situation, when the trained personnel is not available.

Propose and develop an algorithm for beat detection using ICA.

The beat detection is one of the most important preprocessing steps in ECG signal analysis. Without beat position no other analysis could be done. One needs to identify positions of beats in order to measure other waves such as P wave or T wave. Their morphology provides the medical personnel with important information. Beat detection is the second step in ECG processing chain – the first one is filtering, which should reduce noises presented in ECG, but sometimes the filtering fails or could not be done. In that case one needs to deploy algorithm, which is efficient to detect beats in noise corrupted ECG data. We decided to develop such an algorithm with help of ICA. The algorithm should have same or better sensitivity and specificity as the most common algorithms (Pan-Tompkins algorithm, Christov's algorithm), but it should be able to work in presence of strong uncommon noises. In order to evaluate algorithm efficiency we will use freely available data from Physionet.org database [7].

Develop a testing framework for evaluation of proposed algorithms.

Developed algorithms must be tested by standardized procedure, which provides us with information about their performance compared with other state-of-the-art methods. This implicates the necessity for developing a testing framework, which will be easily modifiable for different tasks performed in ECG signal processing chain.

Chapter 3

Independent Component Analysis and its applications in biomedical engineering

3.1 The principles of ICA

Independent Component Analysis (ICA) is described in detail in many publications, for example [2, 8, 9]. ICA represents one solution of the Blind Source Separation problem (BSS), which is the extraction of a set of signals based merely on their mixtures. In particular let us mention ECG, which is a mixture of signals from nodes presented in the heart, or EEG, which is a mixture of neurological activity of centres in brain. Basic ICA model assumes linear combination of source signals (called components):

$$\mathbf{X} = \mathbf{AS}, \tag{3.1}$$

where $\mathbf{X}$ is a mixture of source signals, $\mathbf{A}$ is the mixing matrix that characterizes environment, through which source signals pass, and $\mathbf{S}$ are the source signals. $\mathbf{X}$ and $\mathbf{S}$ get the size n x m, where n is number of sources and m is length of record in samples. Mixture matrix $\mathbf{A}$ is then of size n x n (in general $\mathbf{A}$ does not need to be square, but many algorithms assume this "property"). Figure 3.1 shows schematic representation of the mixing process. Components can be obtained using the following expression:

$$\mathbf{S} = \mathbf{A}^{-1}\mathbf{X} = \mathbf{WX}, \tag{3.2}$$

where matrix **W** is inverse to matrix **A**. From Equation 3.2 it is obvious that estimation of a components is reduced to search of matrix **W**.

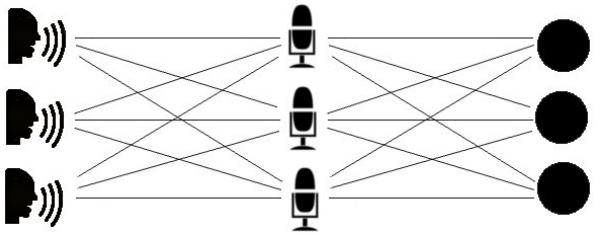

Figure 3.1: Schematic representation of a signal mixing process. It shows a demonstrative example used for ICA explanation - cocktail party problem. Three speakers (left side of the figure) speech is recorded on three microphones (middle of the picture). On each record the mixture of 3 speeches is presented. ICA de-mixes these records and obtains "original" speakers speech on each component(right side of the figure)

The BSS/ICA methods try to estimate components that would be as independent as possible and their linear combination is original data. Estimation of components is done by iterative algorithm, which maximizes function of independence, or by a non-iterative algorithm, which is based on joint diagonalization of correlation matrices.
ICA has one large restriction, which is based on principle of the method - **the original sources must be statistically independent**. This is the only assumption we need to take into account in general. As other methods, ICA has also certain disadvantages:

- **We cannot specify order of components**
  The order of rows in matrix **S** and columns in matrix **A** could be randomly changed without any effect on the result. Formally permutation matrix **P** and its inverse can be substituted into Eq. 3.1: $\mathbf{X} = \mathbf{A}\mathbf{P}^{-1}\mathbf{P}\mathbf{S}$, where **PS** is the original source in another order and $\mathbf{A}\mathbf{P}^{-1}$ is new unknown mixing matrix.

- **We cannot estimate energy of components**
  This problem arises because we have no prior information about matrices **A** and **S** - multiplication of random row with scalar value in matrix **S** and division of competent column in matrix **A** with the same value leads to random change of the amplitude of components. This problem can be partially fixed by reducing variance to one. But this still does not solve the problem with $\pm$ sign (in sense of multiplication by ± 1) of the components.

In many ICA algorithms it is assumed that the data is centred and whitened. Without loss of generality data could be centred:

$$\mathbf{x} = \mathbf{y} - E\{\mathbf{y}\}, \tag{3.3}$$

where $\mathbf{y}$ is original data, $E\{\}$ is expectation of data and $\mathbf{x}$ is centered data.
Whitening can be expressed by:

$$\mathbf{z} = \mathbf{V}\mathbf{x} = \mathbf{V}\mathbf{A}\mathbf{s}, \tag{3.4}$$

where $\mathbf{z}$ is whitened data, $\mathbf{V}$ is whitening matrix, $\mathbf{x}$ are mixed signals, $\mathbf{A}$ is mixing matrix and $\mathbf{s}$ are desired source signals. Whitening operation removes correlation between signals (note that correlation does not mean signals are independent)[2]. So correlation matrix of pre-whitened data $\mathbf{z}$ is: $E\{\mathbf{z}\mathbf{z}^T\} = \mathbf{I}$.

3.2 Algorithms

This section provides the quick overview of fundamental ICA algorithms. These are as follows:

- **F**ast **I**ndependent **C**omponent **A**nalysis (**FastICA**)
- **F**ourth-**O**rder **B**lind **I**dentification (**FOBI**)
- **J**oint **A**pproximate **D**iagonalization of **E**igen matrices (**JADE**)
- **A**lgorithm for **M**ultiple **U**nknown **S**ource **E**xtraction based on **E**VD (**AMUSE**)
- **S**econd-**O**rder **B**lind **I**dentification (**SOBI**)

Last two are not in proper sense ICA algorithms because they use only second order statistics for source estimation. They estimate sources without using independence and they solve BSS problem. These algorithms are widely used and are fundamental for other ICA algorithms, therefore we mention them here.

3.2.1 FastICA

FastICA algorithm was introduced by A. Hyvärinen [2] and it has a couple of modifications based on target function. The introduced separation algorithm is based on maximizing non-Gaussianity function.

This algorithm is based on the idea of using central limit theorem as a measure of independence. Central limit theorem states: *The distribution of a sum of independent random variables tends toward a Gaussian distribution* [10]. We can say that sum of two independent random variables has a distribution that is closer to Gaussian than the original two random variables. So maximizing non-Gaussianity leads to obtaining more independent signals.
Non-Gaussianity can be measured in many ways. One way is to use kurtosis, which is basically normalized version of fourth-order moment [8]:

$$kurt(y) = E\{y^4\} - 3(E\{y^2\})^2, \tag{3.5}$$

where y is a random signal. In our case y is normalized to unit variance so Equation 3.5 simplifies to $kurt(y) = E\{y^4\} - 3$.
Basic algorithm needs gradient of kurtosis:

$$\begin{aligned}
&\frac{\partial |kurt(\mathbf{w}^T\mathbf{z})|}{\partial \mathbf{w}} = \\
&sign(kurt(\mathbf{w}^T\mathbf{z}))\left(\frac{E\{(\mathbf{w}^T\mathbf{z})^4\}}{\partial \mathbf{w}} - \frac{3(E\{(\mathbf{w}^T\mathbf{z})^2\})^2}{\partial \mathbf{w}}\right) = \\
&sign(kurt(\mathbf{w}^T\mathbf{z}))\left(4E\{\mathbf{z}(\mathbf{w}^T\mathbf{z})^3\} - 12E\{||\mathbf{w}^T||^2\}E\{\mathbf{w}^T\}\right) = \\
&4sign(kurt(\mathbf{w}^T\mathbf{z}))[E\{\ \mathbf{z}(\mathbf{w}^T\mathbf{z})^3\} - 3\mathbf{w}||\mathbf{w}||^2].
\end{aligned} \tag{3.6}$$

Since $\mathbf{w}$ is calculated on unit sphere it needs to be normalized in every step. Last term in previous equation changes only norm of $\mathbf{w}$ and thus it could be omitted. Using (3.6) an algorithm was obtained:

1. $\mathbf{w}(t) = \mathbf{w}(t-1) + \alpha sign(kurt(\mathbf{w}(t-1)^T\mathbf{z}))E\{\ \mathbf{z}(\mathbf{w}(t-1)^T\mathbf{z})^3\}$
2. $\mathbf{w}(t) = \frac{\mathbf{w}(t)}{||\mathbf{w}(t)||}$

The algorithm stops when the criterion on kurtosis reaches the desired value. In some cases algorithm cannot reach specified desired value and in order to avoid infinite loops the maximal loop count value is specified. This another stopping criterion enables algorithm

to work properly in difficult cases of similar signal distributions.

This basic algorithm is converted to fast fixed point algorithm by equating the gradient of kurtosis with $\mathbf{w}$. This means we obtain:

$$\mathbf{w} = \alpha[E\{\ \mathbf{z}(\mathbf{w}^T\mathbf{z})^3\} - 3\mathbf{w}||\mathbf{w}||^2], \tag{3.7}$$

this equation suggests the following algorithm:

1. $\mathbf{w}(t) = \alpha[E\{\ \mathbf{z}(\mathbf{w}(t-1)^T\mathbf{z})^3\} - 3\mathbf{w}(t-1)]$
2. $\mathbf{w}(t) = \frac{\mathbf{w}(t)}{||\mathbf{w}(t)||}$

3.2.2 FOBI

FOBI was proposed by Cardoso [11]. Consider quadratically weighted covariance matrix:

$$\Omega = E\{\mathbf{z}\mathbf{z}^T||\mathbf{z}||^2\}, \tag{3.8}$$

where $\mathbf{z}$ is pre-whitened data (see Eq. 3.4). Assuming data pre-whitened by ICA model it follows:

$$\Omega = E\{\mathbf{VAss}^T(\mathbf{VA})^T||\mathbf{VAs}||^2\} = \mathbf{W}^T E\{\mathbf{ss}^T||\mathbf{s}||^2\}\mathbf{W}, \tag{3.9}$$

where $\mathbf{VA}$ is orthogonal and $\mathbf{W} = (\mathbf{VA})^T$. Using independence and unit variance (it does not affect independence property of signals) of s_i matrix Ω stands for:

$$\begin{aligned}
&\Omega = \mathbf{W}diag(E\{s_i^2||\mathbf{s}||^2\})\mathbf{W} = \\
&\mathbf{W}diag(E\{s_i^2\sum_{j=1}^{n} s_j^2\})\mathbf{W} = \\
&\mathbf{W}diag(E\{s_i^2(s_i^2 + \sum_{j=1, j\neq i}^{n} s_j^2)\})\mathbf{W} = \\
&\mathbf{W}diag(E\{s_i^4\} + \sum_{j=1, j\neq i}^{n} E\{s_i^2\}E\{s_j^2\})\mathbf{W} = \\
&\mathbf{W}diag(E\{s_i^4\} + n - 1)\mathbf{W}
\end{aligned} \tag{3.10}$$

Last equation shows that matrix $\mathbf{W}$ can be obtained by eigenvalue decomposition of matrix Ω, which is decomposed to diagonal matrix consisting of the fourth order cumulants of s_i and to orthogonal matrix $\mathbf{W}$. This algorithm is the most efficient algorithm for ICA

computation. **FOBI** has restriction, under which it works, namely all ICs must have different kurtosis.

3.2.3 JADE

JADE [3] is an extension of **FOBI**. For whitened data, we can write fourth-order-cross-cumulant tensor [8] as:

$$F(\mathbf{M}) = E\{(\mathbf{z}^T\mathbf{M}\mathbf{z}\mathbf{z}\mathbf{z}^T)\} - 2\mathbf{M} - tr(\mathbf{M})\mathbf{I}, \tag{3.11}$$

where $\mathbf{M}$ is eigenmatrix of cumulant, $\mathbf{z}$ is whitened data, $\mathbf{I}$ is unit matrix and $tr(\mathbf{M})$ is trace of matrix defined as:

$$tr(\mathbf{M}) = \sum_{i}^{n} m_{ii}. \tag{3.12}$$

Using (3.11) whitened correlation matrices can be defined alternatively as:

$$\Omega = F(\mathbf{I}) = E\{||\mathbf{z}||^2\mathbf{z}\mathbf{z}^T\} - (n+2)\mathbf{I}. \tag{3.13}$$

Thus we can take a matrix $\mathbf{M}$ and replace matrix $\mathbf{I}$ in **FOBI** algorithm. This matrix would have a linear combinations of cumulants of independent components as its eigenvalues. Now we take more than one matrix, jointly diagonalize them and find the best result.

3.2.4 AMUSE

AMUSE [12] is an algorithm based on prior knowledge of data structure - data are signals so they are time dependent. Let us denote lag-time covariance matrix as:

$$C_\tau^{\mathbf{x}} = E\{\mathbf{x}(t)\mathbf{x}^T(t-\tau)\}, \tag{3.14}$$

where $\mathbf{x}$ is vector of signals samples in time t and τ is lag-time.

An issue is that whitening data does not make data independent. The key for solving this problem is time-lagged covariance matrix, it can be used instead of high-order statistics. Using this time-lagged covariance matrix gives us certain extra information to estimate model, under certain conditions (samples of signals must be taken at the same times and delayed correlations between different output signals vanish), and no high-order

information is needed. **AMUSE** uses the simplest case with only one time lag τ. Mostly τ equals 1.

Consider whitened data $\mathbf{z}$, then we can write for separating matrix $\mathbf{W}$:

$$\begin{aligned} \mathbf{W}\mathbf{z}(t) &= \mathbf{s}(t), \\ \mathbf{W}\mathbf{z}(t-\tau) &= \mathbf{s}(t-\tau), \end{aligned} \tag{3.15}$$

where $\mathbf{s}$ are samples of signals in given time. Next consider lagged covariance matrix:

$$C_\tau^{\mathbf{z}} = \frac{1}{2}\left[C_\tau^{\mathbf{z}} + (C_\tau^{\mathbf{z}})^T\right] \tag{3.16}$$

Substituting $\mathbf{z}$ from (3.15) we get:

$$C_\tau^{\mathbf{z}} = \frac{1}{2}\mathbf{W}^T\left[E\{\mathbf{s}(t)\mathbf{s}^T(t-\tau)\} + E\{\mathbf{s}(t-\tau)\mathbf{s}^T(t)\}\right]\mathbf{W} = \mathbf{W}^T C_\tau^{\mathbf{s}}\mathbf{W} \tag{3.17}$$

Due to the independence of signals $s_i(t)$ the covariance matrix $C_\tau^{\mathbf{s}}$ is diagonal, name it $\mathbf{D}$ and rewrite previous equation:

$$C_\tau^{\mathbf{z}} = \mathbf{W}^T\mathbf{D}\mathbf{W} \tag{3.18}$$

We can see that mixing matrix $\mathbf{W}$ is a part of eigenvalue decomposition of $C_\tau^{\mathbf{z}}$. From the previous the following algorithm could be constructed:

1. Whiten data $\mathbf{x}$ to $\mathbf{z}$
2. Compute eigenvalue decomposition of $C_\tau^{\mathbf{z}}$.
3. Rows of matrix $\mathbf{W}$ are given by eigenvectors.

3.2.5 SOBI

SOBI [1] is an extension of **AMUSE** algorithm. It uses more than one time-lag τ. The diagonalization of all corresponding lagged covariance matrices is needed. Because the covariance matrices got different eigenvalues, the formulation of functions, which express the degree of diagonalization of matrices, is needed.
Simple function for measuring this degree of diagonalization of matrix $\mathbf{M}$ is:

$$off(\mathbf{M}) = \sum_{i \neq j} m_{ij}, \tag{3.19}$$

which is the sum of off-diagonal elements. Minimization of sum of off-diagonal elements in several matrices is desired. Denoting S a set of chosen time lags τ criteria for minimization stands for:

$$J(\mathbf{W}) = \sum_{\tau \in S} off(\mathbf{W}\mathbf{C}_\tau^{\mathbf{x}}\mathbf{W}^T)^2, \tag{3.20}$$

where $J(\mathbf{W})$ is objective function, $\mathbf{W}$ is separating matrix, $\mathbf{C}_\tau^{\mathbf{x}}$ is time-lagged covariance matrix of data $\mathbf{x}$. Minimization under this constraint gives the estimation method and it is performed by gradient descend method or simultaneous estimation of eigenvalue decomposition for several matrices.

3.3 Example

As an example serves us mixture of ECG signal and uniformly distributed random noise (Figure 3.2). Both signals are 10 seconds long. Signals have zero mean.

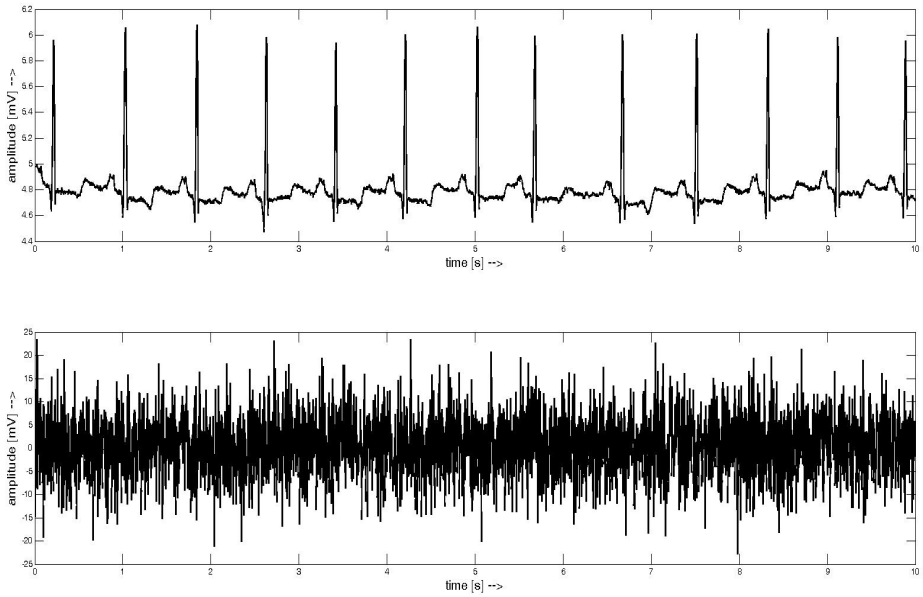

Figure 3.2: Example signals - upper is ECG signal, lower is uniformly distributed random noise.

Next both signals were mixed with randomly generated mixing matrix of size 2x2:

$$\mathbf{A} = \begin{pmatrix} 0.416494 & 0.374777 \\ 0.652350 & 0.885340 \end{pmatrix} \tag{3.21}$$

The mixing result is shown on (Figure 3.3). It is obvious that noise totally corrupted useful signal.

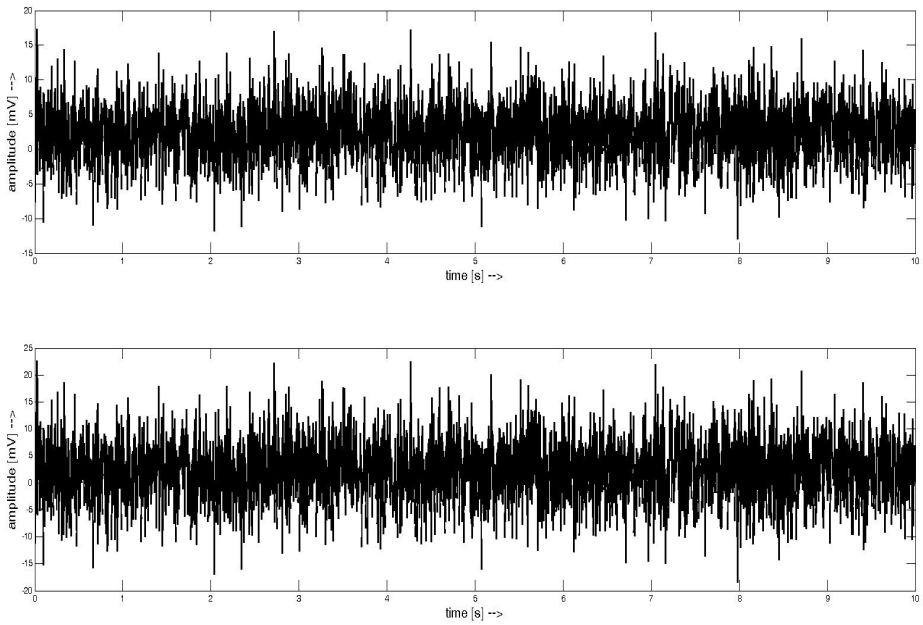

Figure 3.3: Mixture of signals from Figure 3.2. Noise corrupted signal completely. Both signals look similar, but they are different. If we look at the y-scale, we can observe the difference in amplitudes.

Figure 3.4 shows resulting signals computed using estimated de-mixing matrix (result of FastICA algorithm):

$$\widehat{\mathbf{W}} = \begin{pmatrix} -0.184404 & -0.002134 \\ 0.135876 & 0.002434 \end{pmatrix} \tag{3.22}$$

The ECG signal is separated from noise. Results in Figure 3.4 show two disadvantages of ICA. First - scale of resulting signal is the not same as of original data. Second - signal

is "inverted" by x axis. Both problems are caused because ICA cannot estimate energy of results. These problems are rather minor when compared with ICA usefulness. Simplest way to estimate separation quality one can compute multiplication of matrices $\mathbf{A}$ and $\widehat{\mathbf{W}}$ and than create ratio between diagonal and offdiagonal elements of resulting matrix. The resulting matrix should be identity matrix and the ratio should be 0, but any sufficiently small number still means good separation quality. The ratio number in our case is 0.000959, which is a good result.

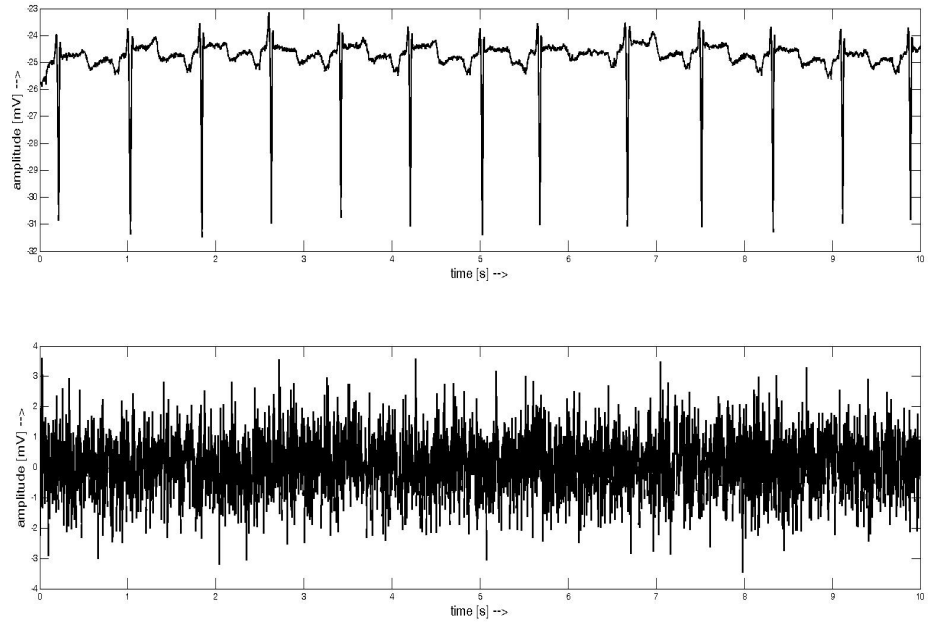

Figure 3.4: Result of ICA source separation.

3.4 Applications

This section covers wide variety of ICA application covering research areas such as EEG, ECG signal processing or more uncommon research areas such as fMRI or EGG signal processing. The section is divided in to several parts each dealing with one part of ICA biomedical applications.

3.4.1 ECG applications

At present only few ECG problems have been addressed. First problem, on which ICA was applied, was **artefact and noise removal**. Pioneer work of *Wisbec et al.*[13] in 1998 deployed Fast ICA algorithm for breath artefacts removal. It presents preliminary results. The ECG with artefacts were measured by a non-standard electrode system and the method was tested on 10 records. The results are interesting - breathing artefact has sub-Gaussian distribution and it was separated in one component.

In the same year *Barros et al.*[14] presented their work, where ICA was implemented using neural networks. ICA gradient based algorithm was adapted for neural network with self-adaptive step size calculation. Performance of the algorithm was measured on artificial data created using MIT-BIH noise stress database, which contains 3 types of noise. The data have been preprocessed by high pass filter. Resulting algorithm provides faster convergence than standard ICA algorithm because of neural network deployment. Researchers employed a measure for separation quality based on knowledge of mixing and demixing matrix.

After these two works other researchers provided their solutions of noise removal problem based on ICA [5, 15, 16, 17, 18, 19, 20, 21, 22, 23, 24, 25, 26]. From them we selected as the most interesting the following ones:

- *He et al.* [5] (2006) proposed an automatic method based on JADE algorithm. ECG records used in this study were measured from three electrodes. The noise removal technique for selection of noisy components is based on thresholding of kurtosis and variance of components. The presented algorithm deals only with low amplitude noises.

- *Chawla et al.* [15] (2008) deployed JADE algorithm on three channel ECG. No comparable results were reported and the method is vaguely described, so the reproducibility of research is limited. This work employed kurtosis and variance for detection of noisy component in the same way as He et al.[5].

- *Milanesi et al.* [17] (2008) deployed FastICA and its modification for motion artefact removal from holter recordings. They studied ICA for convolutive mixtures and constrained ICA. The study proposes two measures of noise elimination - error estimate and correlation coefficients. It also employed statistical analysis of results obtained on data from 9 patients, which are over 5 minutes long.

- *Chawla* [20] (2011) presents and summarizes his latest work. This article contains approach for noise removal presented by Milanesi et al. [17] and combines it with author's own PCA-ICA method. His technique is tested on CSE database [27].

- *Acharyya et al.* [22] (2010) deployed FastICA algorithm on MIT-BIH 3 channel ECG database in order to remove artefacts from electrocardiogram. They developed an algorithm for detection of component containing ECG based on Pearson correlation coefficient. This approach does not deal with signal reconstruction and noise reduction. The ECG morphology changes were not discussed.

- *DiPietroPaolo et al.* [23] (2006) used TDSEP [28] algorithm in magnetocardiography (MCG) analysis in order to reduce artefacts accompanying the MCG measurement. For detection of artifact-containing components three rules have been used. They are based on kurtosis, Pearson's correlation coefficient and power spectra computation. The authors used data from rest and exercise MCG.

- *Oster et al.* [25] (2009) applied JADE algorithm for detection of ECG in recordings done during magnetic resonance imaging (MRI). The data are strongly corrupted by MRI artefacts and the JADE algorithm in combination with wavelet transform is able to extract ECG from the measured signals.

Further ICA application area in ECG processing is **extraction of fetal ECG** (fECG) from records obtained by electrodes placed on mother body. *Lathauwer et al.* [29] presented his pioneer work in 1994. Here blind separation of fECG was based on 4th order cumulants. Researchers mathematically formulated problem of fECG estimation and presented an example of extracted signals. In 2000 *Lathauwer et al.* [30] continued their work, extended database of records and discussed applicability of ICA on twin fECG. *Cardoso* [31] worked on this problem in 1998 and showed usability of ICA in this problem. *Zaroso et al.* [32] (2001) presented their method based on Givens rotations and compared their method with method based on Adaptive Noise Canceller filter. For comparison they projected extracted sources from the component domain back to the signal domain showing contribution of different electrodes to fECG. In 2006 *Sameni et al.* [33] proposed their method based on JADE algorithm for fECG extraction. The work tries to interpret independent components and compares them with vector cardiogram. The researchers reported good separation quality. Another application of JADE algorithm for fECG arose in 2009 when *Lee et al.* [34] proposed their method for fetal magnetocardiogram (fMCG) extraction.

The automatic method selects components containing fMCG based on their kurtosis. In 2011 *Camargo-Olivares et al.* [35] presented their method based on multidimensional ICA (MICA) approach. In order to get better fECG separation results, they estimated maternal ECG and used it as another input to ICA method. In MICA algorithm different ICA algorithms were used (JADE, FastICA, πCA), but the results were considered as similar.

Another application is **extraction of atrial activity for atrial flutter analysis**. In 2000 *Rieta et al.* [36] applied ICA for QRST cancellation problem. They used synthetic and real data for evaluation of algorithm effectiveness. Data were preprocessed by notch and bandpass filter in order to remove noises before extracting atrial activity. Researchers compared their method with other two standard methods. Research uncovered that ICA based separation is better. In following years they extended their work and in 2003 presented FastICA application on extraction problem [37]. Finally in 2004 a summary paper [38] was released comparing different algorithms (FastICA, JADE, AMUSE). This paper also explains why ICA can be applied to this problem and introduced ordering of separated components based on kurtosis. Presented analysis was done on 7 recordings of different patients. *Castells et al.* [39] (2005) continued work of Rieta and they introduced two stage separation algorithm based on FastICA and SOBI. Their paper also introduces measures for estimation of separation quality - Root-Mean-Square error, correlation coefficients and degree of spectral content around main peak. Another work came from *Zaroso et al.* [40] (2008). Paper proposed RobustICA method in framework defined by Castells et al. [39]. *Chang et al.* (2010) extended the methodology proposed by Rieta and Castells [36, 37, 38, 39]. They used JADE and SOBI algorithm in order to extract sources containing atrial fibrillation and then used these sources for classification of atrial fibrillation. The method increased specificity of atrial fibrillation classification. In 2011 *Donoso et al.* [41] proposed method for atrial fibrilation extraction based on FastICA algorithm. They reported preliminary results on data from 4 subjects. In the same year (2011) *Taralunga et al.* [42, 43] applied JADE algorithm in combination with Event Synchronous Canceller (ESC) on data from St. Peterburg DB [7]. They proved that ESC enhanced the JADE algorithm ability for extraction of atrial activity.

Application of ICA in **ECG signal classification** is another biomedical research area with increasing number of research papers. The first papers proposed by *Yu et al.* [44, 45] in 2007 and 2008 presented an application of FastICA for beat classification combining independent components and RR interval as a feature vector for different classification systems. *Yu et al.* [46] proposed beat classification based on selection of independent com-

ponents obtained by FastICA or JADE algorithm. The classification itself is done by SVM [47] classifier on MIT/BIH Arrhythmia Database [48]. In 2011 *Wu et al.* [49] presented the SVM based classification of ECG using features extracted by FastICA algorithm. Finally in 2012 *Huang et al.* [50] proposed method for beat classification using ECG extracted features combined with features obtained from independent components computed by FastICA algorithm.

Newly emerging application of ICA is **ECG beat detection**. The very first research has been done by *Wiklund et al.* [51] in 2007. The researchers present beat detection method for smart clothing application. The first step of method is preprocessing of data done by FastICA algorithm. Next work proposed *Chawla et al.* [52] in 2008, who presented PCA-ICA R-peak detection algorithm using JADE for denoising and PCA for estimation of data segment. The paper discusses the method only. He continues his work and presented new results in 2011 in [6].

Previous papers represent main-stream research in ECG applications of ICA, but there are several other papers presenting **other applications**:

- *Vetter et al.* [53] (2000) presented application for measuring cardiac output based on ICA applied on RR and QT intervals.

- *Zhu et al.* [54] (2008) presented a method for separation of interesting waveforms into different components using 98 channel ECG data obtained from 6 subjects. The method reported several components containing waves of interest. Content of other components was not discussed.

- *Owis et al.* [55] (2002) applied convolutive ICA for classification of arrhythmias. Independent components serve as input for k-NN, Bayes and minimum distance classifiers. Data from MIT-BIH Arrhythmia database were cropped into 3 second segments.

- *Granegger et al.* [56, 57] (2009) used JADE algorithm in application with data collected on ICU patients during cardio pulmonary resuscitation (CPR). The work aims at CPR artefact removal in order to enhance work of automatic external defibrillator. The authors used algorithm based on kurtosis calculation.

- *Ostertag et al.* [58] (2011) proposed method for reconstructing ECG precordial leads using FastICA algorithm. They developed a patient specific transformation, which provides good results.

- *Monasterio et al.* [59] compare several BSS techniques and other separation techniques for multilead T-wave alternans detection. They conclude that BSS algorithms are not well suited for this type of task.

3.4.2 EEG applications

Electroencephalographic and magnetoencephalographic (EEG/MEG) signal processing using ICA was its first application in biomedical field. Many researchers use the same principles in their work and thus we will review only selected papers representing the fundamentals of EEG ICA applications.

The first application of ICA was **event related potential (ERP) detection and analysis**. The first works were published by *Makeig et al.* [60, 61] in 1996 and 1997. Researchers used InfoMax algorithm [62] for separation of EEG activities (alpha, theta) for detection of ERP. Experiments were performed on 10 recordings containing 30 minutes of EEG. Makeig's work was extended by *Jung et al.* [63, 64] (2000, 2001). Database used for ERP analysis contains 50 patient recordings and researchers used ERP image technique for evaluation of separated components. *Vigário et al.* [65] (2000) applied FastICA algorithm to EEG data for ERP and ocular artefacts detection and removal. This paper summed up their research and did not contain results. In 2003 *Richards* [66] used extended Infomax algorithm [62] for source localization from 128 lead EEG measurements. The algorithm was tested on 5 simulated datasets and the author concludes that ICA is better for source localization task than PCA. Two years later *Debener et al.* [67] (2005) used RUNICA algorithm within the EEGLab [68] framework in order to detect auditory ERP. The patients were split into two groups differing with strength and frequency of tones, which were played to them. The algorithm clustered components obtained from RUNICA into two groups corresponding to patients groups. In 2008 *Debener et al.* [69] used the Infomax algorithm for source localization in patient with cochlear implant during the auditory ERP trial. They showed that cochlear implant patient used the same sources for resolving auditory events as "normal" patients. *Liu et al.* [70] in 2011 presented comparison of several ICA algorithm for ERP detection in presence of noise. They conclude that SOBI algorithm outperforms all other ICA algorithms in solving ERP task. Finally *Chen et al.* [71] (2012) used Infomax for ERP extraction. The identification of independent components containing ERP is based on standard deviation computation.

Artefact removal in EEG by ICA was first reported by *Vigário* [72] in 1997. FastICA algorithm was applied on simulated and real children data preprocessed by bandpass

filter. Research reported separation of ocular artefacts and K-complexes in different components. Following first paper in this area several others appeared [73, 74, 75, 76, 77, 78, 79, 80, 81, 82, 83, 84, 85, 86, 87, 88, 89, 90]. We selected the most interesting ones:

- *Tang et al.* [73, 74] (2002) applied SOBI algorithm on 122 channel MEG data in source localization and artefact removal issues. The data from 4 patients were first preprocessed and then components were obtained. The papers explores possibilities of SOBI usage in MEG data processing.

- *Ossadtchi et al.* [75] (2002) used Infomax algorithm for preprocessing during epileptic spikes localization task. Components with artefact activity were discarded for next steps of the algorithm. The algorithm was tested on 4 patients and provides efficient way to deal with epileptic spikes detection.

- *Porée et al.* [76] (2006) used FastICA for hypnogram estimation from EEG, EOG and EMG data obtained from 14 patients. Researchers reported very good results in their study.

- *Hu et al.* [77] (2007) deployed FastICA algorithm for identification and removal of scalp reference signal in intracranial recordings of three patients. The method for selection of relevant components is fully automatic.

- *Joyce et al.* [78] (2004) proposed automatic method for EOG artefacts reduction in EEG data. They employed SOBI algorithm for independent components estimation.

- *McMenamin et al.* [79] (2011) validated approach of ICA applying for EMG artefact removal from EEG data. Infomax algorithm was used for estimation of independent components. Researchers concluded that ICA can deal with strong artefacts, but it could not be used as only one noise removal technique.

- *Le Van et al.* [82] (2006) deployed FastICA in combination with Bayess classifier for detection of epilepsy seizures. Researchers used wide variety of features computed on independent components in order to identify correct epileptic seizure components.

- *Cao et al.* [83] (2003) developed a new algorithm for high-level additive noise extraction from EEG signals. Researchers used variation of EASI algorithm [91], which works very efficiently with sub- and super-Gaussian distributions.

- *Milanesi et al.* [84] (2008) developed a modification of FastICA algorithm for dealing with convolutive mixtures. The key idea is that convolution changes into linear mixing in frequency domain and ICA could estimate sources as usually. The FastICA needs to be adapted for dealing with complex values. The paper show interesting result obtained by the application of algorithm to 9 EEG recordings.

- *Korhonen et al.* [86] (2011) used FastICA modification for large muscle artefacts removal from transcranial magnetic stimulation (TMS). The TMS artefacts have been completely removed by the applied algorithm.

- *Ma et al.* [87] (2011) used SOBI and Infomax algorithm for detection of EOG artefact using comparison of components with artefact pattern. The detection of components with EOG is based on Euclidian distance and it is patient and threshold dependent.

- *Cong et al.* [90] (2010) employed FastICA modification for de-noising of EEG. The key idea of modification lies in re-computation of de-mixing matrix after each learning step according to filtering of components. The final de-mixing matrix is then de-mixing and denoising matrix. Proposed method was tested on 102 patients.

Preceding two research areas represent a main stream research in EEG ICA applications. Following papers represent the **other** published works dealing with EEG using ICA in other than previous applications:

- *Zhukov et al.* [92] (2000) proposed a method for multiple source localization based on ICA. They used simulated 32 channels data for validation of the approach. Results proved that ICA is able to extract extra information from the data.

- *Tang et al.* [93] (2005) applied SOBI algorithm on 128 channel EEG in order to test its abilities on high-density EEG. The paper concludes that SOBI algorithm could be used in several applications such as noise reduction, neuronal sources extraction, SNR improvement in somatosenzory evoked potentials or for source activity localization.

- *Cichocki et al.* [94] (2005) used AMUSE algorithm for detection of early stages of Alzheimer's disease.

- *Swan et al.* [95] (2011) used Infomax algorithm for blink artefact removal during Deep Brain Stimulation of the subthalamic nucleus within the Parkinson's disease patients.

- *De Lucia et al.* [96] (2008) deployed FastICA algorithm for epileptic spikes detection. The researchers used independent component domain features for classification task using Bayess classifier.
- *Selvam et al.* [97] (2011) used Wavelet-ICA algorithm (Wavelet transform + SOBI algorithm) for detection of brain tumors from 19 lead EEG. Again researchers used features computed on independent components for classification using multilayer feed forward neural network.

3.4.3 Other biomedical applications

This part deals with minor biomedical research areas, in which has been BSS/ICA methods used.

3.4.3.1 EMG applications

Electromyography (EMG) is another research area, where ICA has been successfully deployed. There are several papers describing research efforts in processing EMG using ICA:

- *Costa Jr. et al.* [98] (2010) employed FastICA algorithm in order to remove ECG artefact from EMG recording of lumbar muscles. He reported two approaches - one failed in separation of ECG and EMG and second based on using time-delayed signals was successful in separating activities.
- *Mak et al.* [99] (2010) used also FastICA algorithm for removal of ECG from trunk muscle surface EMG. Researchers tested their approach on simulated data and reported good separation results.
- *Ahsan et al.* [100] (2010) reviewed the applications of ICA in EMG signal processing in context of improvement of quality of live for elderly people.
- *Ren et al.* [101] (2010) deployed ICA for extraction of motor units activities within the EMG recording.
- *Farina et al.* [102, 103] (2004,2008) applied SOBI algorithm for separation of two muscle activities during the force-varying task.
- *Subasi et al.* [104] (2010) used FastICA algorithm for dimension reduction during the detection of muscle fatigue task. Artificial neural network was deployed for classification task and ICA served as preprocessing step.

- *Willigenburg et al.* [105] (2012) deployed FastICA for ECG removal from EMG recordings. Researchers compared ICA technique to high-pass filtering and adaptive filtering and concluded that ICA performs better in several cases. The performance of ICA algorithm strongly depended on type of data.

3.4.3.2 fMRI and other medical image processing applications

Another application fields of ICA are functional Magnetic Resonance Imaging (fMRI) and Magnetic Resonance Spectroscopy (MRS). In last decade there were several papers published in this field:

- *McKeown et al.* [106, 107] (1998) first used ICA in fMRI application. Researchers used Infomax and JADE algorithms for detection of region of interest in fMRI images. ICA increased accuracy of separation and localization of sources.
- *Calhoun et al.* [108] (2003) published review paper comparing performances of JADE, FastICA and Infomax algorithms. Researchers used their own data for the evaluation of the ICA algorithms. The comparison criteria was based on Kullback-Leibler divergence [109].
- *Pulkkinen et al.* [110] (2005) published a work about application of FastICA algorithm on MRS data. FastICA was used for tumour detection.
- *Debener et al.* [111] (2006) written an overview of methods for analysis of simultaneously recorded EEG and fMRI. Researchers mentioned ICA as one method for separation of non-brain signals from EEG during the trial.
- *Wang et al.* [112] (2012) presented Fast-FENICA algorithm for detection of functional networks in fMRI data. ICA increased the detection rate.
- *Rodriguez et al.* [113] (2012) used Infomax algorithm for denoising fMRI data. The approach was tested on 16 patient and the noise reduction was increased.
- *Zhang et al.* [114] (2012) employed Infomax and ICASSC (modification of FastICA) algorithms in fMRI stop signal task. BSS/ICA increased ability to localize cognitive centres within the brain in all 59 patients.
- *Lei et al.* [115] (2011) used FastICA algorithm for blink removal in EEG and region detection in fMRI during the analysis of EEG-fMRI analysis of subcortical regions of brain.

- *Kim et al.* [116] (2011) employed FastICA for detection of regions during fMRI semantic decision task. Research reported increased number of regions detected.
- *Moeller et al.* [117] compared ICA with General Linear Model analysis in application within EEG-fMRI recordings. Both methods have similar results.

3.4.3.3 Abdominal phonograms application

In year 2009 *Jiménez-González et al.* [118] initialized research of abdominal foetal phonograms using Single-channel Independent Component Analysis (SCICA) which combines ICA algorithm TDSEP with back projection of components in order to obtain information from a single channel recording. Research was extended and the deeper analysis of resulting components [119, 120].

3.4.3.4 EGG applications

Another minor application field of ICA is EGG signal processing. There have been several papers published in this research area:

- *Wang et al.* [121] (1997) applied neural network implementation of FastICA for detection of EGG activity within the recording contaminated by respiratory, motion and ECG artefacts.
- *Peng et al.* [122] (2007) compared FastICA with ICA with reference algorithm for extraction of slow gastric wave. Both methods increased the probability of correct extraction of gastric wave.
- *Mika et al.* [123] used FastICA algorithm for extraction of normogastric rhythm from the EGG measurement.

3.4.3.5 Measuring HR and temperature from video

Finally ICA is used for analysis of video sequences in order to estimate heart rate (HR) by *Poh et al.* [124] in 2010. ICA was able to extract enough information from RGB video images of face to estimate the HR correctly. Another paper from this interesting research area comes from *Tsouri et al.* [125] (2012). ICA was able to extract pulse rate from video using constrained ICA.

Chapter 4

Electrocardiography and signal processing

Although the main focus of the thesis is on ICA application to ECG signals, we also need to describe briefly the heart and its function. This chapter is written for this purpose - it summarizes basic facts about heart anatomy, its function and the basics of ECG measurement and showing the most common lead system used in electrocardiography. All figures used in this section are from [126], which provides every picture freely available for any use.

4.1 Anatomy and function of human heart

The heart (Fig. 4.1) is an organ, which pumps oxygenated blood throughout the body to important organs and deoxygenated blood to lungs. It can be understood as two separate pumps - one pump (left) pumps the blood to peripheral organs, and second pump (right) pumps the blood to lungs.

Left and right sides of the heart consist of two chambers - an atrium and a ventricle. For controlling of the blood flow there exist four valves - tricuspid, pulmonary, mitral and aortic. The mitral valve separates left atrium and ventricle and the tricuspid valve separates right atrium and ventricle. Pulmonary valve control the blood flow from heart to lungs and the aortic valve directs blood to the body circulation system.

Walls of the heart are formed by cardiac muscle (myocardium). This muscle is responsible for the mechanical work done by the heart (= pumping the blood). For controlling the pumping process specialized muscle cells that conduct electrical impulses evolved. These

impulses are called action potential and they are responsible for forming the ECG waveform on the body surface.

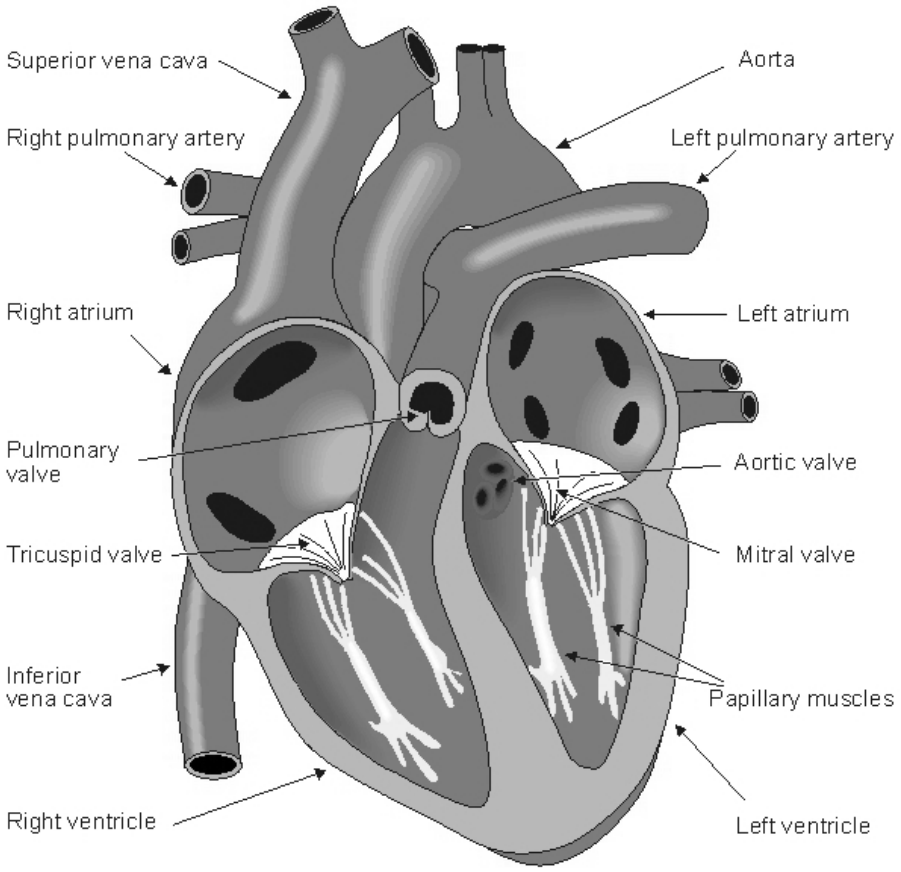

Figure 4.1: Basic heart anatomy schema - there are four chambers, two on the left (right heart) side responsible for pumping the blood to lungs and two on the right (left heart) responsible for pumping the blood to body. Picture used with permission from [126].

In order to distribute oxygen to whole body human heart never stops. It works in periodic cycles. A cycle works as follows: Deoxygenated blood flows through supererior vena cava to the right atrium. When the atrium is contracted, blood is pumped to the right ventricle. From the right ventricle the blood flows through pulmonary artery to the lungs. Lungs remove carbon dioxide from blood cells and replace it with oxygen. Oxygenated blood returns to the left atrium and after another contraction it is pumped to the left ventricle. Finally the blood is forced out of the heart through aorta to the systemic circulation. The contraction period is called systole, during which the heart fills with blood. The relaxation period is called diastole. From electrical point of view the cycle has two stages - depolarization (activation) and repolarization (recovery).

4.2 The conduction system of the heart

To maintain the cardiac cycle the heart developed a special cell system for generating electrical impulses and by these impulses mechanical contraction of the heart muscle is ensured. This system is called conduction system (Fig. 4.2). It conveys impulses rapidly through the heart. Normal rhythmical impulse, which is responsible for contractions, is generated in the sinoatrial (SA) node. Then, propagates to the right and left atrium and to the atrioventricular node (AV). The impulse is delayed in the AV node in order to allow proper contraction of the atria. Thus all blood volume in the atria is forced out to the ventricles before its contraction. Atrium and ventricles are electrically connected by bundle of His. From here, the impulse is conducted to the right and left ventricle. The pathway to the ventricles is divided to the left bundle branch and right bundle branch. Further, the bundles ramify into the Purkinje fibers that diverge to the inner sides of the ventricular walls.

The primary pacemaker of the heart is the sinoatrial node. However, other specialized cells in the heart (AV node, etc.) can also generate impulses but with lower frequency. If the connection from the atria to the atrioventricular node is broken, the AV node is considered as the main pacemaker. If the conduction system fails at the bundle of His, the ventricles will beat at the rate determined by their own region. All cardiac cell types have also different waveform of their action potentials (Fig. 4.3).

4.3 Generation and recording of ECG

Human body is a good electrical conductor, hence electrical activity of the heart can be measured using surface electrodes. Electrodes record the projection of summary resultant vector, which describes the main direction of electrical impulses in the heart. The projection is named electrocardiogram. Different placement of electrodes provides spatio-temporal variations of the cardiac electrical field. The difference between a pair of electrodes is referred to as a lead. A large amount of possible lead systems has been invented; depending on a diagnostic purpose, a lead system is chosen and electrodes placed on accurate position. The most commonly used system is standard 12-lead ECG system defined by Einthoven [127]:

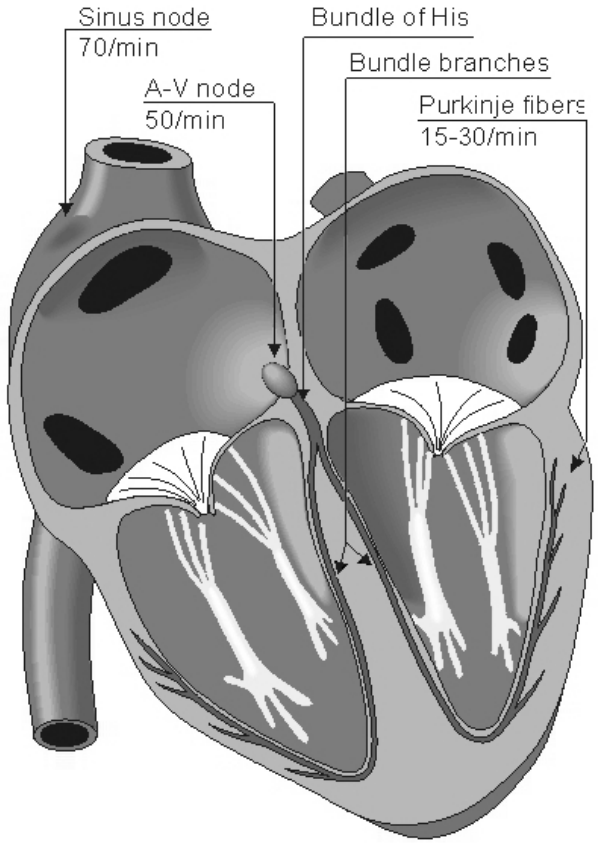

Figure 4.2: Conduction system of the heart consists of Sinus node, Atrioventricular node, Bundle of His, bundle branches and Purkinje fibers. Picture used with permission from [126].

- Three bipolar limb leads (I, II, III) - electrodes are placed to the triangle (left arm, right arm and left leg) with heart in the center (Fig. 4.4). This placement is called the Eithoven's triangle.
- The augmented unipolar limb leads (aVF, aVL, aVF) - electrodes are placed on same positions as in case of leads I, II and III. The difference is in the definition of leads. Leads are calculated as the difference between potential of one edge of the triangle and the average of remaining two electrodes (Fig. 4.5).
- Unipolar precordinal leads (V1-6) - leads are defined as the difference between potential of electrode on chest and central Wilson terminal (constant during cardiac cycle and is computed as average of limb leads). For details see Fig. 4.6.

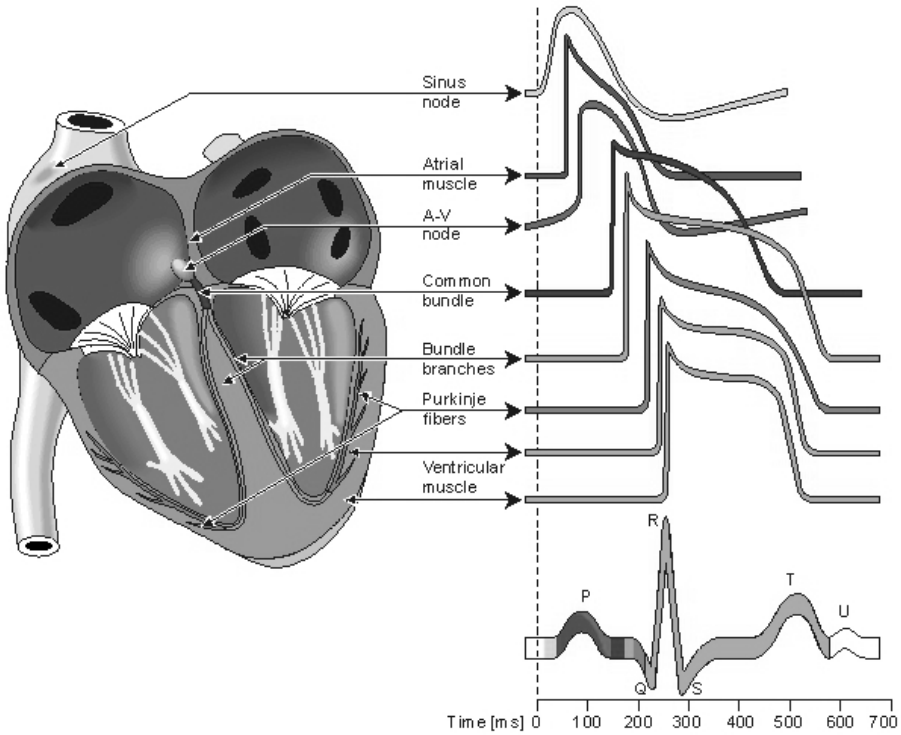

Figure 4.3: Schematic representation of ECG waveform generation by summing of different action potentials. Picture used with permission from [126].

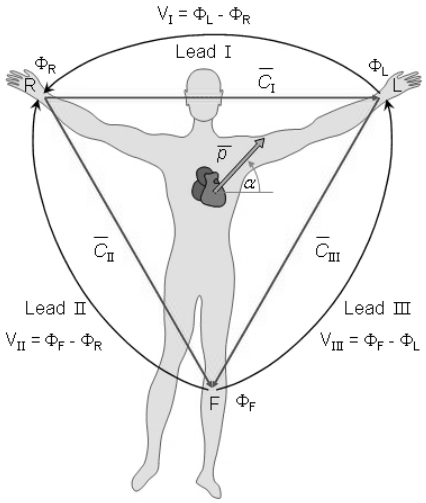

Figure 4.4: Schematic representation of Einthoven triangle electrode placement. Picture used with permission from [126].

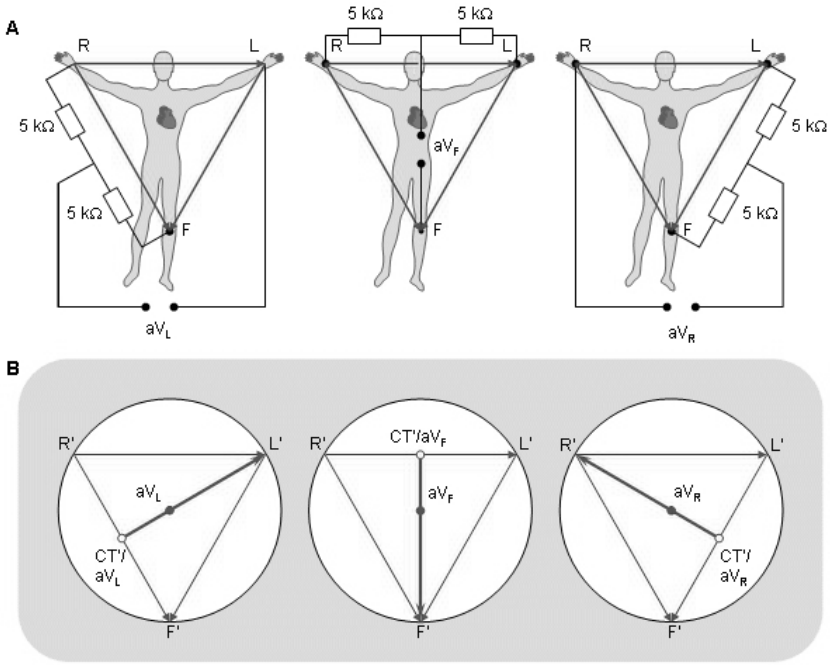

Figure 4.5: Schematic representation of augmented limb leads calculation. Picture used with permission from [126].

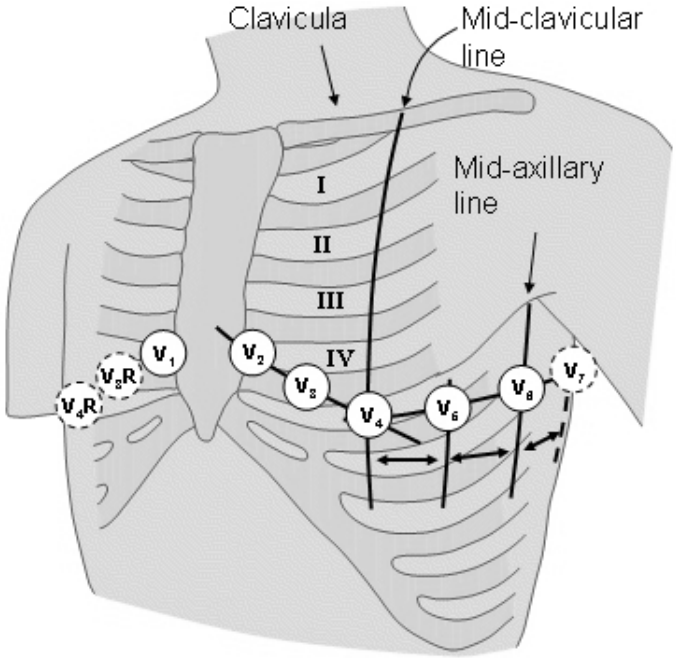

Figure 4.6: Precordial leads electrodes positions. Picture used with permission from [126].

4.3.1 ECG wave form description

As we mentioned earlier ECG wave is formed as a projection of summarized potential vector of the heart. ECG wave has several peaks and "formations", which is useful for its diagnosis (Fig. 4.7). These are:

- P wave - Represents the wave of depolarization that spreads from the SA node throughout the atria, and is usually 0.08 to 0.1 seconds (80-100 ms) length.
- PR interval - Reflects the time the electrical impulse takes to travel from the sinus node through the AV node and entering the ventricles. Usually 120 to 200 ms long.
- PR segment - Corresponds to the time between the end of atrial depolarization to the onset of ventricular depolarization. Last about 100 ms.
- QRS complex - Represents ventricular depolarization. The duration of the QRS complex is normally 0.06 to 0.1 seconds.
- Q wave - Represents the normal left-to-right depolarisation of the interventricular septum.
- R wave - Represents early depolarization of the ventricles.
- S wave - Represents late depolarization of the ventricles.
- S-T segment - Following the QRS is the time at which the entire ventricle is depolarized and roughly corresponds to the plateau phase of the ventricular action potential.
- Q-T interval - Represents the time for both ventricular depolarization and repolarization to occur, and therefore roughly estimates the duration of an average ventricular action potential. This interval can range from 0.2 to 0.4 seconds depending upon heart rate.
- T wave - Represents ventricular repolarization and is longer in duration than depolarization.

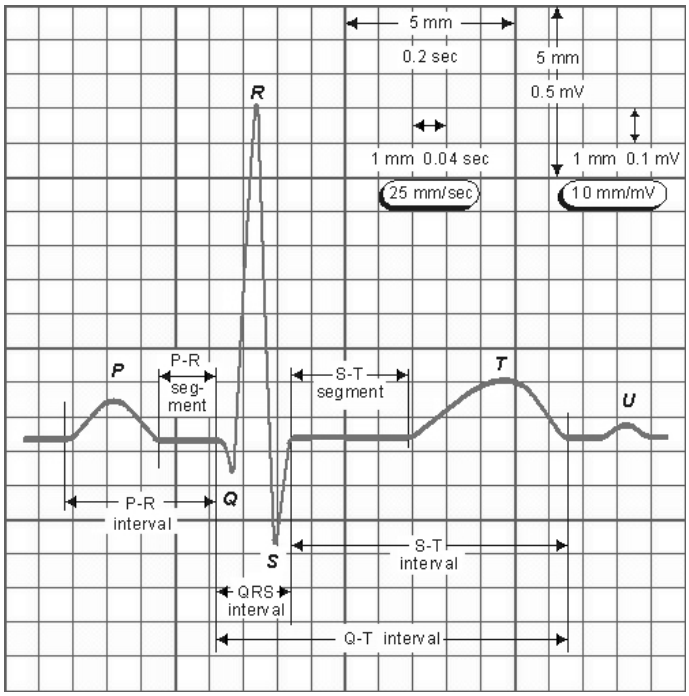

Figure 4.7: Normal ECG waveform. Picture used with permission from [126].

Chapter 5

Independent Component Analysis for ECG de-noising: proposed method

5.1 Introduction

During recording of ECG the recorded signal is disturbed with interferences coming from both technical and biological sources, thus the very first step of any ECG analysis is noise reduction. Any noise reduction technique must be very accurate in order to preserve as much information in data as possible. At present many ECG applications are connected with holter measurement and telemedicine applications. In these cases various types of uncommon noise disturb the useful signal. Many techniques are used for noise reduction in ECG - current most used techniques are traditional filtering (basic digital filters, adaptive filters) and wavelet filtering. As we presented in Chapter 3 there are still many problems in current algorithms, which result in imperfect noise reduction or distortion of useful signal. These facts led us to the idea of a new algorithm proposal satisfying our requirements on de-noising.

We developed an algorithm for solving the problem of electrode cable movement (ECM) artefact, which appears during ECG measuring with a holter device. This artefact mimics normal ECG activity in frequency domain (Fig. 5.1) thus standard filtering cannot be used because it also removes ECG. Our method deploys the JADE algorithm, which is a well-known BSS algorithm based on joint diagonalization of cumulant matrices. The JADE is able to separate ECM artefact from ECG activity in component domain. Combination of JADE and basic classifier for noise component detection provides us with framework capable to deal with ECM artefact.

The work described here is based on several other authors publications [128, 129] and it is available at `http://bio.felk.cvut.cz/~kuziljak/`.

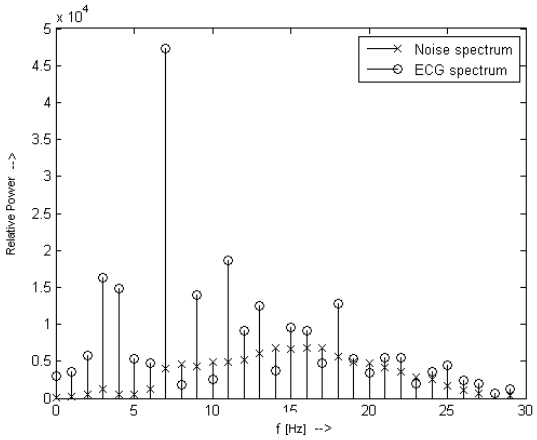

Figure 5.1: Power spectra of noise signal and ECG data. Both spectra are overlapping and noise is mimicking normal ECG signal.

5.2 Proposed Algorithm

As we said before the main concept of our algorithm lies in performing JADE separation algorithm on ECG signal containing noise. The resulting components can be divided into two groups - components containing mostly noise and components containing mostly ECG activity. Because of well-known permutation indeterminacy of ICA the order of components is random and thus one needs to develop a detection algorithm for identification of noise components. The algorithm work-flow is shown in Algorithm 1. Next we will describe each important step of the algorithm.

Algorithm 1 De-noising algorithm

Input: ECG signal

1: Pre-process (subtract mean of signals)
2: Estimate components using JADE
3: Compute features
4: Detect noisy components using CART
5: Set noisy components to zero
6: Transform components back to signal domain
7: Post-process

Output: Filtered ECG signal

5.2.1 Preprocessing and component estimation

Very first step of the algorithm contains mean subtraction. Next independent components are estimated using JADE algorithm. The algorithm is based on joint diagonalization of fourth order cross-cumulant tensor and is explained in the section 3.2.3.

5.2.2 Feature computation

In order to detect noise containing components the algorithm computes set of features for each component. These features are chosen based on prior knowledge of data. The selected feature set contains these features:

- Mean of component samples – mean is defined as:

$$\overline{x} = \frac{1}{N}\sum_{i=0}^{N-1} x_i, \tag{5.1}$$

  where x_i is the i-th sample selected from component x with length N.

- Variance of component samples – unbiased estimate of variance is defined as:

$$var(x) = \frac{1}{N-1}\sum_{i=0}^{N-1}(x_i - \overline{x})^2. \tag{5.2}$$

- Kurtosis of component samples – kurtosis is normalized version of fourth-order moment:

$$kurt(x) = E\{x^4\} - 3(E\{x^2\})^2, \tag{5.3}$$

  where $E\{\}$ is the expectation of component x. Kurtosis has been chosen because it was shown that ECG has super-Gaussian distribution [5, 6, 4].

- Correlation coefficient of component with 50 Hz sinus wave and p-value of hypothesis of no correlation. Pearson correlation coefficient is defined as [130]:

$$\rho_{x,y} = corr(x,y) = \frac{cov(x,y)}{\sigma_x \sigma_y} = \frac{E\{(x-\overline{x})(y-\overline{y})\}}{\sigma_x \sigma_y}, \tag{5.4}$$

  where $cov(x,y)$ is covariance of signal x and y and σ_x,σ_y are their standard deviations defined as:

$$\sigma_x = \sqrt{var(x)}. \tag{5.5}$$

P-value for hypothesis of no correlation between signals is estimated using t value [130]:

$$t = \frac{r}{s_r}, \tag{5.6}$$

where r is correlation coefficient and s_r is standard error of correlation coefficient: $s_r = \sqrt{\frac{1-r^2}{n-2}}$.

- Standard deviation of peak-to-peak distances and number of detected peaks – this feature is used, because ECG has periodical rhythm with dominant R peaks, thus we can asume that ECG component standard deviation is smaller than standard deviation of noisy component deviation, which has no dominant peaks by its nature. Peaks were detected using Pan-Tomkins detection algorithm (see section 7.3.1.2). For the same reason the number of peaks detected in the recording normalized by the length of recording were used.

5.2.3 Noise component detection using CART algorithm

Features discussed in previous section are then classified using a classification tree, which has been learned with CART algorithm using Gini's impurity index [131] using annotated components data obtained by application of JADE to recordings from MIT/BIH Arrhythmia Database. The algorithm constructs a binary tree by splitting data into left and right node using maximalization of decrease of impurity defined as:

$$id(t) = i(t) - p_L i(t_L) - p_R i(t_R), \tag{5.7}$$

where $i(t) = \sum_{j=1}^{J} p(j|t)(1 - p(j|t)) = 1 - \sum_{j=1}^{J} p^2(j|t)$ with $j = 1, 2, ..., J$ and J is the number of items in the training set, $p_L(p_R)$ is the proportions of data in left (right) node. Gini's impurity index is the measure how often a randomly chosen element from the set would be incorrectly labelled if it were randomly labelled with one label in the set according to the distribution of the labels in the set. It reaches zero when all cases fall into one category.

After constructing the CART tree we deployed 10-fold cross-validation in order to estimate best level for tree pruning. The error from cross-validation is shown on Fig. 5.2 with selected number of nodes. Pruning is performed as removal of n lover levels of binary tree according to selected level from cross-validation. Resulting tree is shown on Fig.5.3.

We can see, that only two features were selected for classification of components, namely kurtosis and standard deviation of RR intervals.

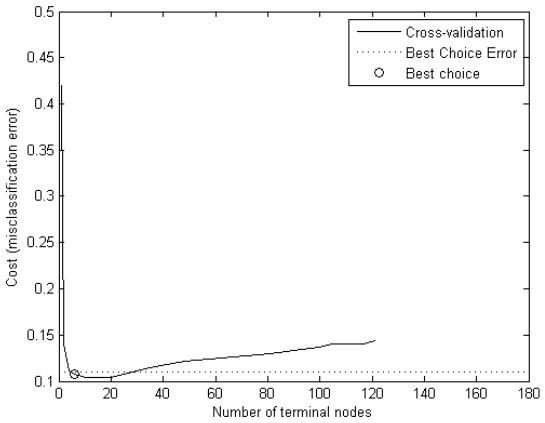

Figure 5.2: Result of 10-fold cross-validation used for estimation of tree pruning level. The best choice is selected by error and number of terminal nodes.

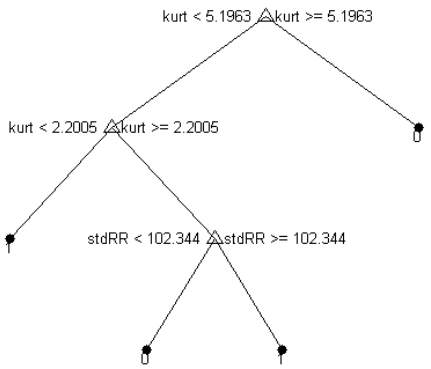

Figure 5.3: Resulting binary classification tree for noise component detection. (0 – ECG component, 1 – Noise component)

5.2.4 Removing noisy components and backward transform

Components identified as noise containing are removed by setting their values to zero. This leads to removal of these components from all ECG signals in signal domain after backward transform. Zeroing can be performed also as zeroing corresponding column in

mixing matrix. This leads to the same result. The backward transform is performed by multiplying components with the mixing matrix, which is computed as inverse to the de-mixing matrix.

5.2.5 Postprocessing

After removal of components containing noise and transforming them back to the signal domain the high frequency noise sometimes appears. Therefore the final step contains the low pass filter with first zero at 117 Hz, delay 5 samples and gain 0.93. Filter frequency response is shown on Fig. 5.4.

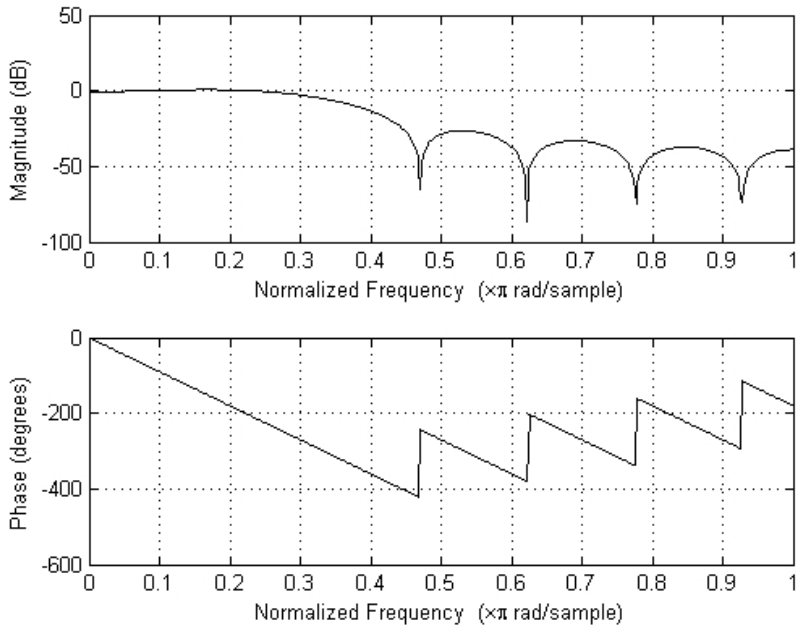

Figure 5.4: Frequency response of postprocessing low pass filter

5.3 Algorithm summary

The algorithm works with signal in predetermined way. First the mean value is subtracted from the data, then independent components using JADE algorithm are estimated. After estimation of components the algorithm points out those containing noise corrupting the ECG using decision tree and finally the components with noise are set to zero. After zeroing data are projected back into signal domain and smoothing filter is applied.

Our method is efficient to deal with electrode cable movement artefact, for which it has been developed, but its performance is good in presence of other noises. Its main disadvantage is wrong estimation of independent components, which could lead to reduction of useful signal. This problem could be solved by applying different BSS/ICA algorithm.

Experiments with developed algorithm are described in Chapter 7 and the results are presented in Chapter 8.

Chapter 6

Independent Component Analysis for ECG beat detection enhancing: proposed method

6.1 Introduction

Beat detection is the most fundamental task in electrocardiography, the positions of QRS or ventricular beats serve as a basis for further analysis of electrocardiogram (ECG). It is for example the most crucial task in heart rate variability (HRV) analysis, which analyses RR interval changes during long periods of time in order to detect heart disorders. The necessity of correct detection arises with each application of QRS detection algorithms. Many researchers proposed large variety of methods for solving this task, eg.[132, 133, 134, 135, 6]. The most commonly used in the real world applications are Pan-Tompkins QRS detection algorithm [134] and its modification introduced by Hamilton and Tompkins [136] or Christov's beat detection algorithm [135].

Pan-Tompkins and its modification Hamilton-Tompkins algorithms are based on patient-specific detection threshold. The algorithms work on single lead ECG, which is modified by set of preprocessing digital filters in order to enhance positions of QRS complexes.

More recently, Christov released his beat detection algorithm, which is based on combined adaptive threshold and transformation of multidimensional ECG signal in to single complex lead data. The complex lead transformation is more robust in presence of noise corrupting useful ECG and the algorithm is more stable.

In many applications strong artefacts from biological or technical sources could appear

and cause distortion of ECG signals. Many algorithms for beat detection perform much worse in that case. Christov's detection algorithm deals with noise that accompanies the ECG by transforming the ECG signal to signal called complex lead, which enhances position of QRS complex and reduces effect of common artefacts presented in ECG. But this algorithm has its limits, too. We try to improve its performance by transforming ECG signal to components using Independent Component Analysis (ICA).

In our study we used JADE [3], which is from the family of joint diagonalization based ICA algorithms. It works with fourth order cross-cummulant tensor in order to obtain best solution for BSS problem.

The offline algorithm successfully combines ICA method JADE with Christov's beat detection algorithm creating a signal called complex component, on which beats were detected using combined adaptive threshold. The transformation to complex component is similar to transformation to the complex lead, but it introduces one more step - independent components estimation and selection of ECG activity. Thus the algorithm works properly in presence of strong artefacts and noises.

This algorithm has been published in [137] and all source codes are available at `http://bio.felk.cvut.cz/~kuziljak/`.

6.2 Christov's beat detection algorithm

The Christov's beat detection algorithm has been developed in 2004 for purpose of beat detection in multidimensional ECG. It combines information from every available ECG signal (originally from orthogonal lead system X-Y-Z) in recording creating so-called complex lead, which is used for detection of beat positions. This algorithm contains several processing steps as it is shown on work-flow chart in Fig. 6.1. In the next subsection we will describe each step in detail and at the end we will summarize the algorithm and its efficiency.

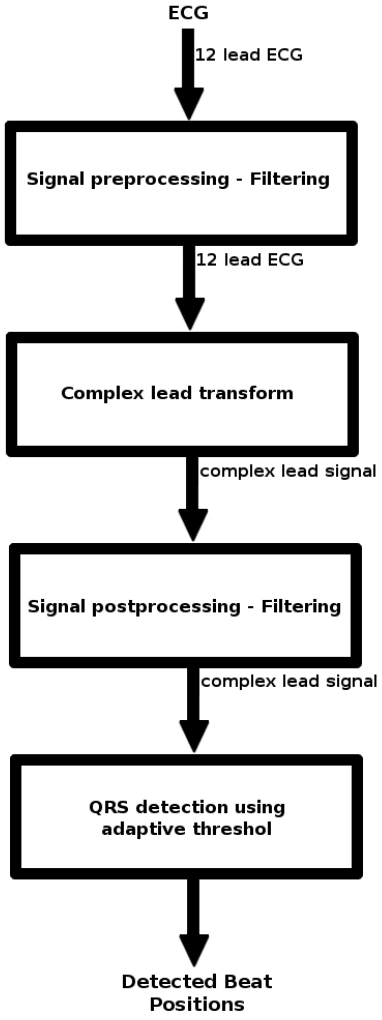

Figure 6.1: Christov's beat detection algorithm work-flow

6.2.1 Signal preprocessing

At the very first beginning ECG signals are processed by set of moving average (MA) filters in order to remove power line interference and electromyographic noise:

- Power line interference moving average filter has first zero on frequency of power grid (for EU is 50 Hz).

- Electromyographic moving average filter average over 28 ms interval of ECG signal, which means that the first zero of the filter is around 35 Hz.

We implemented both filters using recursive moving average defined by equation:

$$y[n] = \frac{x[n]}{N} - \frac{x[n-N]}{N} + y[n-1], \tag{6.1}$$

where y is the output signal, x is the input signal, n is the signal sample index and N is the filter order. The main advantage of recursive filter is its smaller impulse response and faster computation. On the other hand it could be unstable because it is an IIR filter. The order of filter N can be computed using: $N = \frac{f_s}{f_n}$, where f_s is sampling frequency and f_n is frequency of noise. The frequency response of filter is shown on Fig. 6.2 for f_s=500 Hz and f_n=50 Hz.

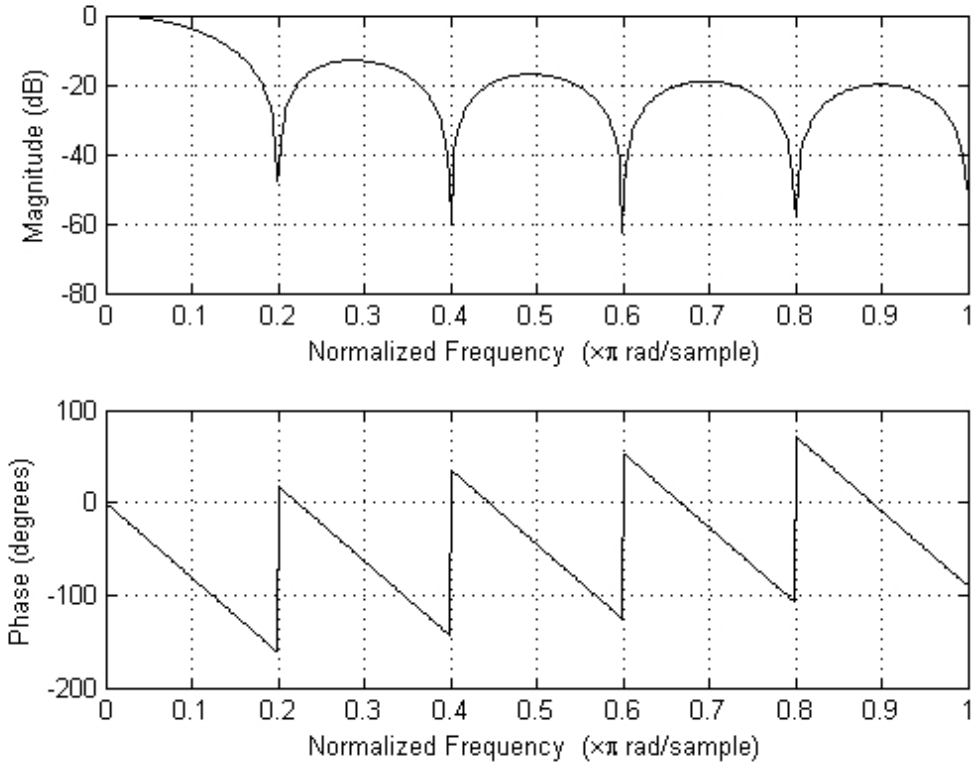

Figure 6.2: Frequency response of recursive MA filter with first zero at 50 Hz for f_s=500 Hz.

6.2.2 Complex lead transform and post-processing filtration

The Christov's beat detection algorithm is based on complex lead transform, which is defined as follows:

$$X[n] = \frac{1}{L}\sum_{j=1}^{L} |x_j(n+1) - x_j(n-1)|, \tag{6.2}$$

where $X[n]$ is n^{th} sample of signal calculated by complex lead transform, L is number of measured ECG leads, $x_j(n)$ is n^{th} sample from j^{th} lead. The transform can be seen as average difference calculated from all leads. Example of calculated complex lead is shown in Fig. 6.3.

After complex lead transform the signal is filtered with MA filter with first zero around 25 Hz in order to suppress noise created by differentiation procedure in complex lead transform. We again used the recursive MA implementation defined by Eq. 6.1.

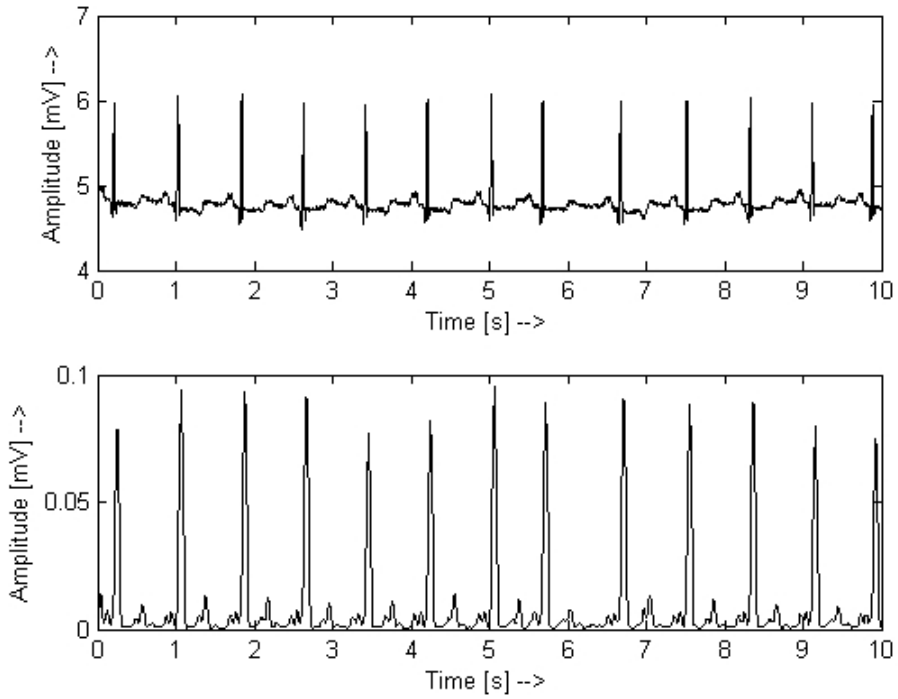

Figure 6.3: Complex Lead (down) estimated from ECG (top)

6.2.3 Combined adaptive threshold for beat detection

After the calculation of complex lead Christov employed combined adaptive threshold **MFR** (see Fig. 6.4 for example) to find peaks, which correspond to beat positions. The combined adaptive threshold is calculated as sum of three thresholds:

- Threshold **M** (adaptive steep-slope threshold) - reflects the amplitude of currently detected beats
- Threshold **F** (adaptive integrating threshold) - reflects the presence of high frequency noise in data and increases the combined threshold in that case
- Threshold **R** (adaptive beat expectation threshold) - intended to deal with heartbeats of normal amplitude followed by beats with very small amplitude

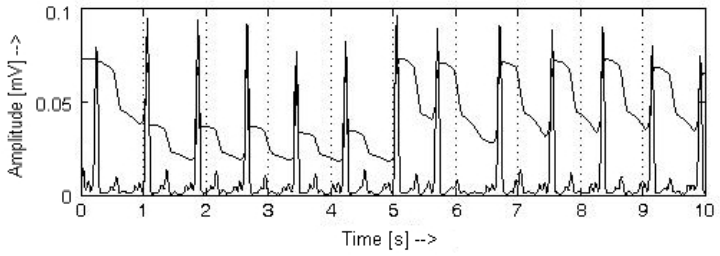

Figure 6.4: Complex Lead with combined adaptive threshold **MFR**

6.2.4 Algorithm summary

The algorithm can work in two modes, namely real-time and pseudo-real-time, which performs back search in case of no detection for long time. The algorithm is then pushed back to last detected beat and starts search with lowered combined adaptive threshold.

Christov's algorithm is robust against the presence of common noises (base line wander, grid noise, EMG, etc.), because of MA filters used in preprocessing step of the algorithm. On the other hand its performance in presence of non-standard noises is not sufficient. The algorithm time performance is strongly affected by back search procedure and our implementation in MATLAB needs around 6.4 seconds for 30 minutes 2-lead ECG to process it.

6.3 Proposed algorithm

The main idea, which lies behind our proposed algorithm is the question - can we enhance ECG activity before ECG is transformed into complex lead? The algorithm, which enhances the activity, should have extracted ECG from unknown mixture of ECG and other signals (power line interference, breathing, etc.) and passed this extracted sources into the complex lead transform.

The problem formulation contains the answer: use method for solving BSS such as ICA to enhance ECG activity. The algorithm is then easily derived from preceeding one – instead of using the ECG use selected components obtained by JADE algorithm and these components transform into complex component (similar to complex lead). JADE preserves overall spatial distribution of ECG activity and separates it from other activities. The algorithm work flowchart is shown in Algorithm 2. At first the algorithm looks the same as original Christov's algorithm, however our change is hidden in the method for estimation of complex lead - it is replaced with method for estimation of complex component.

Algorithm 2 QRS detection algorithm

Input: ECG signal
1: Estimate **complex component** (see Alg. 3)
2: Initialize thresholds (**M**, **F**, **R**) and their buffers
3: **for** all samples of complex component **do**
4: Update weights (**M**, **F**, **R**)
5: **if** current sample $>$ (**M** + **F** + **R**) (beat detected) **then**
6: Update thresholds buffers and thresholds
7: Store detected beat position
8: **else if** beat is not detected for longer than twice average RR interval **then**
9: Start detection again from last detected beat with lowered threshold
10: **end if**
11: **end for**
Output: Beat positions

6.3.1 Complex component transform

Complex component transform is our modification of complex lead transform described in Christov's original paper. The preprocessing using recursive MA filters remains the same. The change lies in adding one more step between preprocessing and complex lead transform – the component estimation step.

As we mentioned above the algorithm used for component estimation is JADE. This algorithm is fully described in Section 3.2.3. Here we will use only basic notation for ICA formulation:

$$\mathbf{S} = \mathbf{W}\mathbf{X}, \tag{6.3}$$

where $\mathbf{S}$ are estimated components, $\mathbf{W}$ is demixing matrix and $\mathbf{X}$ are originally measured ECG signals containing ECG and noise. After the components estimation we need to identify components containing ECG and noise. Because JADE is data driven transformation, we never know, in which order and with which scale we obtain the estimated components. In order to make the algorithm fully automatic, one needs to create a robust decision system for detection of ECG activity.

Our decision algorithm is based on the observation that ECG has super-Gaussian distribution [5, 6, 4], thus the values of its kurtosis are larger than kurtosis values of other presented signals (e. g., EMG is nearly Gaussian with kurtosis close to zero). Kurtosis is defined as:

$$kurt(s) = E\{s^4\} - 3(E\{s^2\})^2, \tag{6.4}$$

where $E\{\}$ is the expectation and s is one of estimated components. Now we need to identify ECG components in $\mathbf{S}$. Because JADE is data driven algorithm, we need to normalize kurtosis in order to find general solution for component identification:

$$kurt_i = \frac{kurt_i}{\sum_{j=0}^{N-1} kurt_j}, \tag{6.5}$$

where $kurt_i$ is kurtosis of one component and N is the number of components.

Using combination with sorting this normalization enables us to find components, whose sum of kurtosis is larger than 75% of sum of all kurtosis values. All components found by previous algorithm are identified as ECG activity and used for computation of complex lead using transform defined by Eq. 6.2. After computation the recursive MA filter is applied similarly to application in original algorithm and the resulting signal is returned to main procedure. Algorithm for computing complex component transform is depicted in Algorithm 3.

6.3.2 Algorithm summary

The algorithm works in pseudo-realtime mode, which contains search-back procedure for identification of low amplitude beats.

Algorithm 3 Algorithm for complex component estimation

Input: ECG signal

1: Pre-process input signal (Remove mean; Filter power line interference and muscle artefacts)
2: Estimate components using *JADE* algorithm
3: Calculate kurtosis of components
4: Normalize values of kurtosis with maximal kurtosis calculated
5: Sort descending normalized values of kurtosis and permute components accordingly to order of their normalized kurtosis
6: Select first n components whose sum $\geq$ threshold
7: Calculate complex component from n selected components
8: Post-process complex component (Filter noise magnified by complex lead transformation)

Output: Complex component

Our method adds one more step between filter preprocessing of original signals and complex lead transform to original Christov's algorithm. This step estimates the ECG activity using JADE algorithm, which makes (see in next Chapters) the algorithm much more robust in presence of strong noises and artefacts. Our implementation with JADE algorithm is slower than original Christov's algorithm. This is understandable and the algorithm needs 7.6 seconds to complete the detection on 30 minutes 2-lead ECG.

6. INDEPENDENT COMPONENT ANALYSIS FOR ECG BEAT DETECTION ENHANCING: PROPOSED METHOD

Chapter 7

Evaluation of proposed algorithms

This chapter summarizes the experiments with our proposed algorithms. First we will speak about used data and procedure for creation of noise in them. Next the evaluation criteria will be mentioned and the state-of-the-art algorithms will be discussed.

7.1 Data

7.1.1 Databases

In the evaluation experiments we used data freely available on MIT medical data storage Physionet [7]:

- MIT-BIH Arrhytmia database [48] - contains 48 half-hour two channel ambulatory ECG recordings digitized at 360 samples per second with 11-bit resolution over 10 mV range annotated by two or more cardiologist. All recordings contain modified limb lead II. Second lead is usually modified lead V1, occasionally V2 or V5 and in one instance V4. Four recordings contain paced beats.

- Normal Sinus Rhythm database [7] - contains 18 long-term two channel ECG recordings of subjects with no significant arrhythmias digitized at 128 samples per seconds per channel with 12-bit resolution over 10 mV range.

- European ST-T database [138] - contains 90 long-term two channel ambulatory ECG recordings of subjects with myocardial ischemia diagnosis or suspicion. The recordings were digitized at 250 samples per second with 12-bit resolution over 20 mV range.

- Long Term ST database [139] - contains 86 lengthy ECG recordings of 80 subjects with significant ST changes. Individual recording contains two or three ECG leads. Each signal was digitized at 250 samples per second with 12-bit resolution over ± 10 mV range.
- QT database [140] - contains 105 fifteen minutes two channel ECG recordings without significant baseline wander or artefacts. Recordings were digitized at 250 samples per second.
- MIT Long Term database [7] - contains 7 long term two or three channel ECG recordings digitized at 128 samples per second.
- MIT-BIH ST Change database [141] - contains 28 ECG two channel recordings of different length recorded during exercise and exhibiting ST depression. Signals were digitized at 360 samples per second.

7.1.2 Simulated noise

According to [132] one can expect various kinds of noise presented in ECG. The most common ones are:

- Power line interference - consists of 50 Hz (60 Hz in U.S.) pickup and its harmonics, typical amplitude is up to 50 percent of peak-to-peak ECG amplitude
- Motion artifacts - transient baseline changes caused by changes in electrode-skin impedance, the cause of impedance change is the slow motion of electrode on the body surface, typical amplitude is up to 500 percent of peak-to-peak ECG amplitude
- Muscle contraction - generates artefactual millivolt-level potentials, its standard deviation is around 10 percent of peak-to-peak ECG amplitude
- Baseline drift and ECG amplitude modulation with respiration - is represented as slow sinusoidal component at respiration frequency, its amplitude variation is 15 percent of peak-to-peak ECG amplitude and typical frequencies at 0.15 Hz to 3 Hz

In addition to these four noises we observed noise typically generated by electrode cable movement during holter recording of ECG. This noise has large amplitudes up to 200 percent of peak-to-peak ECG amplitudes and typical power spectra with peaks at 1.5, 3.16, 6.3 and 8 Hz.

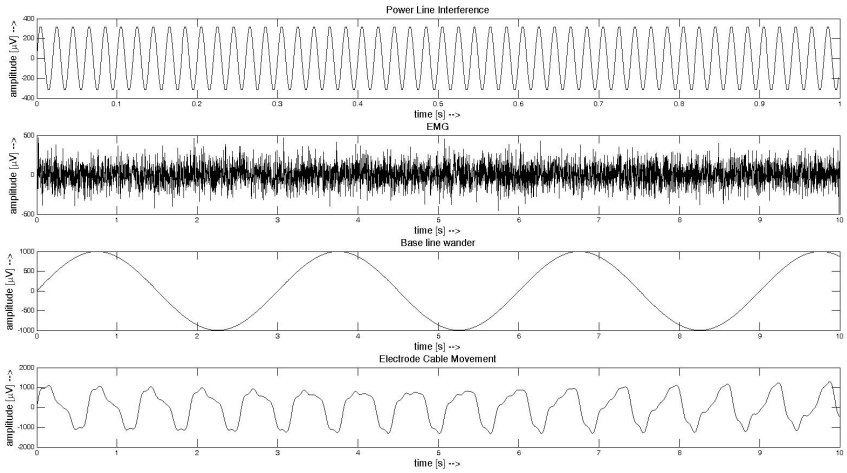

Figure 7.1: Examples of artefacts artificially added to ECG signals

In order to test performance of the algorithm we artificially added noises to ECG recordings. The noises were artificially generated as follows:

- Electromyographic noise - is simulated as random Gaussian signal with deviation around 10 percent of peak-to-peak ECG amplitude
- Power line interference - 50 Hz sinusoid with amplitude 0.333 mV
- Baseline wander - slow sinusoid (0.333 Hz) with the amplitude around 1 mV
- Electrode cable movement - generated as sum of sinusoids with different amplitudes and frequencies ranging from 0.1 to 1 mV and 1.5 to 8 Hz

Each type of simulated noise is added to ECG at four different levels: 25, 50, 75, 100 percent of the maximum amplitude. The noise is added to each lead of ECG with different amplitude estimated from ECG amplitude. The examples of generated noises are shown in Fig. 7.1.

7.2 Evaluation criteria

This section describes evaluation criteria used for "scoring" algorithms performance. First we will speak about de-noising performance criteria and then about QRS detection performance criteria.

7.2.1 De-noising algorithm

For evaluation of de-noising algorithm we used Root-Mean-Square Error ($RMSE$), which is good statistical index for case, when the original clear signal is known. $RMSE$ is defined as:

$$RMSE = \sqrt{\frac{1}{N}\sum_{i=0}^{N-1}(x_i - y_i)^2}, \tag{7.1}$$

where x_i is the i-th sample of original signal, y_i is the i-th sample of filtered signal and N is the number of samples in both signals. The values of $RMSE$ close to 0 means that filtering technique reduces noise efficiently with minimal changes in useful signal.

7.2.2 QRS detection algorithm

For evaluation of QRS detection algorithm we used standard statistical indices [142] Sensitivity (Se), Positive predictivity (P^+) and F-measure (F), which are derived from three parameters:

- Correctly detected beats (True positives=TP)
- Falsely detected beats (False positives=FP)
- Undetected beats (False negatives=FN)

Sensitivity is the parameter describing how many beats are correctly detected. Thus its value is calculated using this equation:

$$Se = \frac{TP}{TP + FN}. \tag{7.2}$$

Positive predictivity characterizes the algorithm in sense of the false detection of beats. Its value is estimated as follows:

$$P^+ = \frac{TP}{TP + FP}. \tag{7.3}$$

The F-measure statistics is defined as harmonic mean of Sensitivity and Positive predictivity:

$$F = 2\frac{Se * P^+}{Se + P^+}. \tag{7.4}$$

All statistical indices range from 0 % (worst) to 100 % (best). The values over 95 % are considered as good results.

7.3 Evaluation methods

This section provides detailed review of referential methods used for comparison with our algorithms. Then we will describe the testing methodology.

7.3.1 State-of-the-art methods

Here we describe the state-of-the-art methods used for comparison with our methods. First we will describe de-noising algorithms and then beat detection algorithms.

7.3.1.1 De-noising algorithms

Standard filtering algorithm is based on set of filters designed for suppression of each common type of noise.

First deployed filter is single-frequency adaptive noise canceller (ANC) [143]. This type of adaptive filter is based on LMS algorithm. The structure of filter is depicted on Fig. 7.2. The ANC filter has two inputs: measured distorted signal x and noise model signal u'. Signal u' is phase-shifted by $\frac{\pi}{2}$ and both original u' and shifted signal u'' are multiplied by weights computed by LMS algorithm. Signals are then summed up into signal $\overline{u}$ and added to measured signal x with switched sign. Resulting error signal e is the desired filtered signal and also serves as input to update LMS rule for weights w_1 and w_2. The update equation has form:

$$\mathbf{w}[n+1] = \mathbf{w}[n] + \mu e[n] \begin{bmatrix} u'[n] \\ u''[n] \end{bmatrix}, \tag{7.5}$$

where $\mathbf{w} = \begin{bmatrix} w_1 \\ w_2 \end{bmatrix}$ is weight vector, e is error signal, μ is convergence constant and u', u'' are input noise model signals.

Second filter in the set is notch filter for EMG artefact suppression. Notch filter is band-stop IIR filter with transfer function [144]:

$$H(z) = \frac{1}{2} \frac{(1+a_2) - 2a_1 z^{-1} + (1+a_2) z^{-2}}{1 - a_1 z^{-1} + a_2 z^{-2}}, \tag{7.6}$$

where:

$$\begin{aligned} a_1 &= \frac{2\cos(\frac{2\pi f_n}{f_s})}{1+\tan(\frac{2\pi BW}{2f_s})}, \\ a_2 &= \frac{1-\tan(\frac{2\pi BW}{2f_s})}{1+\tan(\frac{2\pi BW}{2f_s})}, \end{aligned} \tag{7.7}$$

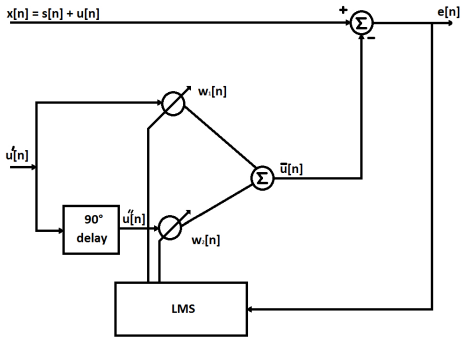

Figure 7.2: Single-frequency adaptive noise canceller

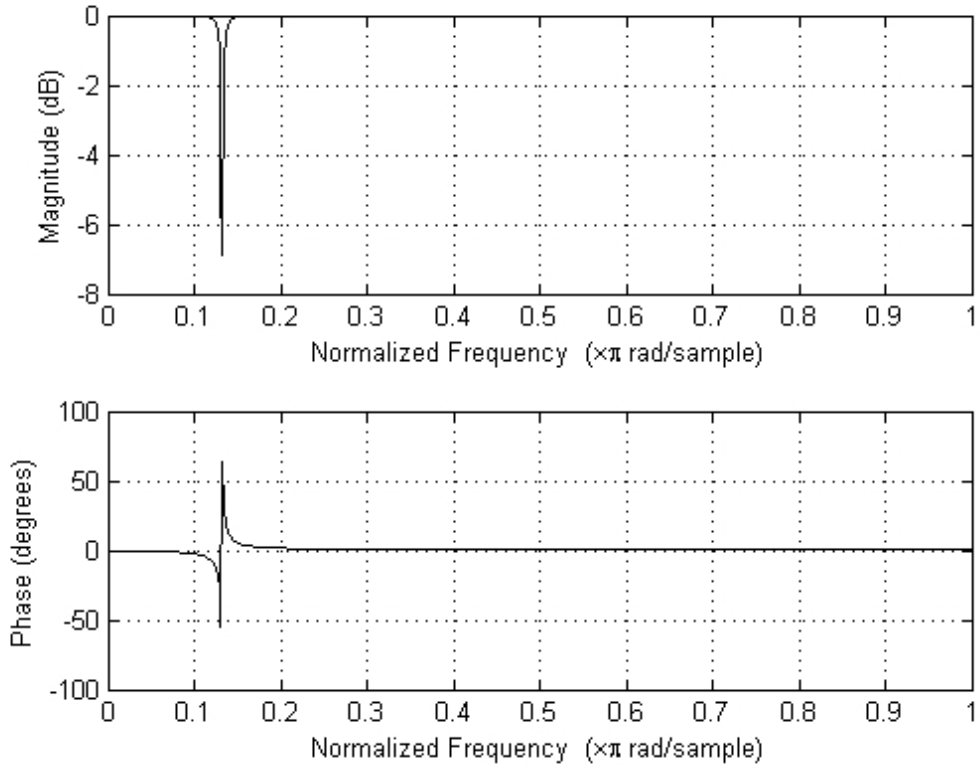

Figure 7.3: Notch filter frequency response for f_n=33 Hz, BW=0.8 and f_s=500 Hz

where f_n is noise frequency, BW is bandwidth and f_s is sampling frequency. Frequency response of notch filter used in set is shown on Fig. 7.3.

Last filter deployed in the set is a median filter for suppression of baseline wander. The algorithm of applying of median filter follows:

- Decimate ECG signal with decimation factor 20.
- Filter resulting signal with median filter of length 10.
- Interpolate filtered signal into original length with low-pass interpolation. Interpolated signal represents base line wander.
- Subtract interpolated signal from original ECG.

Median filter removes any remaining parts of ECG remaining in data and the signal could be considered as base line wander. Median filter is defined by equation:

$$y[n] = median\{x[n+i], i = 0, ..., N-1\}, \tag{7.8}$$

where y represents filtered signal, x represents original signal and N is length of filter.

Wavelet decomposition based algorithm is described in [145]. The wavelet decomposition is widely used algorithm for denoising of various signals, thus we decided to use it as one of the comparison methods. The algorithm contains three steps:

- Wavelet decomposition step – choose wavelet and perform wavelet decomposition of the signal at level N
- Threshold detail coefficients using hard thresholding method
- Wavelet reconstruction step – perform reconstruction based on original approximation coefficients and modified detail coefficients

Wavelet transform is defined as [146]:

$$Wf(u,s) = \int_{-\infty}^{\infty} f(t)\frac{1}{\sqrt{s}}\psi^*(\frac{t-u}{s})dt, \tag{7.9}$$

where u is translation constant, s is scale of transform, $f(t)$ is the original signal and ψ is a wavelet function.

Inverse wavelet transform is then defined:

$$f(t) = \int_{-\infty}^{\infty} Wf(u,s)\frac{1}{\sqrt{s}}\psi(\frac{t-u}{s})dt, \tag{7.10}$$

The signal thresholding algorithm was developed by Donoho [147]. We used hard-thresholding of detail wavelet coefficients. Hard thresholding is defined as follows:

$$f(n) = \begin{cases} X, & \text{for } |X| > \lambda, \\ 0, & \text{for } |X| \leq \lambda, \end{cases} \tag{7.11}$$

where X is the detail coefficient and λ is defined threshold.

In our study we used Daubechies wavelet DB6, which is depicted on Fig. 7.4.

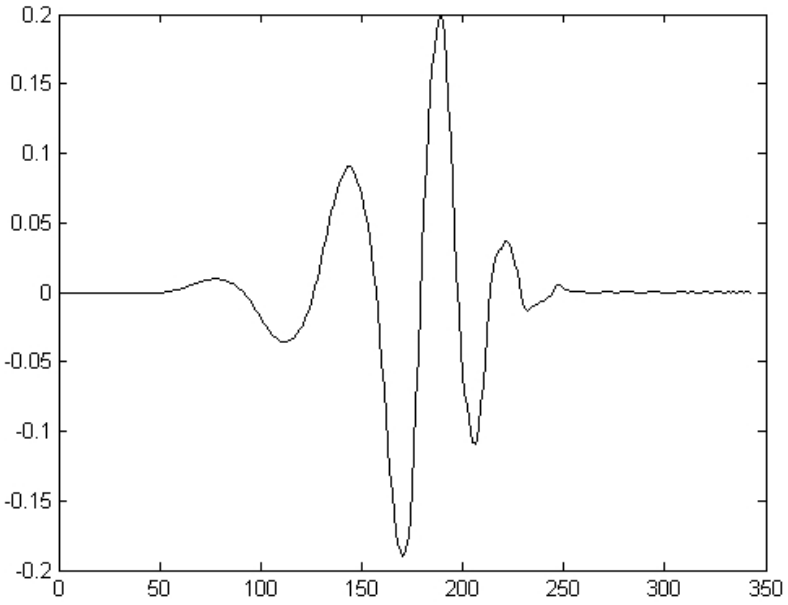

Figure 7.4: Daubechies wavelet DB6

7.3.1.2 QRS detection algorithms

Christov's beat detection algorithm was described in Chapter 6. It is a basis of our algorithm for beat detection and it was used as one state-of-the-art method for evaluation.

Pan-Tompkins beat detection algorithm was published in 1985 [134]. It is one of the most commonly used algorithms. The algorithm works on one dimensional signal (preferred is lead II). It works as shown in Fig. 7.5 – first the signal is transformed by set of filters in order to enhance beat position and second the adaptive threshold is deployed for detection of correct positions.

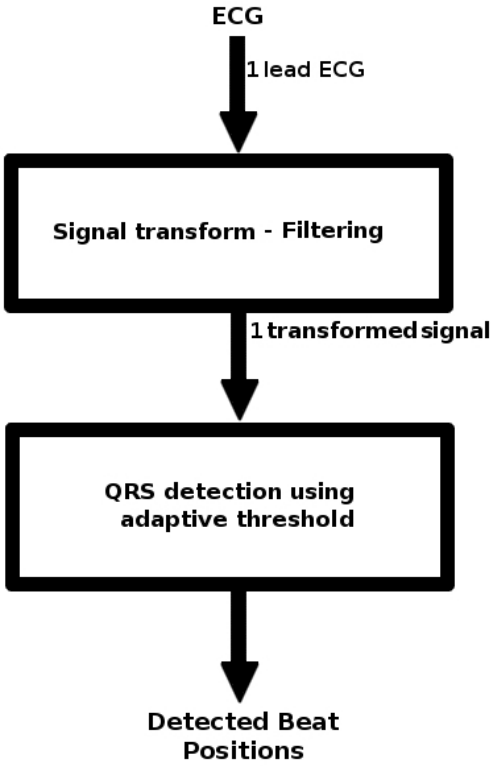

Figure 7.5: Pan-Tompkins beat detection algorithm work-flow

The set of filters starts with low-pass filter for reduction of muscle and power line noise. Its transfer function is as follows:

$$H(z) = \frac{(1 - z^{-6})^2}{(1 - z^{-1})^2}. \tag{7.12}$$

This low-pass filter has cut-off frequency about 11 Hz and gain is 36. Filter processing delay is five samples. Filter frequency response is shown on Fig. 7.6.

Next the signal is passed through high-pass filter, which has low cut-off frequency around 5 Hz, gain 1 and group delay is 16 samples (frequency response is shown on Fig. 7.7). Its transfer function is:

$$H(z) = \frac{-1 + 32z^{-16} - 32z^{-17} + z^{-32}}{1 - z^{-1}}. \tag{7.13}$$

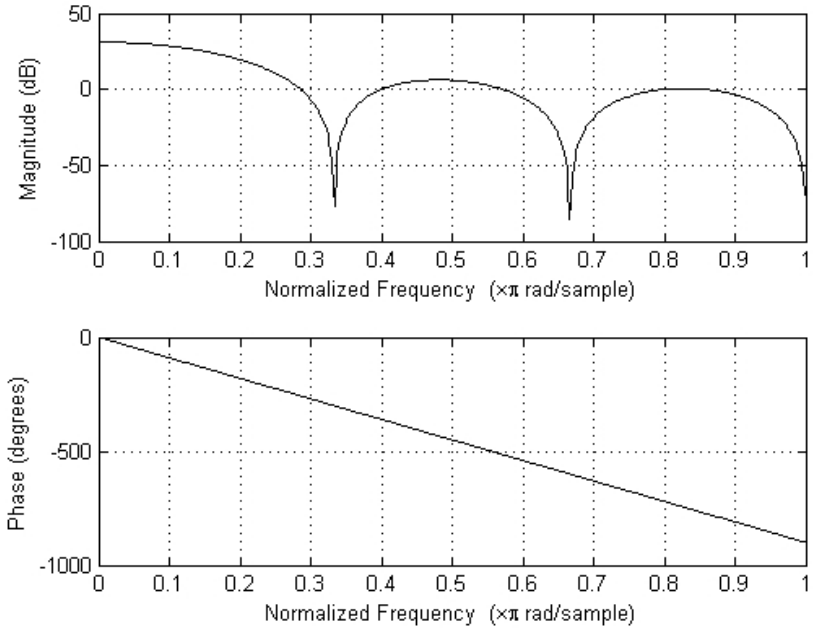

Figure 7.6: Low-pass filter frequency response for f_s=200 Hz

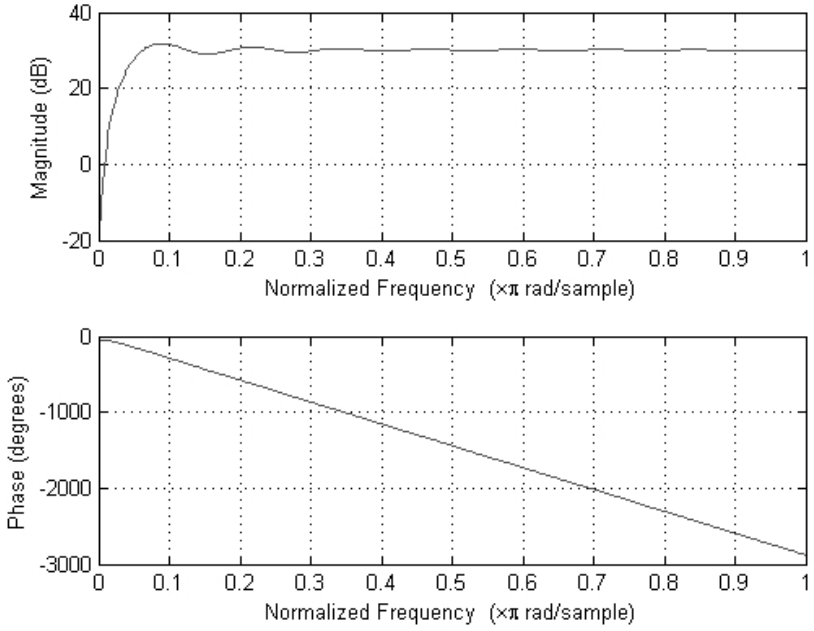

Figure 7.7: High-pass filter frequency response for f_s=200 Hz

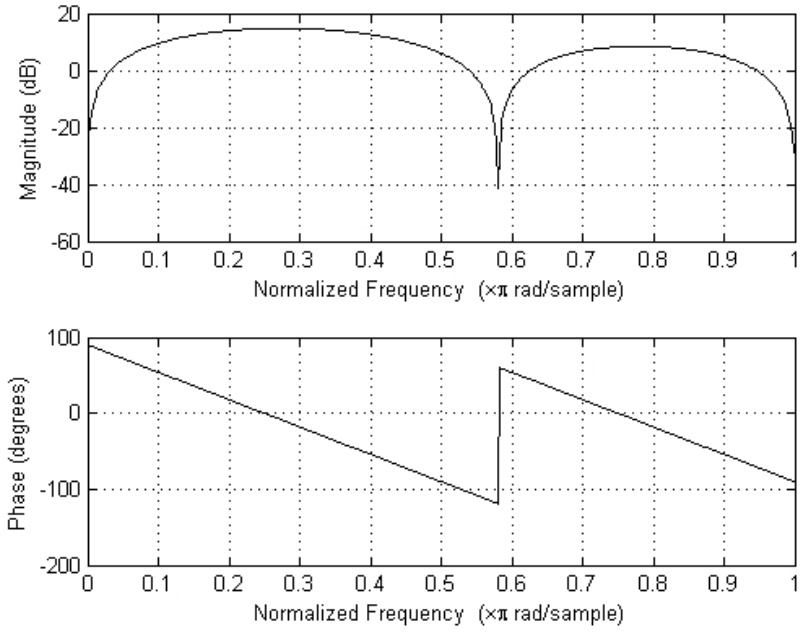

Figure 7.8: Derivative filter frequency response for f_s=200 Hz

After band-pass filtering (implemented by low-pass and high-pass filter) the signal 5-point derivative is taken using derivative filter with transfer function:

$$H(z) = \frac{1}{8}(2 + z^{-1} - z^{-3} - 2z^{-4}). \tag{7.14}$$

The derivative approximates ideal derivative between dc and 30 Hz and has group delay 2 samples. Filter frequency response is shown on Fig. 7.8.

The output of derivative filter is squared and finally it is filtered by MA filter of length 30 samples. Its frequency response is shown on Fig. 7.9.

After averaging resulting signal (for example see Fig. 7.10) is passed to second step of algorithm, which detects beat position using adaptive thresholds. Thresholds are computed from two parameters:

- SPKI - running estimate of signal (ECG) peak,

- NPKI - running estimate of the noise peak.

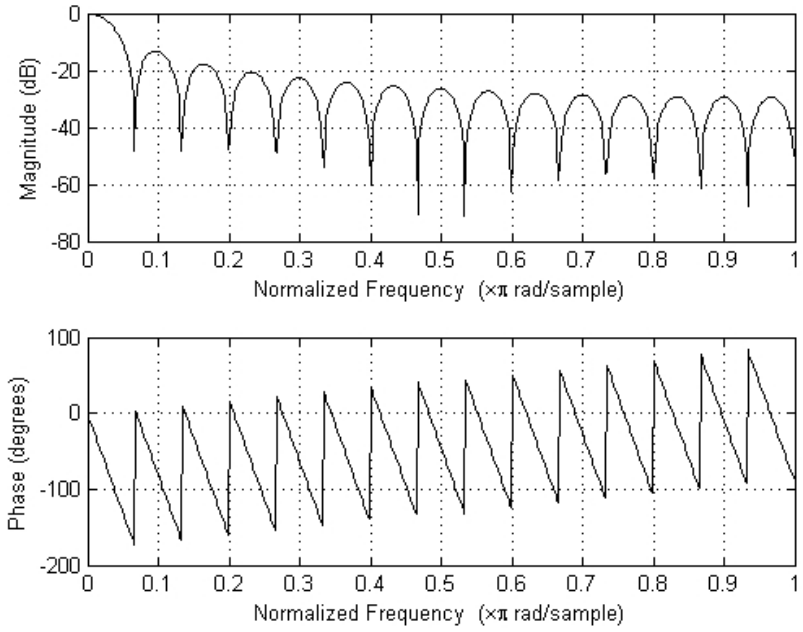

Figure 7.9: MA filter frequency response for f_s=200 Hz

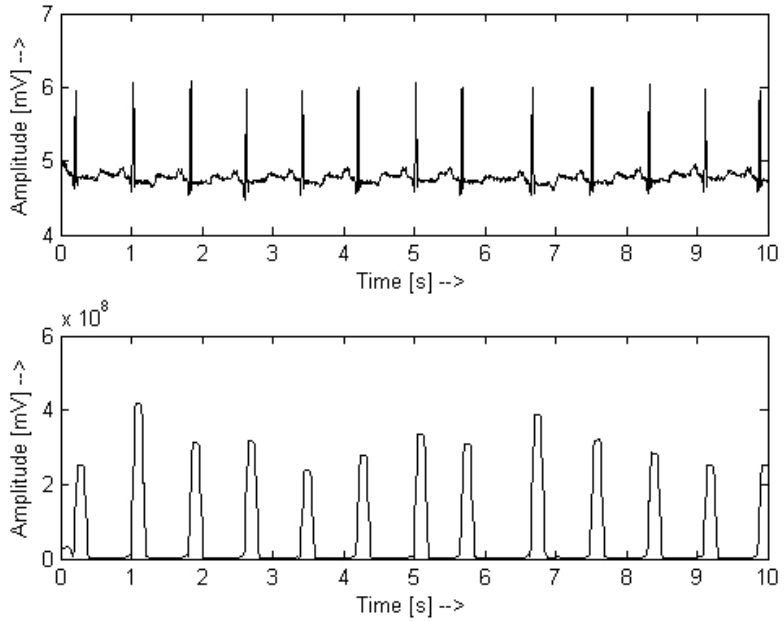

Figure 7.10: Example of ECG transformed by filter set used in Pan-Tompkins algorithm

These two parameters are recomputed every time the peak in ECG is found (PEAKI). The parameters are recomputed as follows:

$$\begin{aligned} SPKI &= 0.125PEAKI + 0.875SPKI, \texttt{if PEAKI is ECG} \\ NPKI &= 0.125PEAKI + 0.875NPKI, \texttt{if PEAKI is noise}. \end{aligned} \tag{7.15}$$

Every time the SPKI and NPKI parameters are recomputed adaptive thresholds are recomputed:

$$\begin{aligned} TH1 &= NPKI + 0.25(SPKI - NPKI), \\ TH2 &= 0.5TH1, \end{aligned} \tag{7.16}$$

where $TH1$ is basic detection threshold and $TH2$ is threshold used during search-back procedure, when no ECG beat is detected for long duration of time. The time duration required for starting search-back procedure is determined as 1.66∗average of last eight RR intervals.

7.3.2 Evaluation algorithm

The evaluation procedure was developed in order to test ECG processing algorithms on standard ECG databases (mentioned above) contaminated with different types of noise with different strength. Our methodology provides general framework for this testing. The evaluation algorithm work flow is shown in Algorithm 4. Basically the method has three main parts:

- Noisy recording creation part - in which the noise is created and added to ECG records according to procedure described in Section 7.1.2.
- ECG processing algorithms part - in this part all tested algorithms "do their work" and the results are stored.
- Evaluation criteria computation part - here the evaluation criteria for tested algorithms are computed according to Section 7.2.

Algorithm 4 Algorithm for complex component estimation

Input: ECG signal database

1: Noisy recording creation and adding to ECG signals
2: ECG processing using evaluated algorithms
3: Evaluation of results

Output: Results according to selected criteria

Chapter 8

Results of proposed algorithms

This Chapter summarizes results of our algorithms compared to state-of-the-art methods. First we will present the de-noising algorithm and its results and then the beat detection algorithm. Results are demonstrated using graphs showing the important information at a glance.

8.1 Denoising algorithm

This section describes results obtained by our de-noising algorithm and the referential methods. First part of the section describes results using graphical description and all available ECG databases. Second part provides testing conclusions.

8.1.1 Results

Figures 8.1, 8.2, 8.3, 8.4, 8.5, 8.6, 8.7 and 8.8 show summarized results of our algorithm, basic filtering algorithm and Wavelet de-noising algorithm. Each figure shows the evolution of RMSE according to the percentage of noise amplitude added to signals (Section 7.1.2). For more detailed results see Appendix A. This section is divided into subsections according to databases used for algorithm testing. The last subsection shows performance of tested algorithms on all available data.

8.1.1.1 Results on MIT-BIH Arrhythmia Database

Figure 8.1 shows summarized results on MIT/BIH Arrhythmia Database. First observation shows us that our de-noising algorithm is similar or better in presence of all noises than other methods - basic filtering has problems in presence of strong EMG artefact and electrode cable movement and the Wavelet based de-noising algorithm has difficulties with base line wander and the electrode cable movement.

The main purpose, for which the algorithm was designed, was removal of electrode

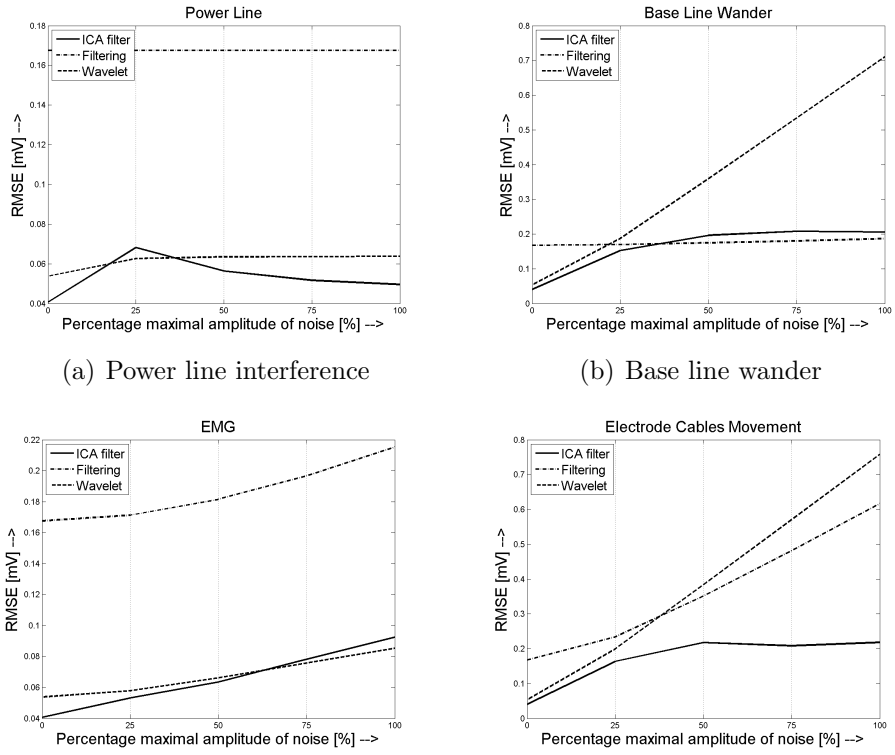

(a) Power line interference

(b) Base line wander

(c) EMG

(d) Electrode cable movement

Figure 8.1: Summarized values of RMS for the developed algorithm and different types of artefacts on MIT/BIH Arrhythmia Database. We can observe that our algorithm performs correctly in presence of all noises. The filtering method has problem with strong EMG artefact and Wavelet method with Base line wander artefact.

cable movement artefact and we can observe that our algorithm is the only one, which was able to reduce noise from ECG, thus we can say our algorithm is more stable in presence of uncommon noise than the other tested algorithms but it works properly in presence of any type of tested noise.

In presence of standard noises state-of-the-art algorithms work properly - filters remove

the power line interference. The biggest surprise is the result of Wavelet method on base line wander artefact, but this problem is probably due to the simulation of noise using sinus wave. Wavelet decomposition uses different basis than sinus wave and thus the sinus wave is split into several details and could not be properly removed. The basic filtering method has difficulties with EMG artefact. EMG has normal distribution and the artefact covers large frequency band in spectrum. Thus the filters designed for suppression of exact frequencies can not work properly.

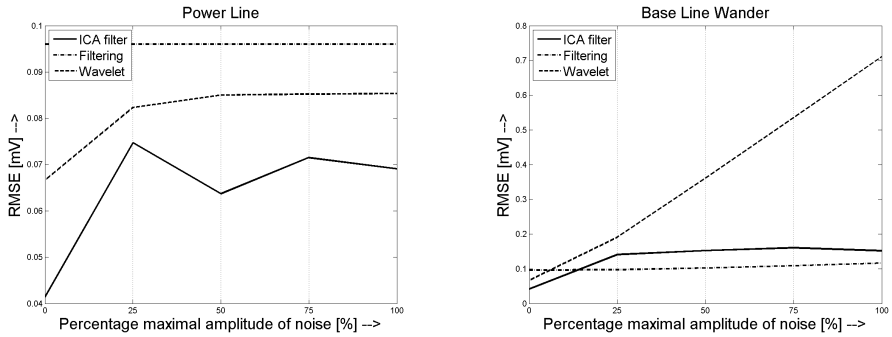

(a) Power line interference

(b) Base line wander

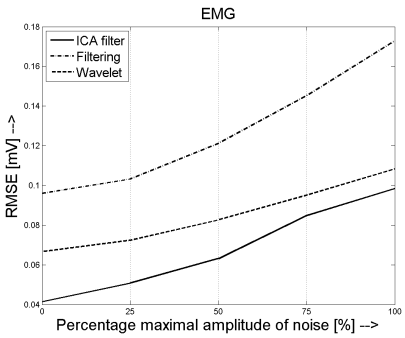

(c) EMG

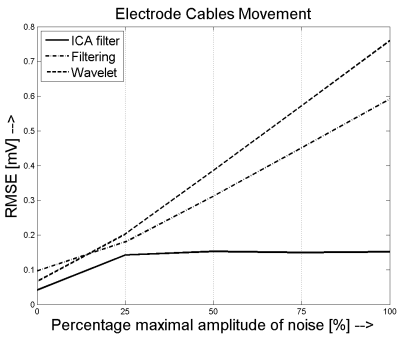

(d) Electrode cable movement

Figure 8.2: Summarized values of RMS for the developed algorithm and different types of artefacts on Normal Sinus Rhythm Database. Again we can observe similar results as on MIT/BIH Arrhythmia Database. Our algorithm works sufficiently in presence of any artefact type.

8.1.1.2 Results on Normal Sinus Rhythm Database

Figure 8.2 shows summarized results on MIT Normal Sinus Rhythm Database. Again we can observe similar performance of our algorithm as in case of MIT/BIH Arrhythmia Database. Again we can say that our algorithm is very successful in presence of electrode

cable movement artefact and it works similar or better in presence of common noises. One exception is base line wander artefact, where our algorithm has slightly worse performance than standard filtering method. Wavelet method has difficulties with base line wander and electrode cable movement. On the other hand basic filtering shows that it has problems with EMG and power line artefacts.

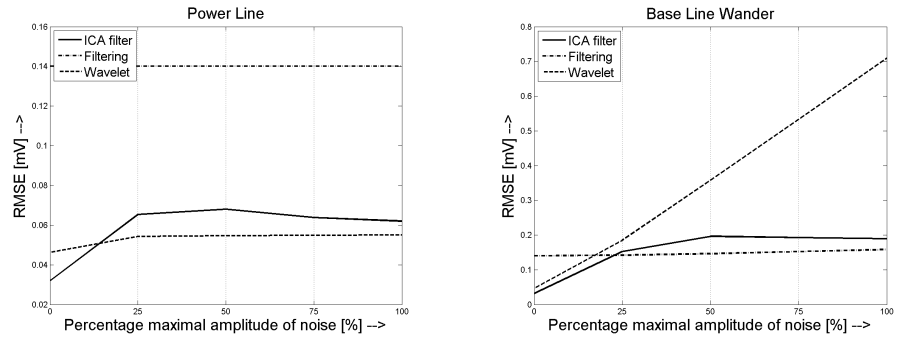

(a) Power line interference

(b) Base line wander

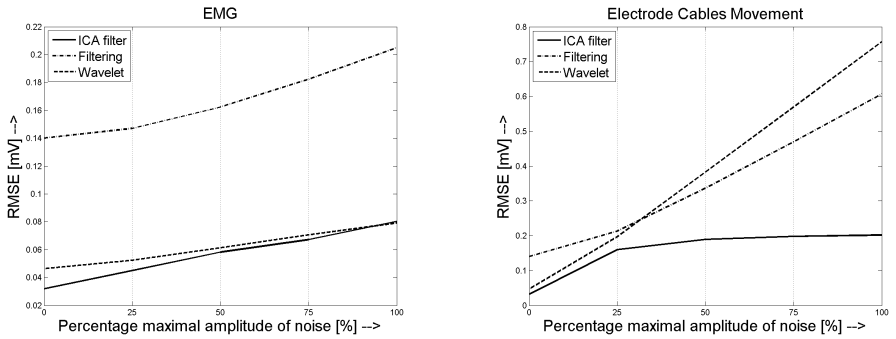

(c) EMG

(d) Electrode cable movement

Figure 8.3: Summarized values of RMS for the developed algorithm and different types of artefacts on European ST-T database. We can observe results similar to previous databases. Our algorithm works properly in presence of all noises types. Wavelet method again fails in case of base line wander and electrode cable movement and standard filtering fails in case of EMG.

8.1.1.3 Results on European ST-T database

Figure 8.3 shows the results on European ST-T database. As in previous case we observe similar results - our algorithm works similar or better than tested referential methods. In case of power line interference our algorithm performance is slightly worse than performance of Wavelet method and in presence of base line wander than performance of basic filtering.

8.1.1.4 Results on Long Term ST database

Figure 8.4 shows the results on Long Term ST database. The performance of our algorithm and referential methods on Long Term ST database is similar to performance on previous tested databases. ICA base algorithm works similar or better than other tested methods. Wavelet de-noising performance is reduced in case of base line wander. Probably due to simulation of artefact by slow sinus wave. Standard filtering technique has difficulties with EMG because of covered frequencies by EMG artefact.

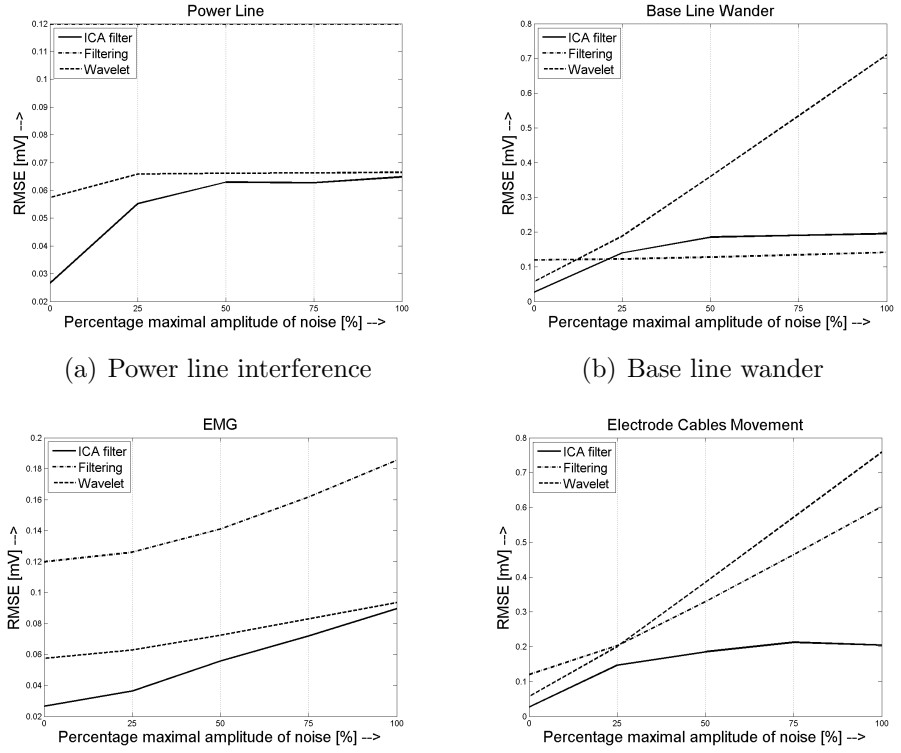

(a) Power line interference

(b) Base line wander

(c) EMG

(d) Electrode cable movement

Figure 8.4: Summarized values of RMS for the developed algorithm and different types of artefacts on Long Term ST database. The results are self-explanatory - the algorithm works similar or better than referential methods. Our method performed better in case of 3 artefacts (power line, EMG and electrode cable movement) and slightly worse than standard filtering in case of base line wander. Wavelet filtering and standard filtering was unable to reduce electrode cable movement artefact efficiently.

8.1.1.5 Results on QT database

Figure 8.5 shows the results on QT database. Our method performance is slightly worse than standard filtering method in presence of power line artefact and base line wander, but its performance is still comparable with it. We can again observe that our algorithm excelled in reduction of electrode cable movement artefact.

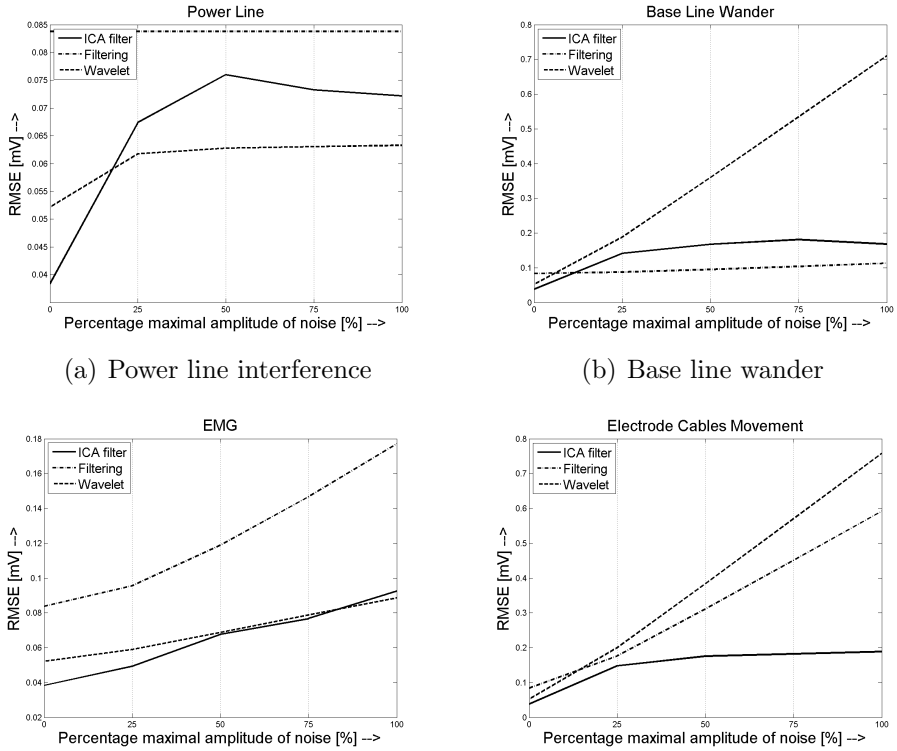

(a) Power line interference

(b) Base line wander

(c) EMG

(d) Electrode cable movement

Figure 8.5: Summarized values of RMS for the developed algorithm and different types of artefacts on QT database. In presence of all four tested noises our algorithm performance is similar or better than performance of referential methods.

8.1.1.6 Results on MIT Long Term database

Figure 8.6 shows results on MIT Long Term database. Again the results of our algorithm are similar to previous results. Our algorithm is capable to deal with all tested noises. In presence of EMG and base line wander our method performance is slightly worse than better of referential methods.

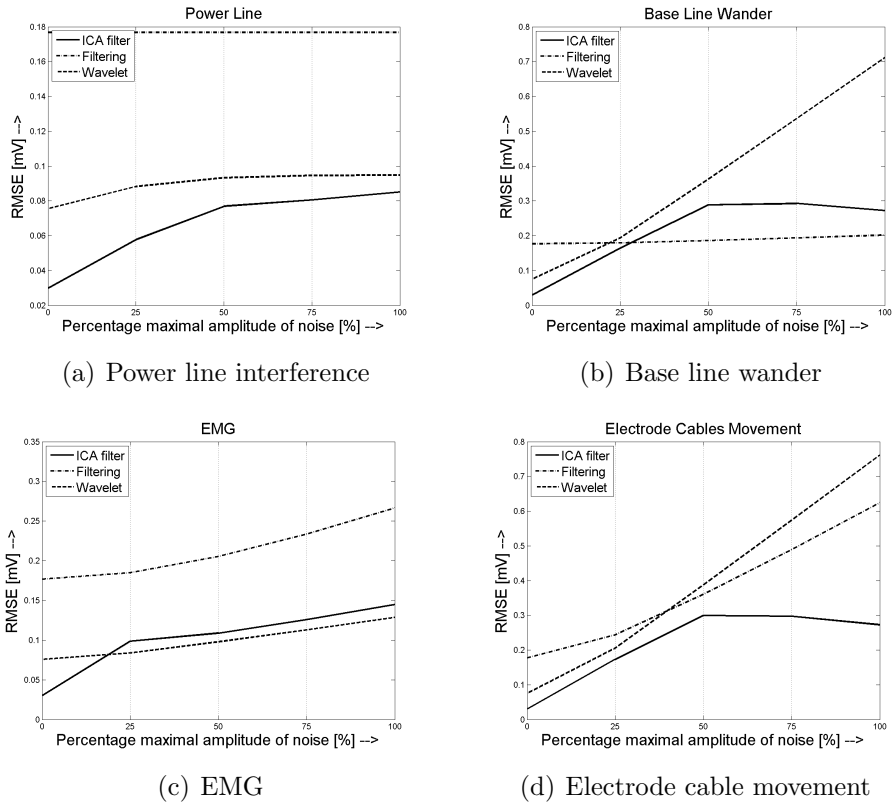

(a) Power line interference

(b) Base line wander

(c) EMG

(d) Electrode cable movement

Figure 8.6: Summarized values of RMS for the developed algorithm and different types of artefacts on MIT Long Term database. The results are similar to results on previously mentioned databases.

8.1.1.7 Results on MIT-BIH ST Change database

Figure 8.7 shows results on MIT-BIH ST Change database. Results on MIT-BIH ST Change database are similar to previous results. All algorithms work similarly to the case of MIT Long Term database. Our method, which was designed for electrode cable movement artefact, is capable to deal with all tested types of noise presented in signal. Wavelet de-noising performs slightly worse than filtering in case of power line interference.

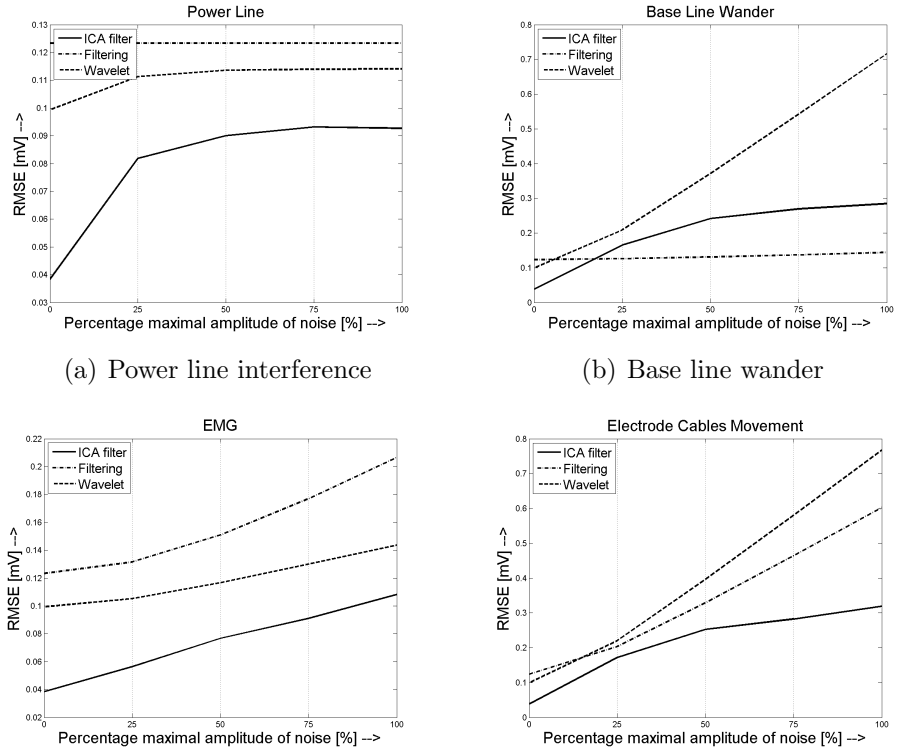

(a) Power line interference

(b) Base line wander

(c) EMG

(d) Electrode cable movement

Figure 8.7: Summarized values of RMS for the developed algorithm and different types of artefacts on MIT-BIH ST Change database. The results are similar to previous results and we can observe that our algorithm performed similar or better than referential methods.

8.1.1.8 Summary results on all databases

Summary results obtained across all databases show (Fig. 8.8) that our algorithm, which was designed for purpose of removal of electrode cable movement artefact, is suitable for removal of all types of noises. We can observe that our algorithm performs accurately in general. The method has one big advantage - in case of no artefact/noise presented our method distorts the resulting the ECG signal of at least. This is very desirable property in case of any medical signal.

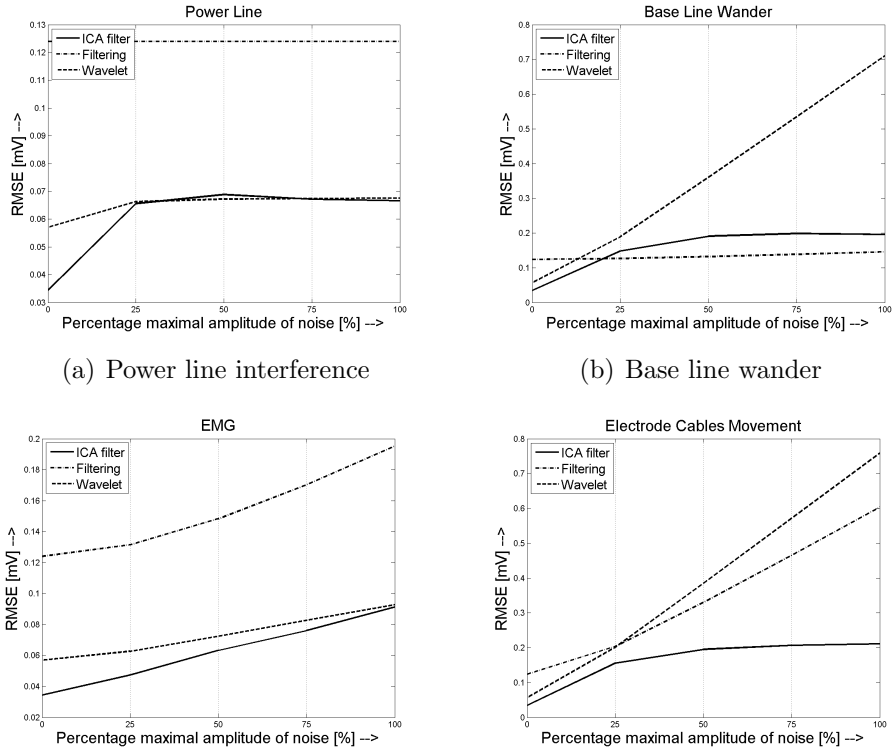

(a) Power line interference

(b) Base line wander

(c) EMG

(d) Electrode cable movement

Figure 8.8: Summarized values of RMS for the developed algorithm and different types of artefacts on all databases. We can observe that our algorithm performs well on all types of artefact. The wavelet de-noising performance is reduced on data containing base line wander and electrode cable movement artefact. Basic filtering performs worse on EMG and electrode cable movement artefact containing data.

Wavelet de-noising works well in case of power line interference and EMG noise, but fails in case of base line wander and electrode cable movement noise. This is probably due to the simulation of base line wander noise using sinus wave. Wavelet decomposition uses different basis than sinus wave and thus the sinus wave is split into several details and could not be properly removed.

Basic filtering procedure performs very accurately on data containing power line interference and base line wander. The problem arises with EMG and electrode cable artefact. EMG artefact was simulated as random vector with normal distribution and it influences all frequency bands in spectrum. Thus the filters designed for suppression of predefined frequencies can not filter whole EMG activity. The same problem is with electrode cable movement artefact, which covers different frequencies than filtered frequencies and artefact was not reduced.

8.1.2 Conclusions

We have developed an ICA based de-noising ECG algorithm for dealing with uncommon noises presented in data during holter and telemedicine applications. This algorithm is able to deal with very strong noises and preserves as much information as possible. Our method connects the well-known JADE algorithm with decision tree in order to identify noise and reduce it.

Method behaviour was tested on standard databases available freely on-line and it was compared to common filtering and Wavelet threshold de-noising techniques. Tests were performed using simulated noises (3 common and 1 uncommon). The uncommon noise tests algorithm ability to deal with unpredictable noise events common for nowadays holter and telemedicine applications.

Our method performs much more stable than other methods – it outperforms both state-of-the-art methods in unpredictable noise events and it works similarly to both methods with ECG data contaminated with base line wander or EMG.

Time requirements of our algorithm is increased due to computational complexity of JADE algorithm and Pan-Tompkins beat detection algorithm (used in feature extraction step), but changing the BSS or QRS complex detection algorithm will lead to better time performance. Memory requirements are also slightly increased but the advantage of our method outperforms its flaws, especially with nowadays hardware development.

8.2 QRS detection algorithm

This section describes results of our QRS detection method based on Christov's beat detection algorithm and referential methods. Results are presented using graphs of F-measure, which is harmonic mean of Sensitivity and Specificity (Section 7.2.2). Last part of the section provides testing conclusions.

8.2.1 Results

Figures 8.9, 8.10, 8.11, 8.12, 8.13, 8.14 and 8.16 show summarized results of our algorithm, Tompkins algorithm and Christov's algorithm. Each figure shows the evolution of F-measure according to the percentage of noise amplitude added to signals. For more details see Appendix B.

8.2.1.1 Results on MIT-BIH Arrhythmia Database

Figure 8.9 shows summarized results on MIT/BIH Arrhytmia Database. The first observation shows that the Tompkins algorithm performance is strongly independent on the noise presence and its power. This is due to the algorithm nature – it uses set of filters in combination with differentiation procedure, which efficiently reduces all types of noise.

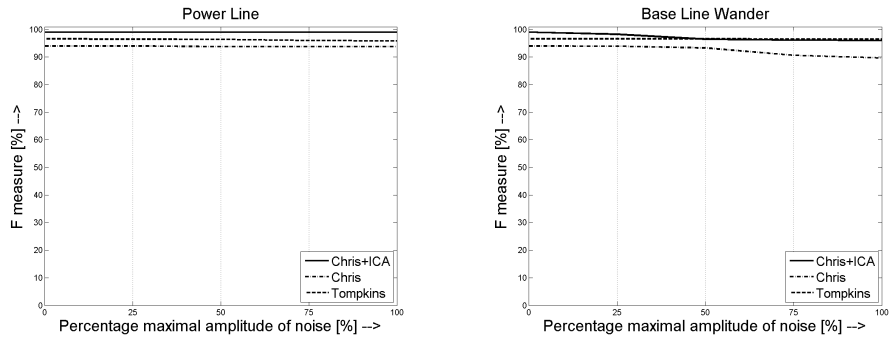

(a) Power line interference (b) Base line wander

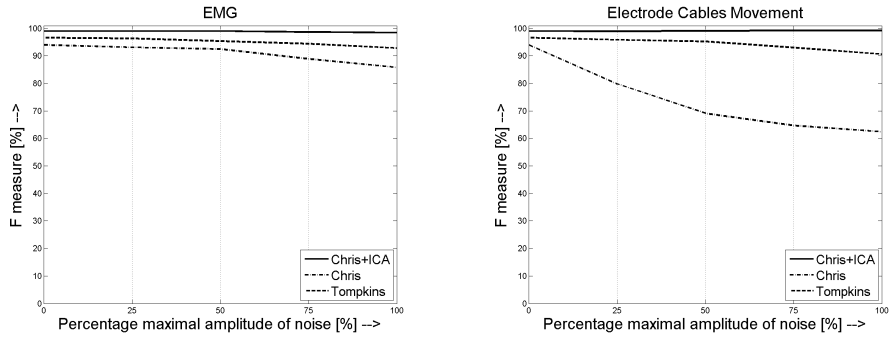

(c) EMG (d) Electrode cable movement

Figure 8.9: Summarized values of F-measure for the developed algorithm and different types of artefacts on MIT/BIH Arrhythmia Database. The results prove stability of our developed method against presence of strong noises. We can observe that our algorithm performance is slightly reduced in presence of base line wander artefact.

On the other hand the Christov's algorithm performance is more affected by introduced noise. Algorithm fails in presence of non-standard noises. The presence of non-standard noises is typical for holter ECG and telemedicine applications, which are by their nature more affected by wide range of noises. The Christov's algorithm performance is then very easily affected by their presence.

Our algorithm is designed to increase stability and robustness of Christov's algorithm

in presence of unpredictable events (artefacts). This goal is achieved.

Our algorithm is very successful in presence of noise, which mimics the QRS complex activity in frequency domain (electrode cable movement artefacts). Its stability is caused by extraction of ECG activity during computation of complex component signal, which is the basis for QRS complex detection.

8.2.1.2 Results on Normal Sinus Rhythm Database

Figure 8.10 shows summarized results on MIT Normal Sinus Rhythm Database. We can observe, again, that Tompkins algorithm performance is stable in presence of any noise presented in ECG. The performance of Christov's algorithm is similar to our method with exception of electrode cable movement artefact. In such a case the Tompkins algorithm

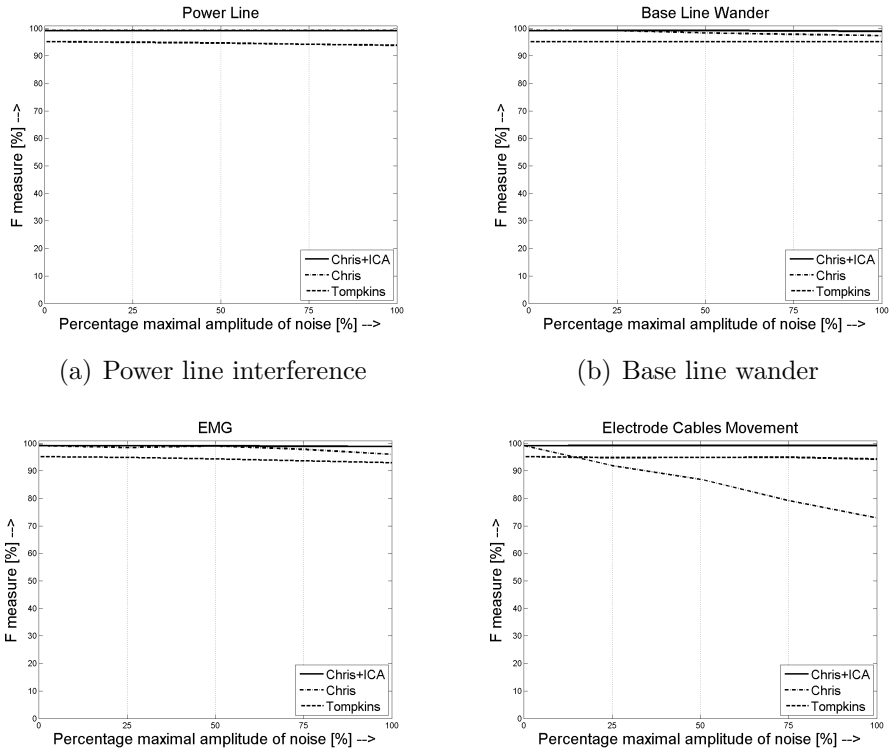

(a) Power line interference

(b) Base line wander

(c) EMG

(d) Electrode cable movement

Figure 8.10: Summarized values of F-measure for the developed algorithm and different types of artefacts on Normal Sinus Rhythm Database. Our algorithm works much more stable in presence of any type of noise. We can also observe that the separation of Base line wander artefact was correct – the results are better than on MIT/BIH Arrhythmia Database.

outperforms the Christov's beat detection algorithm. This shows us that Tompkins algorithm is designed as more independent on data and it performs much better in presence of unpredictable events than Christov's algorithm, which is designed to deal with common noise events. Our algorithm works similar to the performance on the MIT/BIH Arrhytmia Database.

8.2.1.3 Results on European ST-T database

Figure 8.11 shows the results on European ST-T database. We can observe that our algorithm outperforms all referential methods used in our study in presence of all tested artefact types.

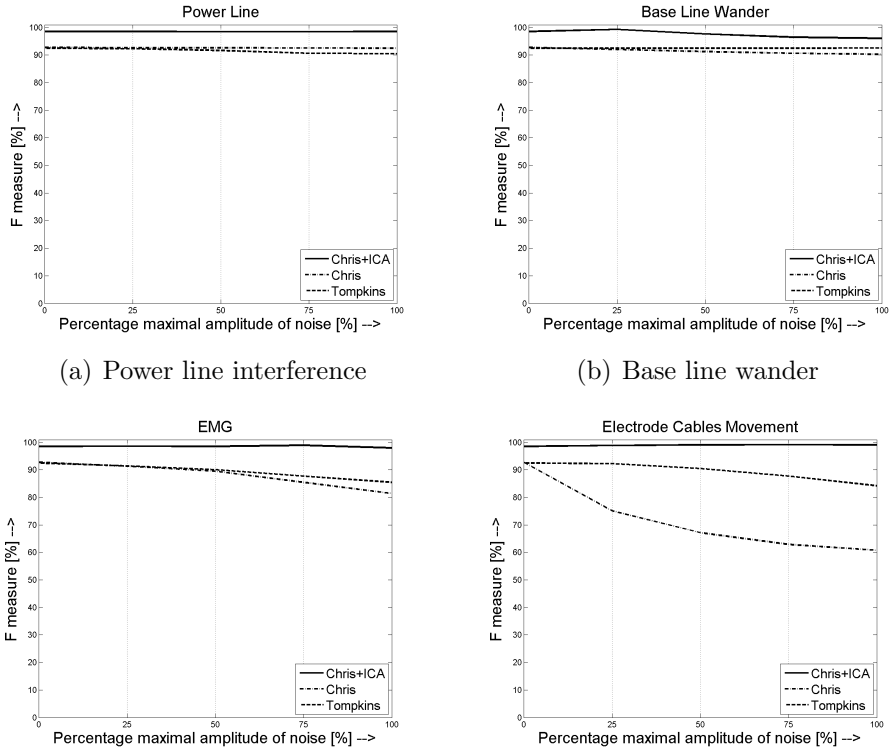

(a) Power line interference

(b) Base line wander

(c) EMG

(d) Electrode cable movement

Figure 8.11: Summarized values of F-measure for the developed algorithm and different types of artefacts on European ST-T database. We can observe that our algorithm works very efficiently and in case of electrode cable movement significantly outperforms other methods.

We can also observe that the performance of Christov's detector is similar or worse than the performance of Tompkins detector. The most significant difference lies in detection of QRS complex in presence of electrode cable movement artefact.

8.2.1.4 Results on Long Term ST database

Figure 8.12 shows results on Long Term ST database. We can again observe that our algorithm performance is stable in presence of all noise types and outperforms the performance of reference methods, whose results are similar to those on previous European ST-T database.

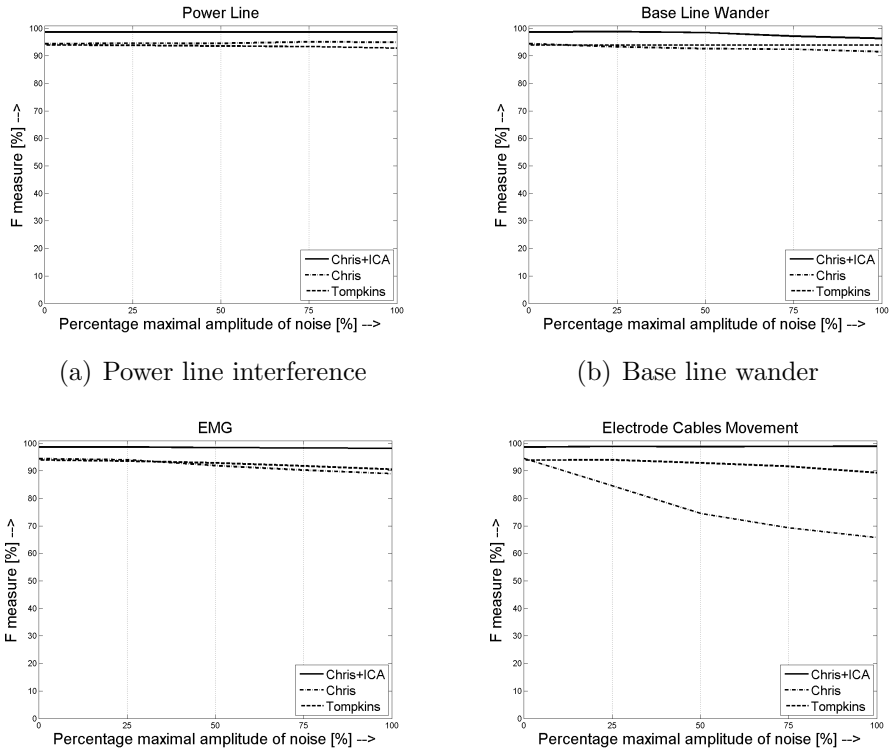

(a) Power line interference

(b) Base line wander

(c) EMG

(d) Electrode cable movement

Figure 8.12: Summarized values of F-measure for the developed algorithm and different types of artefacts on Long Term ST database. Again we can observe that Tompkins and Christov's algorithms has lower F-measure than our algorithm, which means that our algorithm is better.

8.2.1.5 Results on QT database

Figure 8.13 shows summarized results on QT database. As in previous cases, we can observe that our algorithm works very accurately. Referential methods perform with significantly lower accuracy in presence of electrode cable movement artefact and slightly worse in presence of stronger common noises. The performance of Christov's algorithm is similar or slightly worse in presence of standard noises to Tompkins algorithm, on the other hand, its performance in case of electrode cable movement artefact is strongly affected by this artefact. We can observe that Tompkins algorithm is nearly independent on presence of standard artefacts in ECG.

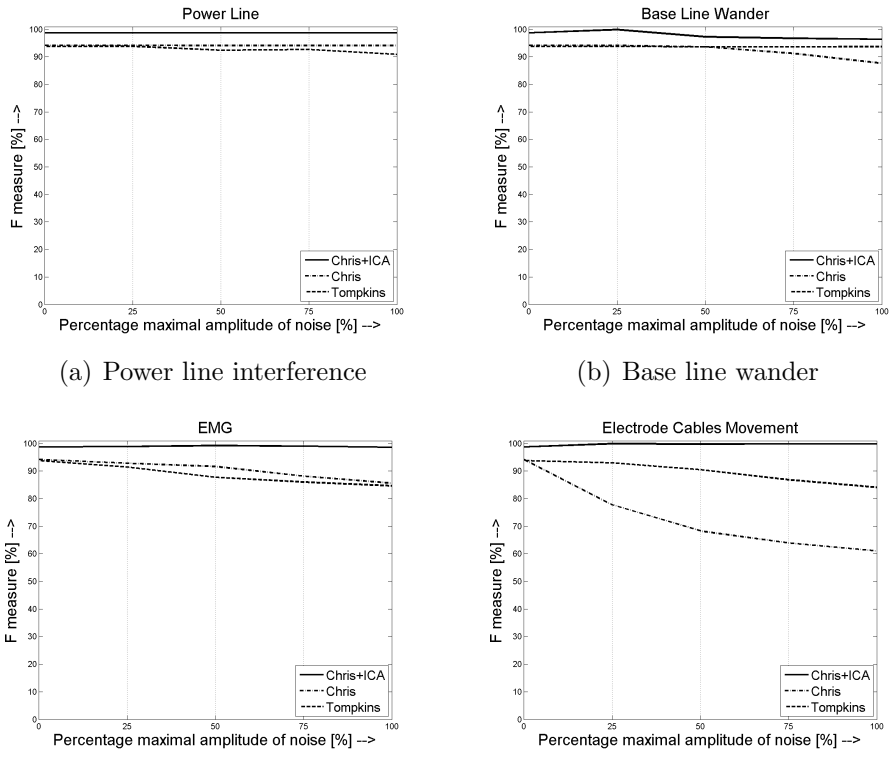

(a) Power line interference

(b) Base line wander

(c) EMG

(d) Electrode cable movement

Figure 8.13: Summarized values of F-measure for the developed algorithm and different types of artefacts on QT database. The performance of our algorithm is less affected by all types of noise due to extraction of ECG activity resulting in better performance than referential methods.

8.2.1.6 Results on MIT Long Term database

Figure 8.14 shows results on MIT Long Term database. We can observe that our algorithm accuracy is significantly increased due to ECG extraction step performed by JADE. On the other hand we can observe that Christov's algorithm accuracy is significantly decreased. We need to keep in mind that results on this database is affected by its size, which is only 7 recordings. Thus the information value of results is small. Again we can observe that Tompkins algorithm accuracy is nearly independent on what type of noise is presented in data – the signal transform performed by set of filters including differential filter makes the algorithm stable.

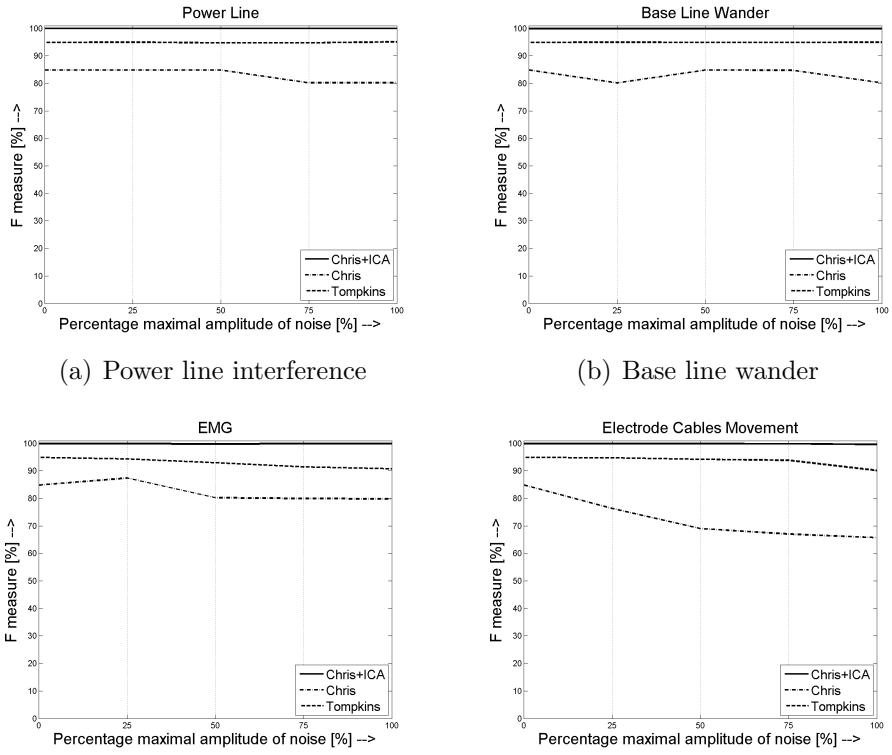

(a) Power line interference

(b) Base line wander

(c) EMG

(d) Electrode cable movement

Figure 8.14: Summarized values of F-measure for the developed algorithm and different types of artefacts on MIT Long Term database. On this database we can observe that Christov's algorithm performance is reduced. We still need to keep in mind that this database contains only 7 recordings, thus the results cannot be viewed as general performance.

8.2.1.7 Results on MIT-BIH ST Change database

Figure 8.16 shows results on MIT-BIH ST Change database. We can observe, again, that our method is able to detect QRS complexes much more accurately than the other tested methods and thus outperforms them in sense of F-measure characteristics.

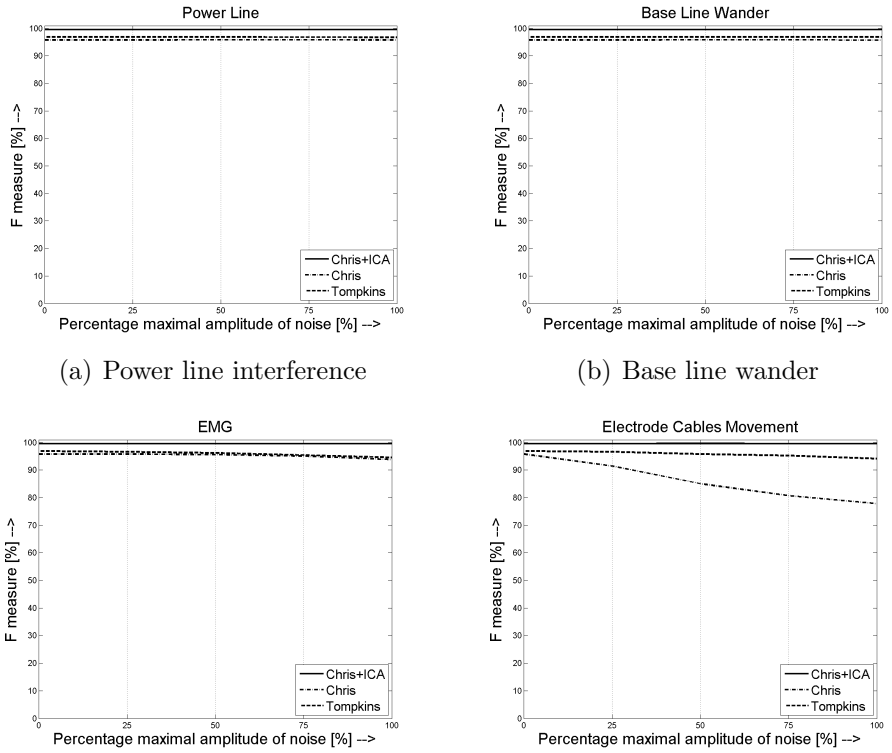

(a) Power line interference

(b) Base line wander

(c) EMG

(d) Electrode cable movement

Figure 8.15: Summarized values of F-measure for the developed algorithm and different types of artefacts on MIT-BIH ST Change database. Again our algorithm outperforms others on data contaminated with different types of noise.

8.2.1.8 Summary results on all databases

Figure 8.16 shows results across all databases. We can observe that performances of all algorithms are stable across all databases. Our algorithm is significantly less affected by electrode cable movement artefact than the others. The performance of both referential algorithms works similar in general on large scale data. One difference between them is in presence of electrode cable movement artefact, which affects significantly harder the performance of Christov's algorithm.

The final summary testing of our algorithm concludes with same result as testing on the partial data – the algorithm performs very stable and is very successful in beat detection.

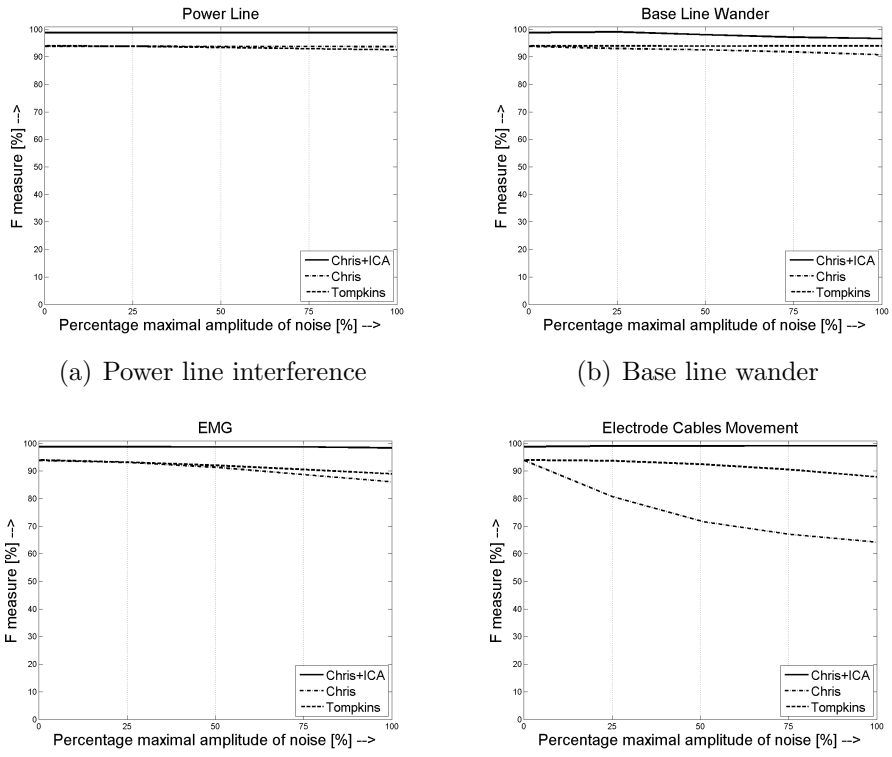

(a) Power line interference

(b) Base line wander

(c) EMG

(d) Electrode cable movement

Figure 8.16: Summarized values of F-measure for the developed algorithm and different types of artefacts on all databases. We can observe that enhancing Christov's original algorithm with JADE in order to enhance the ECG activity leads to significantly increased detection rates.

8.2.2 Conclusions

We have developed an extension of the well-known Christov's beat detection algorithm, which enables dealing with ECG signal highly corrupted by artefacts. Our method introduces JADE algorithm into the complex lead estimation step separating the ECG activity outside the other uninteresting activities, which can be considered as noises in case of beat detection. The JADE algorithm estimated independent components in sense of 4th order statistics.

Algorithm properties were tested on standard databases and its properties were compared to Christov's like beat detection algorithm and Tompkins like detection algorithm.

Tests were performed using simulated noises - power line interference, base line wander, EMG and electrode cable movement. First three noises are common types presented in recorded data and the last one is uncommon one. We decided to add this, because we are dealing with holter ECG recordings and this data contains many unpredictable noise events, which are not usual at all.

Our enhanced version of Christov's beat detection algorithm performs much more stable in presence of noise and it outperforms Christov's and Tompkins like algorithms, which are designed for the typical cases of resting ECGs.

Time requirements of our algorithm is increased only by computational complexity of JADE algorithm, which is one of the fastest BSS algorithms (it runs in milliseconds on 30 minutes 2 lead ECG sampled with sampling frequency 500 Hz, computational complexity could be found in [4, Ch. 18]). So the benefit of ECG activity estimation is much greater than loss of computational time. The amount of space required for data storing is also slightly increased - JADE algorithm stores several matrices with cumulants and the amount of data stored is dependent on number of ECG leads.

Chapter 9

Conclusions

We have developed new algorithms for de-noising and beat detection of ECG signals. We also created extensive state-of-the-art of ICA applications in biomedical research area. This chapter summarizes our results.

Create state-of-the-art of ICA applications in Biomedical Engineering research area with main focus on application in ECG signal processing.

We provided a review of most frequent ICA algorithms and their applications to biomedical signal processing. In detail it is described in Chapter 3.

Independent Component Analysis is a general tool, which could uncover hidden processes within the biomedical signal. The last decade in research proves that ICA has been successfully used in many research areas ranging from traditional areas such as EEG or ECG research to more unconventional such as fMRI or EGG signals analysis.

The power of ICA lies in its basic assumptions - thus it can found processes that cannot be found by any other technique. However results of separation by ICA should be investigated carefully. ICA is a data driven technique and results could seem great but the opposite might be true. The knowledge about data is necessary for differentiation of good and bad separation result. For example we need to be able to differentiate between noise and ECG activity within the estimated component and we need also identify problematic separation, which could have great impact on results.

Many algorithms for solving ICA/BSS task emerged, but only few are commonly used in biomedical research. The best method for biomedical area cannot be selected and one

should test several algorithms when searching for the best suited one for the researched application. Each algorithm has different assumptions, which need to be satisfied. Loosing assumptions from mind could lead to wrong conclusions.

We went through a large amount of papers covering most of the biomedical research using ICA. Several questions arose during this work. First and most crucial question is the reproducibility of experiments – many papers provide relatively clear algorithm explanation, but the algorithm testing is performed on unpublished data, which were collected by the authors of those papers. So the main problem is that nobody could say whether the implementation of proposed method works correctly because it cannot be tested on the same dataset. With this problem several others come – there are not many standard databases freely available online. Of course there are well-known exceptions such as Physionet.org databases. The most reasonable solution is to make data freely available or to test algorithms on both data – own and standard data.

Another problem that many papers have is lack of time and memory requirements of the developed method (algorithm). Also there are missing crucial information such as computer and software specifications, on which the experiments were performed.

According to our opinion, the best solution for solving all these problems is to make implementations of the algorithm freely available to download. This will solve many questions and difficulties, which nowadays researchers deal with. For ICA algorithms there exists an online database of ICA algorithms implementations - ICALAB [148], which could serve as an example to others.

The idea we posted here is not new. We can mention a very interesting paper written by Patrick Vandewalle [149], which deals with similar questions in the area of signal processing.

Based on our extensive analysis of current research efforts in biomedical ICA applications we decided to develop two algorithms. One for de-noising of ECG signals obtained during measuring of holter ECG and second for beat detection in cases of noisy ECG recordings.

Propose and develop the algorithm for denoising of ECG signals using ICA.

We created an algorithm for artefact reduction from ECG. Our algorithm is capable to deal with strong noise in ECG data and enables QRS detection and visual examination (for details see Chapter 5). The algorithm deals with uncommon noises presented in ECG data during holter and telemedicine applications. Our method connects well-known JADE algorithm with decision tree in order to identify noise and reduce it.

Method behaviour was tested on standard databases and it was compared to common filtering and Wavelet threshold de-noising techniques. Tests were performed using simulated noises (3 common and 1 uncommon).

Our method performed similar or better than both referential methods in presence of all common types of artefacts. Our method was the only one method that successfully reduced the electrode cable movement artefact. In that case both referential methods performance was decreased with stronger noise presented.

JADE based filtering has one advantage against both referential methods – our method least distorts the resulting signal in case of no noise presented in data. This ability is very valuable in medical applications. Time requirements of our algorithm is increased due computational complexity of JADE algorithm and Pan-Tompkins beat detection algorithm (used in feature extraction step), but changing the BSS or QRS complex detection algorithm will lead to better time performance. Memory requirements are also slightly increased but the advantage of our method outperforms its flaws, especially with nowadays hardware development.

Propose and develop the algorithm for beat detection using ICA.

We have developed an extension of the well-known Christov's beat detection algorithm, which enables dealing with ECG signal highly corrupted by artefacts (for details see Chapter 6). Our method introduces JADE algorithm into the complex lead estimation step separating the ECG activity outside the other uninteresting activities, which can be considered as noises in case of beat detection.

Algorithm properties were tested on standard databases and its properties were compared to Christov's like beat detection algorithm and Tompkins like detection algorithm. Tests were performed using simulated noises - power line interference, base line wander,

EMG and electrode cable movement. First three noises are common types presented in recorded data and the last one is uncommon one. We decided to add this, because we are dealing with holter ECG recordings and this data contains many unpredictable noise events, which are not usual at all.

Our enhanced version of Christov's beat detection algorithm performs much more stable in presence of noise and it outperformed Christov's and Tompkins like algorithms, which are designed for the typical cases of resting ECGs.

The computational complexity of our algorithm is increased only by computational complexity of JADE algorithm, which is one of the fastest BSS algorithms. So the benefit of ECG activity estimation is much greater than loss of computational time. The amount of space required for data storing is also slightly increased - JADE algorithm stores several matrices with cumulants and the amount of data stored is dependent on number of ECG leads.

Develop a testing framework for evaluation of proposed algorithms.

We developed the standardized procedure, which enables us to test performance of our algorithms against the state-of-the-art methods (see Chapter 7). This procedure is versatile and modular, thus we used it in testing of both methods. The information was easily obtained and analysed. Our framework enables us effective tuning of the methods.

Final remarks and future work

All goals we formulated were successfully fulfilled. We proposed two algorithms – one for de-noising of ECG recording containing noise and second the algorithm for beat detection with noisy ECG recordings. Both algorithms were tested using our testing framework against the state-of-the-art methods and results are good. Both algorithms are capable to deal with common types of noises and also with uncommon ones. This makes them very useful in applications within telemedicine issues and holter recordings, where the environment is rapidly changing and the distortions corrupting ECG signals could be very different for those normally present in ECG within laboratory or ambulatory measurement of ECG.

Our future work will aim at extensive testing of our developed algorithms. We will also test different ICA algorithms within our developed methods in order to test their dependency on performance of used BSS algorithm. We also plan to test new decision algorithms for recognition of noisy components in order to enhance algorithms performance.

Appendix A: Detailed results of de-noising algorithms

Tables show detailed results visualised in graphs plotted

Tables are organized as follows: each type of noise corresponds to one row of the table, each column of the table corresponds to one type of algorithm and noise level (for details see. 7.1.2) used during testing. On top of every four columns, which corresponds to one tested algorithm, one can find performance of corresponding algorithm on clear signal.

We can observe the same results as in above mentioned graphs. Our method is capable to deal with strong noises and also reduce the electrode cable movement artefact efficiently. We can also observe that our method is stable in presence of any type of noise.

ECG signals values is in units of mV, thus the values of RMS around 40 μV should be considered as very good result. They mean that the noise reduction in ECG signal is good enough to preserve ECG signal diagnostics. We can observe that our method provides slightly worse results, but these results are stable in presence of any noise of any strength. This is very desired feature of any ECG signal processing algorithm.

	RMS [μV]											
	ICA filter				Basic Filtering				Wavelet denoising			
Clear signal	34.40				123.97				56.98			
Noise type	Noise level [%]				Noise level [%]				Noise level [%]			
	25	50	75	100	25	50	75	100	25	50	75	100
Power Line Interference	65.58	68.83	67.19	66.64	123.97	123.97	123.97	123.97	66.28	67.20	67.41	67.60
EMG	47.43	63.27	75.96	91.31	131.46	148.33	170.28	195.32	62.79	72.40	82.69	92.86
Base Line Wander	148.07	191.22	198.85	196.15	126.54	132.14	138.87	146.03	189.08	360.17	534.82	710.49
Electrode Cable Movement	155.52	195.36	206.56	210.91	203.88	330.21	465.11	603.35	201.24	385.12	571.72	758.67

Table 1: Detailed summary results on all databases

APPENDIX A: DETAILED RESULTS OF DE-NOISING ALGORITHMS

	RMS [μV]											
	ICA filter				Basic Filtering				Wavelet denoising			
Clear signal	40.59				167.55				53.73			
Noise type	Noise level [%]				Noise level [%]				Noise level [%]			
	25	50	75	100	25	50	75	100	25	50	75	100
Power Line Interference	68.22	56.38	51.69	49.60	167.55	167.55	167.55	167.55	62.65	63.48	63.60	63.79
EMG	53.19	63.47	78.24	92.36	171.32	181.59	196.68	215.25	57.82	66.20	75.81	85.45
Base Line Wander	152.82	196.45	207.80	205.55	169.66	174.42	180.23	186.47	187.30	359.12	534.09	709.94
Electrode Cable Movement	163.78	217.77	208.39	218.47	234.13	351.42	481.53	616.81	199.61	383.98	570.82	757.84

Table 2: Detailed results on MIT/BIH Arrhythmia Database

	RMS [μV]											
	ICA filter				Basic Filtering				Wavelet denoising			
Clear signal	41.36				96.01				66.60			
Noise type	Noise level [%]				Noise level [%]				Noise level [%]			
	25	50	75	100	25	50	75	100	25	50	75	100
Power Line Interference	74.71	63.72	71.50	69.07	96.01	96.01	96.01	96.01	82.34	85.01	85.22	85.36
EMG	50.71	63.13	84.81	98.38	103.23	121.18	145.22	172.82	72.40	82.56	94.98	108.29
Base Line Wander	140.86	152.15	160.26	151.70	97.18	101.92	108.64	116.27	191.04	361.05	535.39	710.92
Electrode Cable Movement	142.42	152.63	149.84	151.88	180.19	312.26	450.71	591.46	202.92	385.88	572.46	759.51

Table 3: Detailed results on Normal Sinus Rhythm Database

	RMS [μV]											
	ICA filter				Basic Filtering				Wavelet denoising			
Clear signal	31.84				140.13				46.29			
Noise type	Noise level [%]				Noise level [%]				Noise level [%]			
	25	50	75	100	25	50	75	100	25	50	75	100
Power Line Interference	65.37	67.99	63.82	62.02	140.13	140.13	140.13	140.13	54.28	54.65	54.82	55.01
EMG	45.00	58.16	67.17	80.35	146.98	162.37	182.29	204.97	52.38	61.51	70.62	79.16
Base Line Wander	152.36	196.43	192.80	189.36	142.03	146.52	152.08	158.07	184.63	357.65	533.09	709.19
Electrode Cable Movement	159.95	189.42	198.31	201.99	213.44	336.42	469.54	606.66	196.94	382.61	569.74	756.83

Table 4: Detailed results on European ST-T database

	RMS [μV]											
	ICA filter				Basic Filtering				Wavelet denoising			
Clear signal	26.56				119.86				57.39			
Noise type	Noise level [%]				Noise level [%]				Noise level [%]			
	25	50	75	100	25	50	75	100	25	50	75	100
Power Line Interference	55.22	62.96	62.74	64.83	119.86	119.86	119.86	119.86	65.89	66.18	66.32	66.49
EMG	36.35	55.64	71.98	89.62	125.96	141.08	161.64	185.50	62.80	72.38	83.03	93.50
Base Line Wander	140.05	185.75	190.66	195.30	122.48	127.98	134.58	141.62	188.42	359.79	534.56	710.31
Electrode Cable Movement	146.93	185.35	213.00	204.55	202.84	329.69	464.58	602.78	200.83	385.18	571.85	758.80

Table 5: Detailed results on Long Term ST database

	RMS [μV]											
	ICA filter				Basic Filtering				Wavelet denoising			
Clear signal	38.37				83.78				52.14			
Noise type	Noise level [%]				Noise level [%]				Noise level [%]			
	25	50	75	100	25	50	75	100	25	50	75	100
Power Line Interference	67.43	76.04	73.28	72.16	83.78	83.78	83.78	83.78	61.76	62.79	63.04	63.27
EMG	49.33	67.74	76.76	92.43	95.64	118.87	146.75	177.20	58.98	68.93	78.85	88.71
Base Line Wander	141.17	167.44	181.08	167.93	87.49	95.15	103.95	113.01	188.23	359.76	534.53	710.26
Electrode Cable Movement	148.07	175.63	182.35	189.02	176.22	311.40	451.07	592.24	200.13	384.14	570.82	757.92

Table 6: Detailed results on QT database

	RMS [μV]											
	ICA filter				Basic Filtering				Wavelet denoising			
Clear signal	29.78				176.82				75.57			
Noise type	Noise level [%]				Noise level [%]				Noise level [%]			
	25	50	75	100	25	50	75	100	25	50	75	100
Power Line Interference	57.75	76.90	80.57	85.11	176.82	176.82	176.82	176.82	88.28	93.34	94.64	94.81
EMG	98.60	108.73	126.04	144.77	184.99	205.51	233.45	266.14	83.80	97.91	112.94	128.60
Base Line Wander	164.79	288.66	292.64	272.36	179.68	186.17	193.99	202.16	193.61	362.39	536.28	711.59
Electrode Cable Movement	173.65	299.37	297.49	272.79	244.06	360.36	489.42	624.22	205.77	387.67	573.90	761.21

Table 7: Detailed results on MIT Long Term database

	RMS [μV]											
	ICA filter				Basic Filtering				Wavelet denoising			
Clear signal	38.41				123.38				99.37			
Noise type	Noise level [%]				Noise level [%]				Noise level [%]			
	25	50	75	100	25	50	75	100	25	50	75	100
Power Line Interference	81.89	90.05	93.15	92.71	123.38	123.38	123.38	123.38	111.29	113.62	113.93	114.09
EMG	56.34	76.69	91.08	108.26	131.51	151.04	177.01	206.67	105.28	116.60	130.00	143.65
Base Line Wander	165.03	241.71	269.39	284.80	126.02	131.09	137.19	143.95	208.61	371.37	542.54	716.36
Electrode Cable Movement	171.68	252.84	282.56	319.58	203.72	329.45	464.57	602.99	220.20	396.70	580.90	766.86

Table 8: Detailed results on MIT-BIH ST Change database

APPENDIX B: DETAILED RESULTS OF DE-NOISING ALGORITHMS

Appendix B: Detailed results of beat detection algorithms

Tables show detailed results visualised in graphs plotted on Fig.

Tables are organized as follows: each type of noise corresponds to one row of the table, each column of the table corresponds to one type of algorithm and noise level (for details see. 7.1.2) used during testing. On top of every four columns, which corresponds to one tested algorithm, one can find performance of corresponding algorithm on clear signal.

Again we can observe the same results as in above mentioned graphs. Our method proves to be more robust to noises than other beat detection methods with one exception - the base line wander artefact, when the estimation of components converge to solution with divided sinus wave into several components with kurtosis higher than standard ECG activity.

We can observe that our method has same performance as original Christov's algorithm, but its strength lies in suppression of irregular types of noises, for which the original Christov's algorithm was not designed.

	F-measure [%]											
	Christov's algorithm + ICA				Christov's algorithm				Hammilton's algorithm			
Clear signal	98.81				93.88				93.99			
Noise type	Noise level [%]				Noise level [%]				Noise level [%]			
	25	50	75	100	25	50	75	100	25	50	75	100
Power Line Interference	98.81	98.80	98.80	98.81	93.89	93.83	93.82	93.76	93.90	93.44	92.98	92.57
EMG	98.85	98.78	98.79	98.39	93.12	91.37	88.69	86.13	93.29	92.10	90.60	89.01
Base Line Wander	99.11	98.09	97.17	96.69	93.05	92.58	91.82	90.81	93.98	93.98	93.98	94.00
Electrode Cable Movement	99.08	99.13	99.19	99.20	80.71	71.87	67.14	64.21	93.77	92.48	90.57	87.91

Table 9: Detailed summarized results on all databases

APPENDIX B: DETAILED RESULTS OF DE-NOISING ALGORITHMS

	F-measure [%]											
	Christov's algorithm + ICA				Christov's algorithm				Hammilton's algorithm			
Clear signal	99.07				94.02				96.61			
Noise type	Noise level [%]				Noise level [%]				Noise level [%]			
	25	50	75	100	25	50	75	100	25	50	75	100
Power Line Interference	99.07	99.07	99.07	99.07	94.03	93.82	93.81	93.80	96.52	96.43	96.04	95.86
EMG	99.04	99.02	98.70	98.52	93.15	92.52	88.92	85.85	96.37	95.41	94.45	92.86
Base Line Wander	98.30	96.49	96.18	96.04	93.93	93.33	90.67	89.65	96.61	96.61	96.59	96.59
Electrode Cable Movement	98.99	99.09	99.24	99.22	79.81	69.12	64.71	62.47	95.89	95.23	93.05	90.63

Table 10: Detailed results on MIT/BIH Arrhythmia Database

	F-measure [%]											
	Christov's algorithm + ICA				Christov's algorithm				Hammilton's algorithm			
Clear signal	99.17				99.24				95.17			
Noise type	Noise level [%]				Noise level [%]				Noise level [%]			
	25	50	75	100	25	50	75	100	25	50	75	100
Power Line Interference	99.17	99.17	99.17	99.17	99.24	99.24	99.24	99.24	95.00	94.73	94.22	93.87
EMG	99.17	99.11	98.98	98.93	98.46	99.02	97.86	96.02	94.90	94.36	93.68	92.98
Base Line Wander	99.22	99.22	99.11	99.00	99.15	98.34	97.85	97.40	95.18	95.16	95.16	95.15
Electrode Cable Movement	99.23	99.22	99.24	99.24	91.96	87.00	79.19	72.98	94.87	94.94	94.98	94.31

Table 11: Detailed results on Normal Sinus Rhythm Database

	F-measure [%]											
	Christov's algorithm + ICA				Christov's algorithm				Hammilton's algorithm			
Clear signal	98.55				92.76				92.50			
Noise type	Noise level [%]				Noise level [%]				Noise level [%]			
	25	50	75	100	25	50	75	100	25	50	75	100
Power Line Interference	98.53	98.52	98.52	98.52	92.65	92.62	92.54	92.53	92.33	91.66	90.67	90.52
EMG	98.65	98.56	98.95	98.04	91.36	89.52	85.46	81.46	91.48	90.11	87.77	85.51
Base Line Wander	99.28	97.67	96.52	96.08	92.04	91.28	90.66	90.29	92.50	92.50	92.53	92.55
Electrode Cable Movement	98.93	99.10	99.20	99.14	75.12	67.18	62.94	60.76	92.27	90.50	87.75	84.25

Table 12: Detailed results on European ST-T database

	F-measure [%]											
	Christov's algorithm + ICA				Christov's algorithm				Hammilton's algorithm			
Clear signal	98.72				94.46				93.93			
Noise type	Noise level [%]				Noise level [%]				Noise level [%]			
	25	50	75	100	25	50	75	100	25	50	75	100
Power Line Interference	98.71	98.71	98.71	98.71	94.62	94.54	95.14	94.99	93.88	93.61	93.39	92.84
EMG	98.69	98.52	98.34	98.21	94.09	91.92	90.32	89.02	93.61	92.89	91.83	90.58
Base Line Wander	98.83	98.51	97.19	96.35	93.35	92.62	92.41	91.53	93.93	93.93	93.93	93.94
Electrode Cable Movement	98.87	98.87	98.88	98.99	84.60	74.57	69.33	65.73	94.00	92.92	91.66	89.37

Table 13: Detailed results on Long Term ST database

	F-measure [%]											
	Christov's algorithm + ICA				Christov's algorithm				Hammilton's algorithm			
Clear signal	98.75				94.23				93.84			
Noise type	Noise level [%]				Noise level [%]				Noise level [%]			
	25	50	75	100	25	50	75	100	25	50	75	100
Power Line Interference	98.76	98.76	98.76	98.76	94.22	94.15	94.14	94.13	93.87	92.45	92.68	90.94
EMG	98.89	99.26	99.05	98.61	92.85	91.64	88.19	85.63	91.45	87.77	86.06	84.63
Base Line Wander	99.94	97.33	96.77	96.44	94.16	93.66	91.27	87.71	93.82	93.70	93.70	93.77
Electrode Cable Movement	99.94	99.77	99.87	99.86	77.75	68.32	63.98	61.08	92.97	90.49	86.85	84.12

Table 14: Detailed results on QT database

	F-measure [%]											
	Christov's algorithm + ICA				Christov's algorithm				Hammilton's algorithm			
Clear signal	99.94				84.85				94.93			
Noise type	Noise level [%]				Noise level [%]				Noise level [%]			
	25	50	75	100	25	50	75	100	25	50	75	100
Power Line Interference	99.94	99.94	99.94	99.94	84.85	84.86	80.28	80.29	94.98	94.77	94.78	95.12
EMG	99.92	99.80	99.94	99.94	87.39	80.29	79.95	79.85	94.33	92.98	91.47	90.79
Base Line Wander	99.96	99.95	99.96	99.96	80.25	84.83	84.80	80.20	94.95	94.94	94.94	94.96
Electrode Cable Movement	99.96	99.94	99.87	99.63	76.34	69.03	67.08	65.74	94.75	94.22	93.88	90.14

Table 15: Detailed results on MIT Long Term database

	F-measure [%]											
	Christov's algorithm + ICA				Christov's algorithm				Hammilton's algorithm			
Clear signal	99.57				95.82				96.87			
Noise type	Noise level [%]				Noise level [%]				Noise level [%]			
	25	50	75	100	25	50	75	100	25	50	75	100
Power Line Interference	99.57	99.57	99.57	99.57	95.83	95.87	95.86	95.83	96.90	96.89	96.84	96.74
EMG	99.57	99.57	99.58	99.59	95.81	95.58	95.15	93.83	96.65	96.18	95.44	94.56
Base Line Wander	99.60	99.62	99.61	99.58	95.80	95.87	95.85	95.72	96.88	96.89	96.89	96.89
Electrode Cable Movement	99.61	99.63	99.62	99.61	91.49	85.06	80.77	77.88	96.64	95.83	95.28	94.15

Table 16: Detailed results on MIT-BIH ST Change database

References

[1] A. Belouchrani, K. Abed-Meraim, J. F. Cardoso, and E. Moulines, "A blind source separation technique using second-order statistics," *Signal Processing, IEEE Transactions on*, vol. 45, no. 2, pp. 434–444, 1997. 1, 11

[2] A. Hyvarinen and E. Oja, "Independent component analysis: algorithms and applications," *Neural Netw.*, vol. 13, pp. 411–430, May 2000. 1, 5, 7, 8

[3] J. F. Cardoso and A. Souloumiac, "Blind beamforming for non-gaussian signals," *Radar and Signal Processing, IEE Proceedings F*, vol. 140, no. 6, pp. 362–370, 1993. 1, 10, 42

[4] P. Comon and C. Jutten, *Handbook of Blind Source Separation.* Elsevier, 2010. 1, 35, 48, 83

[5] T. He, G. Clifford, and L. Tarassenko, "Application of independent component analysis in removing artefacts from the electrocardiogram," *Neural Computing & Applications*, vol. 15, no. 2, pp. 105–116, 2006. 1, 15, 35, 48

[6] M. P. S. Chawla, "Pca and ica processing methods for removal of artifacts and noise in electrocardiograms: A survey and comparison," *Applied Soft Computing Journal*, vol. 11, no. 2, pp. 2216–2226, 2011. 1, 18, 35, 41, 48

[7] A. L. Goldberger, L. A. N. Amaral, L. Glass, J. M. Hausdorff, P. C. Ivanov, R. G. Mark, J. E. Mietus, G. B. Moody, C. K. Peng, and H. E. Stanley, "PhysioBank, PhysioToolkit, and PhysioNet : Components of a New Research Resource for Complex Physiologic Signals," *Circulation*, vol. 101, pp. e215–220, June 2000. 4, 17, 51, 52

[8] A. Hyvärinen, J. Karhunen, and E. Oja, *Independent Component Analysis*. Wiley, 2001. 5, 8, 10

[9] P. Comon, "Independent component analysis, a new concept?," *Signal Process.*, vol. 36, pp. 287–314, April 1994. 5

[10] R. E. Walpole, R. H. Myers, S. L. Myers, and K. E. Ye, *Probability and Statistics for Engineers and Scientists*. Prentice Hall, 2011. 8

[11] J. F. Cardoso, "Source separation using higher order moments," in *Acoustics, Speech, and Signal Processing, 1989. ICASSP-89., 1989 International Conference on*, pp. 2109–2112 vol.4, 1989. 9

[12] L. Molgedey and H. G. Schuster, "Separation of a mixture of independent signals using time delayed correlations," *Physical Review Letters*, vol. 72, pp. 3634–3637, 1994. 10

[13] J. O. Wisbeck, A. K. Barros, A. K. B. Yy, and R. G. Ojeda, "Application of ica in the separation of breathing artifacts in ecg signals," 1998. 15

[14] A. K. Barros, A. Mansour, and N. Ohnishi, "Removing artifacts from electrocardiographic signals using independent components analysis," *Neurocomputing*, vol. 22, pp. 173–186, 11/20 1998. 15

[15] M. P. S. Chawla, H. K. Verma, and V. Kumar, "Artifacts and noise removal in electrocardiograms using independent component analysis," *International journal of cardiology*, vol. 129, pp. 278–281, 9/26 2008. 15

[16] H. Xing and J. Hou, "A noise elimination method for ecg signals," in *Bioinformatics and Biomedical Engineering , 2009. ICBBE 2009. 3rd International Conference on*, pp. 1–3, 2009. 15

[17] M. Milanesi, N. Martini, N. Vanello, V. Positano, M. F. Santarelli, and L. Landini, "Independent component analysis applied to the removal of motion artifacts from electrocardiographic signals," *Medical & biological engineering & computing*, vol. 46, pp. 251–261, MAR 2008. 15, 16

[18] G. Agrawal, M. Singh, V. R. Singh, and H. R. Singh, "Reduction of artifacts in 12-channel ecg signals using fastica algorithm," *JOURNAL OF SCIENTIFIC & INDUSTRIAL RESEARCH*, vol. 67, pp. 43–48, JAN 2008. 15

[19] F. Castells, A. Cebrian, and J. Millet, "The role of independent component analysis in the signal processing of ecg recordings," *BIOMEDIZINISCHE TECHNIK*, vol. 52, no. 1, pp. 18–24, 2007. 15

[20] M. P. S. Chawla, "Pca and ica processing methods for removal of artifacts and noise in electrocardiograms: A survey and comparison," *APPLIED SOFT COMPUTING*, vol. 11, pp. 2216–2226, MAR 2011. 15, 16

[21] M. Milanesi, N. Martini, N. Vanello, V. Positano, M. F. Santarelli, R. Paradiso, D. D. Rossi, and L. Landini 2006. 15

[22] A. Acharyya, K. Maharatna, B. M. Al-Hashimi, and S. Mondal, "Robust Channel Identification Scheme: Solving Permutation Indeterminacy of ICA for Artifacts Removal from ECG," in *2010 ANNUAL INTERNATIONAL CONFERENCE OF THE IEEE ENGINEERING IN MEDICINE AND BIOLOGY SOCIETY (EMBC)*, IEEE Engineering in Medicine and Biology Society Conference Proceedings, pp. 1142–1145, IEEE Engn Med & Biol Soc (EMBS), 2010. 32nd Annual International Conference of the IEEE Engineering-in-Medicine-and-Biology-Society (EMBC 10), Buenos Aires, ARGENTINA, AUG 30-SEP 04, 2010. 15, 16

[23] D. DiPietroPaolo, H.-P. Mueller, G. Nolte, and S. N. Erne, "Noise reduction in magnetocardiography by singular value decomposition and independent component analysis," *MEDICAL & BIOLOGICAL ENGINEERING & COMPUTING*, vol. 44, pp. 489–499, JUN 2006. 15, 16

[24] Y. Tu, X. Fu, D. Li, C. Huang, Y. Tang, S. Ye, and H. Chen, "A Novel Method for Automatic Identification of Motion Artifact Beats in ECG Recordings," *ANNALS OF BIOMEDICAL ENGINEERING*, vol. 40, pp. 1917–1928, SEP 2012. 15

[25] J. Oster, O. Pietquin, R. Abaecherli, M. Kraemer, and J. Felblinger, "Independent component analysis-based artefact reduction: application to the electrocardiogram for improved magnetic resonance imaging triggering," *PHYSIOLOGICAL MEASUREMENT*, vol. 30, pp. 1381–1397, DEC 2009. 15, 16

[26] I. Romero, "PCA and ICA applied to Noise Reduction in Multi-lead ECG," in *2011 COMPUTING IN CARDIOLOGY*, pp. 613–616, European Soc Cardiol; Zhejiang Univ; EMB; IEEE; Drager; Mortara; Philips; Univ Rochester, Telemetr & Holter ECG Warehouse; Physiol Measurement; Mindray; GE Healthcare; Zoll; Edan;

GSMA, 2011. Conference on Computing in Cardiology, Hangzhou, PEOPLES R CHINA, SEP 18-21, 2011. 15

[27] J. L. Willems, C. Abreu-Lima, P. Arnaud, J. H. van Bemmel, C. Brohet, R. Degani, B. Denis, J. Gehring, I. Graham, G. van Herpen, H. Machado, P. W. Macfarlane, J. Michaelis, S. D. Moulopoulos, P. Rubel, and C. Zywietz, "The diagnostic performance of computer programs for the interpretation of electrocardiograms," *New England Journal of Medicine*, vol. 325, no. 25, pp. 1767–1773, 1991. 16

[28] A. Ziehe and K.-R. Müller, "Tdsep - an efficient algorithm for blind separation using time structure," 1998. 16

[29] L. D. Lathauwer, B. D. Moor, J. Vandewalle, G. Spain, L. D. Lathauwer, D. Callaerts, and B. D. Moor, "Fetal electrocardiogram extraction by source subspace separation," in *In Proc. HOS'95*, pp. 134–138, 1994. 16

[30] L. D. Lathauwer, B. D. Moor, and J. Vandewalle, "Fetal electrocardiogram extraction by blind source subspace separation," *IEEE Trans.Biomed.Eng*, vol. 47, pp. 567–572, 2000. 16

[31] J. F. Cardoso, "Fetal electrocardiogram extraction by source subspace separation," in *IEEE International Conference on Acoustics Speech and Signal Processing*, pp. 1941–1944, 1998. 16

[32] V. Zarzoso and A. K. Nandi, "Noninvasive fetal electrocardiogram extraction: blind separation versus adaptive noise cancellation," *Biomedical Engineering, IEEE Transactions on*, vol. 48, no. 1, pp. 12–18, 2001. 16

[33] R. Sameni, C. Jutten, and M. B. Shamsollahi, "What ICA provides for ECG processing: Application to noninvasive fetal ECG extraction," in *2006 IEEE International Symposium on Signal Processing and Information Technology, Vols 1 and 2*, pp. 656–661, IEEE Comp Soc; IEEE Signal Proc Soc, 2006. 6th IEEE International Symposium on Signal Processing and Information Technology, Vancouver, CANADA, AUG 28-30, 2006. 16

[34] Y. Lee and S. Jiang, "Fetal Signal Reconstruction Based on Independent Components Analysis," in *2009 3RD INTERNATIONAL CONFERENCE ON BIOINFORMATICS AND BIOMEDICAL ENGINEERING, VOLS 1-11*, pp. 932–934, IEEE Engineering Med & Biol Soc; Gordon Life Sci Inst; Fudan Univ; Beijing Univ Posts &

Telecommunicat; Beijing Inst Technol; Wuhan Univ; Journal Biomed Sci & Engn, 2009. 3rd International Conference on Bioinformatics and Biomedical Engineering, Beijing, PEOPLES R CHINA, JUN 11-16, 2009. 16

[35] J. L. Camargo-Olivares, R. Martín-Clemente, S. Hornillo-Mellado, M. M. Elena, and I. Román, "The maternal abdominal ecg as input to mica in the fetal ecg extraction problem," *IEEE Signal Processing Letters*, vol. 18, no. 3, pp. 161–164, 2011. 17

[36] J. J. Rieta, V. Zarzoso, J. Millet-Roig, R. Garcia-Civera, and R. Ruiz-Granell, "Atrial activity extraction based on blind source separation as an alternative to qrst cancellation for atrial fibrillation analysis," in *Computers in Cardiology 2000*, pp. 69–72, 2000. 17

[37] J. J. Rieta, F. Castells, C. Sánchez, and J. Igual, "Ica applied to atrial fibrillation analysis," in *ICA 03*, (Nara, Japan), pp. 59–64, apr 2003. 17

[38] J. J. Rieta, F. Castells, C. Sanchez, V. Zarzoso, and J. Millet, "Atrial activity extraction for atrial fibrillation analysis using blind source separation," *Biomedical Engineering, IEEE Transactions on*, vol. 51, no. 7, pp. 1176–1186, 2004. 17

[39] F. Castells, J. J. Rieta, J. Millet, and V. Zarzoso, "Spatiotemporal blind source separation approach to atrial activity estimation in atrial tachyarrhythmias," *Biomedical Engineering, IEEE Transactions on*, vol. 52, no. 2, pp. 258–267, 2005. 17

[40] V. Zarzoso and P. Comon, "Robust independent component analysis for blind source separation and extraction with application in electrocardiography," in *Engineering in Medicine and Biology Society, 2008. EMBS 2008. 30th Annual International Conference of the IEEE*, pp. 3344 –3347, aug. 2008. 17

[41] F. Donoso, E. Lecannelier, E. Pino, and A. Rojas, *Reliable atrial activity extraction from ECG atrial fibrillation signals*, vol. 7042 LNCS of *Lecture Notes in Computer Science (including subseries Lecture Notes in Artificial Intelligence and Lecture Notes in Bioinformatics)*. 2011. 17

[42] D. Taralunga, M. Ungureanu, R. Strungaru, and W. Wolf, "Performance comparison of four ica algorithms applied for fecg extraction from transabdominal recordings," in *ISSCS 2011 - International Symposium on Signals, Circuits and Systems, Proceedings*, pp. 499–502, 2011. 17

[43] D. D. Taralunga, M. Ungureanu, W. Wolf, and R. Strungaru, "Atrial Fibrillation: Evaluation of the ESC/ICA method on simulated ECG signals," in *2011 E-HEALTH AND BIOENGINEERING CONFERENCE (EHB)*, Romania Sect; Romania Sect EMB Chapter; IEEE, 2011. 3rd International Conference on E-Health and Bioengineering (EHB), Univ Med & Pharm, Iasi, ROMANIA, NOV 24-26, 2011. 17

[44] S.-N. Yu and K.-T. Chou, "Integration of independent component analysis and neural networks for ecg beat classification," *EXPERT SYSTEMS WITH APPLICATIONS*, vol. 34, pp. 2841–2846, MAY 4 2008. 17

[45] S.-N. Yu and K.-T. Chou, "A switchable scheme for ecg beat classification based on independent component analysis," *EXPERT SYSTEMS WITH APPLICATIONS*, vol. 33, pp. 824–829, NOV 2007. 17

[46] S.-N. Yu and K.-T. Chou, "Selection of significant independent components for ECG beat classification," *EXPERT SYSTEMS WITH APPLICATIONS*, vol. 36, pp. 2088–2096, MAR 2009. 17

[47] R. O. Duda, D. G. Stork, and P. E. Hart, *Pattern classification and scene analysis.* Wiley, 2 ed., 2000. 18

[48] G. Moody and R. Mark, "The impact of the mit-bih arrhythmia database," *Engineering in Medicine and Biology Magazine, IEEE*, vol. 20, pp. 45 –50, may-june 2001. 18, 51

[49] Y. Wu and L. Zhang, *ECG classification using ICA features and support vector machines*, vol. 7062 LNCS of *Lecture Notes in Computer Science (including subseries Lecture Notes in Artificial Intelligence and Lecture Notes in Bioinformatics)*. 2011. 18

[50] K. Huang, L. Zhang, and Y. Wu, "Ecg classification based on non-cardiology feature," in *Advances in Neural Networks – ISNN 2012* (J. Wang, G. Yen, and M. Polycarpou, eds.), vol. 7368 of *Lecture Notes in Computer Science*, pp. 179–186, Springer Berlin / Heidelberg, 2012. 18

[51] U. Wiklund, M. Karlsson, N. Ostlund, L. Berglin, K. Lindecrantz, S. Karlsson, and L. Sandsjo, "Adaptive spatio-temporal filtering of disturbed ECGs: a multi-channel approach to heartbeat detection in smart clothing," *MEDICAL & BIOLOGICAL ENGINEERING & COMPUTING*, vol. 45, pp. 515–523, JUN 2007. 18

[52] M. P. S. Chawla, H. K. Verma, and V. Kumar, "A new statistical pca–ica algorithm for location of r-peaks in ecg," *International journal of cardiology*, vol. 129, pp. 146–148, 9/16 2008. 18

[53] R. Vetter, N. Virag, J. M. Vesin, P. Celka, and U. Scherrer, "Observer of autonomic cardiac outflow based on blind source separation of ecg parameters," *Biomedical Engineering, IEEE Transactions on*, vol. 47, no. 5, pp. 578–582, 2000. 18

[54] Y. Zhu, A. Shayan, W. Zhang, T. L. Chen, T.-P. Jung, J.-R. Duann, S. Makeig, and C.-K. Cheng, "Analyzing high-density ecg signals using ica," *Biomedical Engineering, IEEE Transactions on*, vol. 55, no. 11, pp. 2528–2537, 2008. 18

[55] M. Owis, A. Youssef, and Y. Kadah, "Characterisation of electrocardiogram signals based on blind source separation," *Medical and Biological Engineering and Computing*, vol. 40, no. 5, pp. 557–564, 2002. 10.1007/BF02345455. 18

[56] M. Granegger, T. Werther, and H. Gilly, "Use of independent component analysis for reducing CPR artefacts in human emergency ECGs," *RESUSCITATION*, vol. 82, pp. 79–84, JAN 2011. 18

[57] M. Granegger, T. Werther, M. Roehrich, and H. Gilly, "CPR Artifact Reduction in the Human ECG Using Independent Component Analysis," in *WORLD CONGRESS ON MEDICAL PHYSICS AND BIOMEDICAL ENGINEERING, VOL 25, PT 4: IMAGE PROCESSING, BIOSIGNAL PROCESSING, MODELLING AND SIMULATION, BIOMECHANICS* (Dossel, O and Schlegel, WC, ed.), vol. 25 of *IFMBE Proceedings*, pp. 980–983, IUPESM; IOMP, 2010. World Congress on Medical Physics and Biomedical Engineering, Munich, GERMANY, SEP 07-12, 2009. 18

[58] M. H. Ostertag and G. R. Tsouri, "Reconstructing ECG Precordial Leads from a Reduced Lead Set using Independent Component Analysis," in *2011 ANNUAL INTERNATIONAL CONFERENCE OF THE IEEE ENGINEERING IN MEDICINE AND BIOLOGY SOCIETY (EMBC)*, pp. 4414–4417, IEEE; Engn Med & Biol Soc (EMBS), 2011. 33rd Annual International Conference of the IEEE Engineering-in-Medicine-and-Biology-Society (EMBS), Boston, MA, AUG 30-SEP 03, 2011. 18

[59] V. Monasterio, G. D. Clifford, and J. Pablo Martinez, "Comparison of Source Separation Techniques for Multilead T-Wave Alternans Detection in the ECG," in *2010 ANNUAL INTERNATIONAL CONFERENCE OF THE IEEE ENGINEERING IN*

MEDICINE AND BIOLOGY SOCIETY (EMBC), IEEE Engineering in Medicine and Biology Society Conference Proceedings, pp. 5367–5370, IEEE Engn Med & Biol Soc (EMBS), 2010. 32nd Annual International Conference of the IEEE Engineering-in-Medicine-and-Biology-Society (EMBC 10), Buenos Aires, ARGENTINA, AUG 30-SEP 04, 2010. 19

[60] S. Makeig, A. J. Bell, T. ping Jung, and T. J. Sejnowski, "Independent component analysis of electroencephalographic data," in *Advances in Neural Information Processing Systems*, pp. 145–151, MIT Press, 1996. 19

[61] S. Makeig, T.-P. Jung, A. J. Bell, D. Ghahremani, and T. J. Sejnowski, "Blind separation of auditory event-related brain responses into independent components," *Proceedings of the National Academy of Sciences of the United States of America*, vol. 94, pp. 10979–10984, 09/30 1997. 19

[62] A. J. Bell and T. J. Sejnowski, "An information-maximization approach to blind separation and blind deconvolution.," *Neural computation*, vol. 7, no. 6, pp. 1129–1159, 1995. 19

[63] T.-P. Jung, S. Makeig, M. Westerfield, J. Townsend, E. Courchesne, and T. J. Sejnowski, "Removal of eye activity artifacts from visual event-related potentials in normal and clinical subjects," *Clinical Neurophysiology*, vol. 111, no. 10, pp. 1745 – 1758, 2000. 19

[64] T.-P. Jung, S. Makeig, M. Westerfield, J. Townsend, E. Courchesne, and T. J. Sejnowski, "Analysis and visualization of single-trial event-related potentials," *Human brain mapping*, vol. 14, pp. 166–185, 2001. 19

[65] R. Vigario, J. Sarela, V. Jousmiki, M. Hamalainen, and E. Oja, "Independent component approach to the analysis of eeg and meg recordings," *Biomedical Engineering, IEEE Transactions on*, vol. 47, no. 5, pp. 589–593, 2000. 19

[66] J. Richards, "Recovering dipole sources from scalp-recorded event-related-potentials using component analysis: principal component analysis and independent component analysis," *INTERNATIONAL JOURNAL OF PSYCHOPHYSIOLOGY*, vol. 54, pp. 201–220, NOV 2004. 19

[67] S. Debener, S. Makeig, A. Delorme, and A. K. Engel, "What is novel in the novelty oddball paradigm? functional significance of the novelty p3 event-related potential

as revealed by independent component analysis," *Cognitive Brain Research*, vol. 22, pp. 309–321, 3 2005. 19

[68] A. Delorme and S. Makeig, "Eeglab: An open source toolbox for analysis of single-trial eeg dynamics including independent component analysis," *Journal of neuroscience methods*, vol. 134, no. 1, pp. 9–21, 2004. 19

[69] S. Debener, J. Hine, S. Bleeck, and J. Eyles, "Source localization of auditory evoked potentials after cochlear implantation," *PSYCHOPHYSIOLOGY*, vol. 45, pp. 20–24, JAN 2008. 19

[70] H. Liu, C. Q. Chang, K. D. K. Luk, and Y. Hu, "Comparison of Blind Source Separation Methods in Fast Somatosensory-Evoked Potential Detection," *JOURNAL OF CLINICAL NEUROPHYSIOLOGY*, vol. 28, pp. 170–177, APR 2011. 19

[71] H. Chen, B. Li, and Z. Chen, "Automatic extracting event-related potentials within several trials using Infomax ICA algorithm," *JOURNAL OF SCIENTIFIC & INDUSTRIAL RESEARCH*, vol. 71, pp. 468–473, JUL 2012. 19

[72] R. N. Vigário, "Extraction of ocular artefacts from eeg using independent component analysis," *Electroencephalography and clinical neurophysiology*, vol. 103, pp. 395–404, 9 1997. 19

[73] A. C. Tang and B. A. Pearlmutter, *Independent components of magnetoencephalography: localization*, pp. 129–162. Cambridge, MA, USA: MIT Press, 2003. 20

[74] A. C. Tang, B. A. Pearlmutter, N. A. Malaszenko, and D. B. Phung, "Independent components of magnetoencephalography: Single-trial response onset times," *NeuroImage*, vol. 17, pp. 1773–1789, 12 2002. 20

[75] A. Ossadtchi, R. M. Leahy, J. C. Mosher, N. Lopez, and W. Sutherling, "Automated interictal spike detection and source localization in meg using ica and spatial-temporal clustering," in *Biomedical Imaging, 2002. Proceedings. 2002 IEEE International Symposium on*, pp. 785–788, 2002. 20

[76] F. Poree, A. Kachenoura, H. Gauvrit, C. Morvan, G. Carrault, and L. Senhadji, "Blind source separation for ambulatory sleep recording," *Information Technology in Biomedicine, IEEE Transactions on*, vol. 10, no. 2, pp. 293–301, 2006. 20

[77] S. Hu, M. Stead, and G. A. Worrell, "Automatic identification and removal of scalp reference signal for intracranial eegs based on independent component analysis," *Biomedical Engineering, IEEE Transactions on*, vol. 54, no. 9, pp. 1560–1572, 2007. 20

[78] C. A. Joyce, I. F. Gorodnitsky, and M. Kutas, "Automatic removal of eye movement and blink artifacts from eeg data using blind component separation," *Psychophysiology*, vol. 41, pp. 313–325, 03 2004. ID: citeulike:1189182. 20

[79] B. W. McMenamin, A. J. Shackman, L. L. Greischar, and R. J. Davidson, "Electromyogenic artifacts and electroencephalographic inferences revisited," *NeuroImage*, vol. 54, no. 1, pp. 4–9, 2011. 20

[80] C. James and O. Gibson, "Temporally constrained ica: an application to artifact rejection in electromagnetic brain signal analysis," *Biomedical Engineering, IEEE Transactions on*, vol. 50, pp. 1108 –1116, sept. 2003. 20

[81] G. Barbati, C. Porcaro, F. Zappasodi, P. Rossini, and F. Tecchio, "Optimization of an independent component analysis approach for artifact identification and removal in magnetoencephalographic signals," *CLINICAL NEUROPHYSIOLOGY*, vol. 115, pp. 1220–1232, MAY 2004. 20

[82] P. LeVan, E. Urrestarazu, and J. Gotman, "A system for automatic artifact removal in ictal scalp EEG based on independent component analysis and Bayesian classification," *CLINICAL NEUROPHYSIOLOGY*, vol. 117, pp. 912–927, APR 2006. 20

[83] J. Cao, N. Murata, S. Amari, A. Cichocki, and T. Takeda, "A robust approach to independent component analysis of signals with high-level noise measurements," *IEEE TRANSACTIONS ON NEURAL NETWORKS*, vol. 14, pp. 631–645, MAY 2003. 20

[84] M. Milanesi, N. Martini, N. Vanello, V. Positano, M. F. Santarelli, and L. Landini, "Independent component analysis applied to the removal of motion artifacts from electrocardiographic signals," *MEDICAL & BIOLOGICAL ENGINEERING & COMPUTING*, vol. 46, pp. 251–261, MAR 2008. 20, 21

[85] D. Mantini, R. Franciotti, G. L. Romani, and V. Pizzella, "Improving MEG source localizations: An automated method for complete artifact removal based on independent component analysis," *NEUROIMAGE*, vol. 40, pp. 160–173, MAR 1 2008. 20

[86] R. J. Korhonen, J. C. Hernandez-Pavon, J. Metsomaa, H. Maki, R. J. Ilmoniemi, and J. Sarvas, "Removal of large muscle artifacts from transcranial magnetic stimulation-evoked EEG by independent component analysis," *MEDICAL & BIOLOGICAL ENGINEERING & COMPUTING*, vol. 49, pp. 397–407, APR 2011. 20, 21

[87] J. Ma, S. Bayram, P. Tao, and V. Svetnik, "High-throughput ocular artifact reduction in multichannel electroencephalography (EEG) using component subspace projection," *JOURNAL OF NEUROSCIENCE METHODS*, vol. 196, pp. 131–140, MAR 15 2011. 20, 21

[88] Y. Lu, P. Cao, J. Sun, J. Wang, L. Li, Q. Ren, Y. Chen, and X. Chai, "Using independent component analysis to remove artifacts in visual cortex responses elicited by electrical stimulation of the optic nerve," *JOURNAL OF NEURAL ENGINEERING*, vol. 9, APR 2012. 20

[89] L. Parra, C. Spence, A. Gerson, and P. Sajda, "Recipes for the linear analysis of EEG," *NEUROIMAGE*, vol. 28, pp. 326–341, NOV 1 2005. 20

[90] F. Cong, I. Kalyakin, T. Huttunen-Scott, H. Li, H. Lyytinen, and T. Ristaniemi, "SINGLE-TRIAL BASED INDEPENDENT COMPONENT ANALYSIS ON MISMATCH NEGATIVITY IN CHILDREN," *INTERNATIONAL JOURNAL OF NEURAL SYSTEMS*, vol. 20, pp. 279–292, AUG 2010. 20, 21

[91] J. . Cardoso and B. H. Laheld, "Equivariant adaptive source separation," *IEEE Transactions on Signal Processing*, vol. 44, no. 12, pp. 3017–3030, 1996. 20

[92] L. Zhukov, D. Weinstein, and C. Johnson, "Independent component analysis for EEG source localization - An algorithm that reduces the complexity of localizing multiple neural sources," *IEEE ENGINEERING IN MEDICINE AND BIOLOGY MAGAZINE*, vol. 19, pp. 87–96, MAY-JUN 2000. 21

[93] A. Tang, M. Sutherland, and C. McKinney, "Validation of SOBI components from high-density EEG," *NEUROIMAGE*, vol. 25, pp. 539–553, APR 1 2005. 21

[94] A. Cichocki, S. Shishkin, T. Musha, Z. Leonowicz, T. Asada, and T. Kurachi, "EEG filtering based on blind source separation (BSS) for early detection of Alzheimer's disease," *CLINICAL NEUROPHYSIOLOGY*, vol. 116, pp. 729–737, MAR 2005. 21

[95] N. Swann, H. Poizner, M. Houser, S. Gould, I. Greenhouse, W. Cai, J. Strunk, J. George, and A. R. Aron, "Deep Brain Stimulation of the Subthalamic Nucleus Alters the Cortical Profile of Response Inhibition in the Beta Frequency Band: A Scalp EEG Study in Parkinson's Disease," *JOURNAL OF NEUROSCIENCE*, vol. 31, pp. 5721–5729, APR 13 2011. 21

[96] M. De Lucia, J. Fritschy, P. Dayan, and D. S. Holder, "A novel method for automated classification of epileptiform activity in the human electroencephalogram-based on independent component analysis," *MEDICAL & BIOLOGICAL ENGINEERING & COMPUTING*, vol. 46, pp. 263–272, MAR 2008. 22

[97] V. S. Selvam and S. Shenbagadevi, "Brain Tumor Detection using Scalp EEG with Modified Wavelet-ICA and Multi Layer Feed Forward Neural Network," in *2011 ANNUAL INTERNATIONAL CONFERENCE OF THE IEEE ENGINEERING IN MEDICINE AND BIOLOGY SOCIETY (EMBC)*, pp. 6104–6109, 2011. 33rd Annual International Conference of the IEEE Engineering-in-Medicine-and-Biology-Society (EMBS), Boston, MA, AUG 30-SEP 03, 2011. 22

[98] J. Costa Junior, D. Ferreira, J. Nadal, and A. Miranda de Sa´ and, "Reducing electrocardiographic artifacts from electromyogram signals with independent component analysis," in *Engineering in Medicine and Biology Society (EMBC), 2010 Annual International Conference of the IEEE*, pp. 4598 –4601, 31 2010-sept. 4 2010. 22

[99] J. N. F. Mak, Y. Hu, and K. D. K. Luk, "An automated ecg-artifact removal method for trunk muscle surface emg recordings," *Medical Engineering and Physics*, vol. 32, no. 8, pp. 840–848, 2010. 22

[100] M. R. Ahsan, M. I. Ibrahimy, and O. O. Khalifa, "Advances in electromyogram signal classification to improve the quality of life for the disabled and aged people," *Journal of Computer Science*, vol. 6, no. 7, pp. 706–715, 2010. 22

[101] X. Ren, S. Mo, H. Hua, and L. Deng, "Resolving superimposed action potentials for emg signal decomposition," in *Bioinformatics and Biomedical Engineering (iCBBE), 2010 4th International Conference on*, pp. 1 –4, june 2010. 22

[102] D. Farina, C. Fevotte, C. Doncarli, and R. Merletti, "Blind separation of linear instantaneous mixtures of nonstationary surface myoelectric signals," *Biomedical Engineering, IEEE Transactions on*, vol. 51, no. 9, pp. 1555–1567, 2004. 22

[103] D. Farina, M.-F. Lucas, and C. Doncarli, "Optimized wavelets for blind separation of nonstationary surface myoelectric signals," *IEEE TRANSACTIONS ON BIOMEDICAL ENGINEERING*, vol. 55, pp. 78–86, JAN 2008. 22

[104] A. Subasi and M. Kiymik, "Muscle fatigue detection in emg using time–frequency methods, ica and neural networks," *Journal of Medical Systems*, vol. 34, pp. 777–785, 2010. 22

[105] N. W. Willigenburg, A. Daffertshofer, I. Kingma, and J. H. van Dieen, "Removing ECG contamination from EMG recordings: A comparison of ICA-based and other filtering procedures," *JOURNAL OF ELECTROMYOGRAPHY AND KINESIOLOGY*, vol. 22, pp. 485–493, JUN 2012. 23

[106] M. J. McKeown, S. Makeig, G. G. Brown, T.-P. Jung, S. S. Kindermann, R. S. Kindermann, A. J. Bell, and T. J. Sejnowski, "Analysis of fmri data by blind separation into independent spatial components," *Human brain mapping*, vol. 6, pp. 160–188, 1998. 23

[107] M. J. McKeown and T. J. Sejnowski, "Independent component analysis of fMRI data: examining the assumptions," *Human brain mapping*, vol. 6, pp. 368–372, 1998. ID: MCK-98a. 23

[108] V. D. Calhoun, T. Adali, L. K. Hansen, J. Larsen, and J. J. Pekar, "Ica of functional mri data: An overview," in *Proceedings of the International Workshop on Independent Component Analysis and Blind Signal Separation*, pp. 281–288, 2003. 23

[109] S. Kullback and R. A. Leibler *The Annals of Mathematical Statistics.* 23

[110] J. Pulkkinen, A. M. Häkkinen, N. Lundbom, A. Paetau, R. A. Kauppinen, and Y. Hiltunen, "Independent component analysis to proton spectroscopic imaging data of human brain tumours," *European Journal of Radiology*, vol. 56, pp. 160–164, 11 2005. 23

[111] S. Debener, M. Ullsperger, M. Siegel, and A. K. Engel, "Single-trial EEG-fMRI reveals the dynamics of cognitive function," *TRENDS IN COGNITIVE SCIENCES*, vol. 10, pp. 558–563, DEC 2006. 23

[112] N. Wang, W. Zeng, and L. Chen, "A Fast-FENICA method on resting state fMRI data," *JOURNAL OF NEUROSCIENCE METHODS*, vol. 209, pp. 1–12, JUL 30 2012. 23

[113] P. A. Rodriguez, V. D. Calhoun, and T. Adali, "De-noising, phase ambiguity correction and visualization techniques for complex-valued ICA of group fMRI data," *PATTERN RECOGNITION*, vol. 45, pp. 2050–2063, JUN 2012. 23

[114] S. Zhang and C.-s. R. Li, "Functional networks for cognitive control in a stop signal task: Independent component analysis," *HUMAN BRAIN MAPPING*, vol. 33, pp. 89–104, JAN 2012. 23

[115] X. Lei, P. Xu, C. Luo, J. Zhao, D. Zhou, and D. Yao, "fMRI Functional Networks for EEG Source Imaging," *HUMAN BRAIN MAPPING*, vol. 32, pp. 1141–1160, JUL 2011. 23

[116] K. K. Kim, P. Karunanayaka, M. D. Privitera, S. K. Holland, and J. P. Szaflarski, "Semantic: association investigated with functional MRI and independent component analysis," *EPILEPSY & BEHAVIOR*, vol. 20, pp. 613–622, APR 2011. 24

[117] F. Moeller, P. Levan, and J. Gotman, "Independent Component Analysis (ICA) of Generalized Spike Wave Discharges in fMRI: Comparison with General Linear Model-Based EEG-fMRI," *HUMAN BRAIN MAPPING*, vol. 32, pp. 209–217, FEB 2011. 24

[118] A. Jimenez-Gonzalez and C. J. James, "Time-structure based reconstruction of physiological independent sources extracted from noisy abdominal phonograms," *Biomedical Engineering, IEEE Transactions on*, vol. 57, no. 9, pp. 2322–2330, 2010. 24

[119] A. Jimenez-Gonzalez and C. J. James, "Extracting sources from noisy abdominal phonograms: a single-channel blind source separation method," *Medical & biological engineering & computing*, vol. 47, pp. 655–664, JUN 2009. 24

[120] A. Jimenez-Gonzalez and C. J. James, "On the interpretation of the independent components underlying the abdominal phonogram: a study of their physiological

relevance," *PHYSIOLOGICAL MEASUREMENT*, vol. 33, pp. 297–314, FEB 2012. 24

[121] Z. Wang, Z. He, and J. Chen, "Blind egg separation using ica neural networks," in *Engineering in Medicine and Biology Society, 1997. Proceedings of the 19th Annual International Conference of the IEEE*, vol. 3, pp. 1351 –1354 vol.3, oct-2 nov 1997. 24

[122] C. Peng, X. Qian, and D. Ye, "Electrogastrogram extraction using independent component analysis with references," *Neural Computing and Applications*, vol. 16, pp. 581–587, 2007. 24

[123] B. Mika, E. Tkacz, P. Kostka, and Z. Budzianowski, "An improvement of normogastric rhythm extraction from electrogastrographic (egg) signal using independent component analysis," in *Engineering in Medicine and Biology Society, 2009. EMBC 2009. Annual International Conference of the IEEE*, pp. 356 –359, sept. 2009. 24

[124] M. Z. Poh, D. J. McDuff, and R. W. Picard, "Non-contact, automated cardiac pulse measurements using video imaging and blind source separation," *Optics Express*, vol. 18, no. 10, pp. 10762–10774, 2010. 24

[125] G. R. Tsouri, S. Kyal, S. Dianat, and L. K. Mestha, "Constrained independent component analysis approach to nonobtrusive pulse rate measurements," *JOURNAL OF BIOMEDICAL OPTICS*, vol. 17, JUL 2012. 24

[126] J. Malmivuo and R. Plonsey, *Bioelectromagnetism : Principles and Applications of Bioelectric and Biomagnetic Fields*. Oxford University Press, USA, 1 ed., July 1995. 25, 26, 28, 29, 30, 32

[127] W. Einthoven, "Weiteres über das Elektrokardiogramm," *Pflugers Archiv-european Journal of Physiology*, vol. 122, pp. 517–584, 1908. 27

[128] J. Kuzilek, L. Lhotska, and M. Hanuliak, "An automatic method for holter ecg denoising using ica," in *Proceedings of the 4th International Symposium on Applied Sciences in Biomedical and Communication Technologies*, ISABEL '11, (New York, NY, USA), pp. 3:1–3:5, ACM, 2011. 34

[129] J. Kuzilek, L. Lhotska, and M. Hanuliak, "Processing holter ecg signal corrupted with noise: Using ica for qrs complex detection," in *Applied Sciences in Biomedical*

and Communication Technologies (ISABEL), 2010 3rd International Symposium on, pp. 1–4, Nov. 34

[130] J. Zar, *Biostatistical analysis*. Prentice Hall, 1984. 35, 36

[131] L. Breiman, *Classification and regression trees*. The Wadsworth and Brooks-Cole statistics-probability series, Chapman & Hall, 1984. 36

[132] G. Friesen, T. Jannett, M. Jadallah, S. Yates, S. Quint, and H. Nagle, "A comparison of the noise sensitivity of nine qrs detection algorithms," *Biomedical Engineering, IEEE Transactions on*, vol. 37, pp. 85 –98, jan. 1990. 41, 52

[133] S. Pal and M. Mitra, "Empirical mode decomposition based ecg enhancement and qrs detection," *Computers in biology and medicine*, vol. 42, no. 1, pp. 83–92, 2012. 41

[134] J. Pan and W. J. Tompkins, "A real-time qrs detection algorithm," *Biomedical Engineering, IEEE Transactions on*, vol. BME-32, no. 3, pp. 230–236, 1985. 41, 58

[135] I. Christov, "Real time electrocardiogram qrs detection using combined adaptive threshold," *BioMedical Engineering OnLine*, vol. 3, no. 1, p. 28, 2004. M3: 10.1186/1475-925X-3-28. 41

[136] P. S. Hamilton and W. J. Tompkins, "Quantitative investigation of qrs detection rules using the mit/bih arrhythmia database.," *IEEE Transactions on Biomedical Engineering*, vol. BME-33, no. 12, pp. 1157–1165, 1986. 41

[137] J. Kuzilek and L. Lhotska, "Electrocardiogram beat detection enhancement using independent component analysis," *Medical Engineering and Physics*, 2012. Article in Press. 42

[138] A. Taddei, G. Distante, M. Emdin, P. Pisani, G. B. Moody, C. Zeelenberg, and C. Marchesi, "The european st-t database: standard for evaluating systems for the analysis of st-t changes in ambulatory electrocardiography," *European heart journal*, vol. 13, no. 9, pp. 1164–1172, 1992. 51

[139] F. Jager, A. Taddei, G. B. Moody, M. Emdin, G. Antolič, R. Dorn, A. Smrdel, C. Marchesi, and R. G. Mark, "Long-term st database: A reference for the development and evaluation of automated ischaemia detectors and for the study of the

dynamics of myocardial ischaemia," *Medical and Biological Engineering and Computing*, vol. 41, no. 2, pp. 172–182, 2003. 52

[140] P. Laguna, R. G. Mark, A. Goldberg, and G. B. Moody, "Database for evaluation of algorithms for measurement of qt and other waveform intervals in the ecg," in *Computers in Cardiology*, pp. 673–676, 1997. 52

[141] P. Albrecht, *ST Segment Characterization for Long Term Automated ECG Analysis*. Massachusetts Institute of Technology, Department of Electrical Engineering and Computer Science, 1983. 52

[142] G. Clifford, F. Azuaje, and P. McSharry, *Advanced methods and tools for ECG data analysis*. Artech House engineering in medicine & biology series, Artech House, 2006. 54

[143] B. Widrow, J. Glover Jr., and J. McCool, "Adaptive noise cancelling: principles and applications," *Proceedings of the IEEE*, vol. 63, no. 12, pp. 1692–1716, 1975. 55

[144] K. Hirano, S. Nishimura, and S. K. Mitra, "Design of digital notch filters.," *IEEE Transactions on Communications*, vol. COM-22, no. 7, pp. 964–970, 1974. 55

[145] P. Patil and M. Chavan, "A wavelet based method for denoising of biomedical signal," in *Pattern Recognition, Informatics and Medical Engineering (PRIME), 2012 International Conference on*, pp. 278–283, March. 57

[146] S. Mallat, *A Wavelt Tour of Signal Processing*. Wavelet Analysis & Its Applications, Acad. Press, 1999. 57

[147] D. L. Donoho, "De-noising by soft-thresholding," *IEEE Transactions on Information Theory*, vol. 41, no. 3, pp. 613–627, 1995. 58

[148] A. Cichocki and S.-i. Amari, *Adaptive Blind Signal and Image Processing: Learning Algorithms and Applications*. New York, NY, USA: John Wiley & Sons, Inc., 2002. 86

[149] P. Vandewalle, J. Kovacevic, and M. Vetterli, "Reproducible research in signal processing," *Signal Processing Magazine, IEEE*, vol. 26, pp. 37 –47, may 2009. 86